TAMPEREEN TEKNILLINEN YLIOPISTO
TAMPERE UNIVERSITY OF TECHNOLOGY

INARI LYYRA

OPTIMISING POLYLACTIDE MELT SPINNING USING REAL-TIME MONITORING

Master's thesis

Examiner: Professor Minna Kellomäki
Examiner and topic approved by the Faculty Council of the Faculty of Engineering Sciences on 5 March 2014.

TIIVISTELMÄ

TAMPEREEN TEKNILLINEN YLIOPISTO
Materiaalitekniikan koulutusohjelma
LYYRA, INARI: Polylaktidin sulakehruun optimointi reaaliaikaisen monitoroinnin avulla
Diplomityö, 85 sivua, 10 liitesivua
Kesäkuu 2015
Pääaine: Biomateriaalitekniikka
Tarkastaja: Professori Minna Kellomäki
Avainsanat: Polylaktidi, sulakehruu, reaaliaikainen monitorointi, hydrolyyttinen hajoaminen

Polylaktidi (PLA) on synteettinen, biohajoava polyesteri. Siitä valmistetaan kuitua yleensä kaksivaiheisella sulakehruulla, jonka vaiheet ovat (i) raaka-aineen sulattaminen ja sulan pakottaminen pienten reikien läpi ja (ii) kuidun vetäminen ja lämpökäsittely sen mekaanisten ominaisuuksien parantamiseksi. Biohajoavien polymeerien prosessointi on haastavaa polymeerin termisen hajoamisen vuoksi, mikä rajoittaa prosessointiparametrien valintaa. Näin ollen on kehitetty reaaliaikaisia monitorointimenetelmiä, joiden avulla materiaalin tärkeimpiä ominaisuuksia voidaan seurata prosessoinnin aikana.

Tämän työn päätavoitteet olivat: (i) tehostaa nelifilamenttisen PLA-kuidun valmistusta päivitetyllä sulakehruulaitteistolla ja (ii) tutkia tavanomaisella linjalla valmistetun PLA-kuidun hydrolyyttista hajoamista. Päivitetty sulakehruulaitteisto koostui suurinopeuksisista kehruutorneista ja kaksiruuviekstruuderista, joka oli varustettu rakosuuttimella myöhemmin tapahtuvaa polymeerin termisen hajoamisen reaaliaikaista mittausta varten. PLA:n sulakehruuparametrien optimointi tehtiin kahdessa osassa; alustavat ajot suoritettiin pakkauslaatuisella PLA:lla ja toinen prosessointisarja GMP-laatuisella poly-L/D-laktidilla, jonka L/D-suhde oli 96/4.

Valmistettuja kuituja tutkittiin vetokokein ja prosessoinnin aikana tapahtuvaa termistä hajoamista arvioitiin sisäisen viskositeetin (i.v.) mittauksilla. Kuitujen ominaisuuksille asetettiin tavoitearvot, joiden tiedettiin mahdollistavan kuitujen jatkokäsittelyn. Osa alustavissa prosessointiajoissa valmistetuista kuiduista oli mekaanisesti suhteellisen hyviä ottaen huomioon käytetyn materiaalin ja osa filamenttien halkaisijoista tavoitearvojen mukaisia. Pakkauslaatuinen PLA ei hajonnut termisesti prosessoinnin aikana, mutta GMP-laatuisen PLA:n i.v. putosi kolmanneksen. Puolet GMP-laatuisista kuiduista oli filamenttien halkaisijoiden ja venymäarvojen suhteen tavoitteessa. Kuitujen mekaaniset ominaisuudet vaativat vielä optimointia, ja tämä tulisi tehdä ensisijaisesti nostamalla vetosuhdetta. Kuitujen vetolujuus ei kuitenkaan ollut kaukana tavoitteesta.

Lisäksi työssä tutkittiin tavanomaisella laitteistolla valmistettujen gammasteriloitujen ja steriloimattomien kuitujen hydrolyyttistä hajoamiskäyttäytymistä 48 viikon hydrolyysisarjalla. Kuitujen mekaanisia, termisiä ja reologisia ominaisuuksia sekä molekyylipainon muutosta tutkittiin hydrolyysisarjan aikana. Kuitujen molekyylipaino ja i.v. laskivat tasaisesti, mutta gammasteriloidun kuidun hajoamisnopeus oli huomattavasti suurempi. Steriloimattoman kuidun mekaaniset ominaisuudet eivät juuri muuttuneet sarjan aikana, mutta steriloitua kuitua ei pystytty 28 viikon jälkeen enää vetokoestamaan. Hydrolyysisarjan tulokset olivat pääasiassa samassa linjassa aikaisempien vastaavien tutkimusten kanssa. Sarjan tuloksia voidaan käyttää referenssinä tuleville päivitetyllä laitteistolla valmistettujen kuitujen hydrolyysisarjoille.

ABSTRACT

TAMPERE UNIVERSITY OF TECHNOLOGY
Degree Programme in Material Science
LYYRA, INARI: Optimising polylactide melt spinning using real-time monitoring
Master of Science Thesis, 85 pages, 10 Appendix pages
June 2015
Major subject: Biomaterials
Examiner: Professor Minna Kellomäki
Keywords: Polylactide, melt spinning, real-time monitoring, hydrolytic degradation

Polylactide (PLA) is a synthetic biodegradable polyester and it is usually processed into fibres by two-step melt spinning, which comprises of (i) melting the raw material and pushing the melt through small orifices and (ii) stretching and heat treating the fibre to increase its mechanical properties. However, processing biodegradable polymers is challenging because the polymer degrades thermally which narrows the choice of the processing parameters. Real-time monitoring allows monitoring of the key properties of the material during the production of the fibre.

There were two objectives for this work: (i) upscaling the production of 4-filament PLA fibre with an updated set-up with real-time monitoring and (ii) studying the hydrolytic degradation of PLA fibres manufactured with the conventional set-up. The updated set-up comprised of high-speed spinning plants and a twin-screw extruder equipped with a slit die for later real-time monitoring of parameters related to thermal degradation of the polymer. The processing conditions of polylactide melt spinning were optimised by two sets of trials; initial trials with a packaging grade PLA and a second set of trials with GMP grade poly(L/D)lactide with an L/D ratio of 96/4.

The obtained fibres were characterised by tensile testing and the temperature-induced chain scission was evaluated by inherent viscosity (i.v.) measurements. Goal values were established to enable the post-processing of the fibres. Mechanically adequate fibre was produced in the initial trials regarding the material used and the filament diameters fulfilled the requirements. The packaging grade PLA did not degrade during extrusion but the i.v. of the GMP grade PLA was decreased by one third. The filament diameter and the strain values were at an acceptable level in half of the spools produced in the GMP grade trials. In the initial trials there was a problem with the fluctuation of the filament diameters but it was largely solved by a change of the feeding equipment in the GMP grade trials. There is a need for further optimisation of the mechanical properties. This should be done by increasing the draw ratio. However, the ultimate tensile strength of the fibre was close to the required value.

In addition a 48-week hydrolysis study was conducted on the fibre produced with the conventional set-up. The molecular, rheological, thermal and mechanical properties of gamma irradiated and non-irradiated fibres were measured. The molecular weights and inherent viscosities of both fibres decreased steadily, but the irradiated fibre degraded more prominently. The mechanical performance of the non-irradiated fibre showed no changes but the irradiated fibre could no longer be tested after 28 weeks. In conclusion, the results of the hydrolytic degradation studies were mainly in line with earlier studies. These results can be used as a reference for the future hydrolytic degradation studies for the fibre manufactured with the upgraded set-up.

PREFACE

This study has been carried out in the Biomaterials and Tissue Engineering group in the Department of Electronics and Communications Engineering in Tampere University of Technology.

First I would like to thank Professor Minna Kellomäki for inspecting the thesis and giving me the opportunity to work in such an interesting project. I would also like to thank Ville Ellä, who instructed me in the beginning of the thesis project. I would like to express special gratitude to Elina Talvitie for inspiring supervision and support.

I would also like to thank the whole Biomaterials and Tissue Engineering research group for creating such a helpful and warm working environment. I am also very grateful to Rami, Jukka and Jaana in the mechanical workshop and Heikki and Suvi in the laboratory. I would also take this opportunity to thank all the other Master's Thesis workers in the research group for giving peer support during the thesis process.

I wish to express my special gratitude to my mother Tiina-Mari for giving me guidance in the academic world. I would also take this opportunity to thank all my family and friends, especially my dear friend and roommate Jenni for her understanding support and for not letting me forget that we are not all engineers.

CONTENTS

TERMS AND DEFINITIONS

Ø	Diameter
Amorphous	A material with a non-organised structure, non-crystalline
ATR	Attenuated Total Reflectance
Bioabsorption	The process of a substance being degraded or dissolved and eventually excreted from the body as a result of cell metabolism
Biodegradation	The process of a substance chemically falling apart as a result of biologic activity
Bioresorption	see bioabsorption
Copolymer	A polymer synthesised by using two or more different monomer types
CV	Coefficient of Variation
Denier	A unit of weight to measure the fineness of yarns, equal to the weight in grams of 9,000 meters of the yarn
DR	Draw Ratio
FTIR	Fourier Transform Infrared
FT-NIR	Fourier Transform Near Infrared
Gy	gray, a unit of absorbed ionizing radiation dose (J/kg)
Homopolymer	A polymer synthesised by using only one monomer type
Hydrolysis	Water-induced process of a substance degrading
In vitro	Outside the body, namely in the laboratory
In vivo	Inside a living organism
iPP	Isotactic Polypropylene
IR	Infrared
I.v.	Inherent viscosity
LED	Light Emitting Diode
MFI	Melt Flow Index
M_n	Number-average molecular weight
Molecular weight	The sum of the atomic weights of the atoms in the molecule
Monomer	A low-molecular-weight substance which is capable of forming polymer chains
MPa	Megapascal, the unit of pressure and stress (N/mm^2)
MSD	Light Emitting Diode Shadow Method
M_w	Weight average molecular weight
N	Newton, the unit of force (kgm/s^2)
NIR	Near Infrared
NMR	Nuclear Magnetic Resonance
PA 6	Polyamide 6
PBS	Phosphate buffered saline solution
PDLA	Poly(D-lactide)
PET	Polyethylene Terephthalate

PLA	Polylactide
PLDLA	Poly(L/D-lactide)
PLLA	Poly(L-lactide)
Polymer	A substance formed by repetition of one or more types of monomers
Polymerisation	A chemical reaction in which the monomers are linked together to form a polymer
POM	Polyoxymethylene
PP	Polypropylene
Racemic	Optically inactive, comprises of equal amounts of optic isomers having opposite specific rotations
Rpm	revolutions per minute
SAXS	Small Angle X-ray Scattering
Scaffold	A porous supporting structure used in tissue engineering
Tensile strength	A measure of force per unit area required to break a test specimen which has been attached of its ends and drawn
T_g	Glass transition temperature
T_m	Melting temperature
UV-vis	Ultra-violet/visible
WAXS	Wide Angle X-ray Scattering

1 INTRODUCTION

Bioresorbable medical devices are implants which give temporary support and shape for the new growing tissue in lesion sites and eventually break down in the body being replaced with the new tissue. These implants have many benefits, including no need for removing surgery, reducing healthcare costs, better biocompatibility and tailorability to each application via a range of properties, for example the rate of hydrolytic degradation. (Tateishi et al. 2002.) However, the development of bioresorbable medical devices can be a long and expensive process. The cost of GMP grade materials is high and their processing difficult as no additives are allowed and the range of the usable processing parameters is narrow. (McAfee & Thompson 2007.) Each batch of the raw material is usually different and the selection of the appropriate processing conditions for each material to obtain acceptable extrudate quality is time-consuming and results in material being wasted during the examination of optimal processing parameters (Liu et al. 2012).

Real-time monitoring removes the need for time-consuming and laborious off-line characterisation of the extrusion products. Real-time monitoring of the properties of the melt and the extrudate enhances the control over the processing event resulting in better quality of the products. (Saerens et al. 2011.) Biodegradable polymers, such as polylactide, degrade in high temperatures. This has to be taken into account in processing of these materials. The thermal degradation results in chain scission seen as a reduction in the melt viscosity and as an increase in monomer content. These events, especially the increase in the monomer content, effect on the hydrolytic degradation rate of the product. (Ellä et al. 2011a.)

Bio-PolyTec is an EU-funded project which aims to develop real-time monitoring of the key properties and improve the quality of biodegradable polymer. In this work the production rate of polylactide fibre is increased by transferring the production to an updated set-up. The set-up comprises of high-speed spinning plants and a twin-screw extruder equipped with a slit die. The slit die enables the real-time monitoring of melt viscosity and monomer content, which both are related to the degree of thermal degradation of the polymer. The processing conditions of polylactide melt spinning are optimised by two sets of trials; initial trials with a packaging grade polylactide and a trial series with GMP grade polylactide. The obtained fibres are characterised by tensile testing and the temperature-induced chain scission is evaluated by inherent viscosity (i.v.) measurements. In addition the hydrolytic degradation behaviour of fibres manufactured by the conventional melt spinning set-up is studied and the molecular, rheological, thermal and mechanical properties of the fibres are examined.

THEORETICAL BACKGROUND

2 POLYLACTIDE

Polylactide (PLA) is a completely biodegradable, linear aliphatic polyester. It can be derived from renewable resources and its applications range from packaging and agriculture to biomedical field. The basic building block of PLA is a simple compound called lactic acid or 2-hydroxypropionic acid. Lactic acid is a chiral molecule which exists in two stereoisomerical forms, L- and D-lactic acid. Humans and other mammals can produce only the L-isomer, whereas bacteria can produce both L- and D-isomers. (Garlotta 2002; Gupta et al. 2007; Carrasco et al. 2010.)

2.1 Structure and synthesis

PLA can be polymerised from lactic acid in two ways; direct polycondensation of lactic acid and ring-opening polymerisation of a cyclic dimer intermediate. Polycondensation of PLA involves splitting water molecules between the monomers to form a polymer. The process requires solvents as well as vacuum and high temperatures to remove the water produced in the synthesis. The resulting polymer has low to intermediate molecular weight and is mechanically poor. In addition, the synthesis allows poor control over the stereoregularity of the resulting polymer. The second polymerisation method is often preferred over the first one as it enables the production of high molecular weight (over 100 000 Da) PLA without solvents and with better stereoregularity control. The method involves an intermediate step of producing a cyclic dimer (commonly referred as lactide) from two lactic acid monomers. Cyclic lactides are then converted into PLA by ring-opening polymerisation (see Figure 2.1.). (Lunt 1998; Kricheldorf 2001; Södergård & Stolt 2002; Gupta et al. 2007; Gupta & Kumar 2007; Slomkowski et al. 2014.)

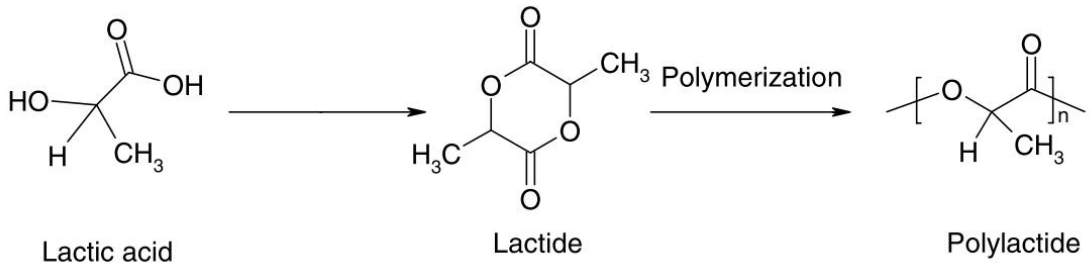

Figure 2.1. *Synthesis of polylactide by ring-opening polymerisation (Gupta & Kumar 2007).*

Since lactic acid exists in two stereoisomeric forms, there can be three different configurations of lactide (see Figure 2.2.). The dimers can have identical (L,L or D,D) or different (L,D) stereochemical centres. The mixed dimer is called meso- or L,D-lactide and it is optically inactive as the specific rotations of the two different lactides cancel

out each other. (Lunt 1998; Kricheldorf 2001; Södergård & Stolt 2002; Gupta et al. 2007; Gupta & Kumar 2007; Slomkowski et al. 2014.)

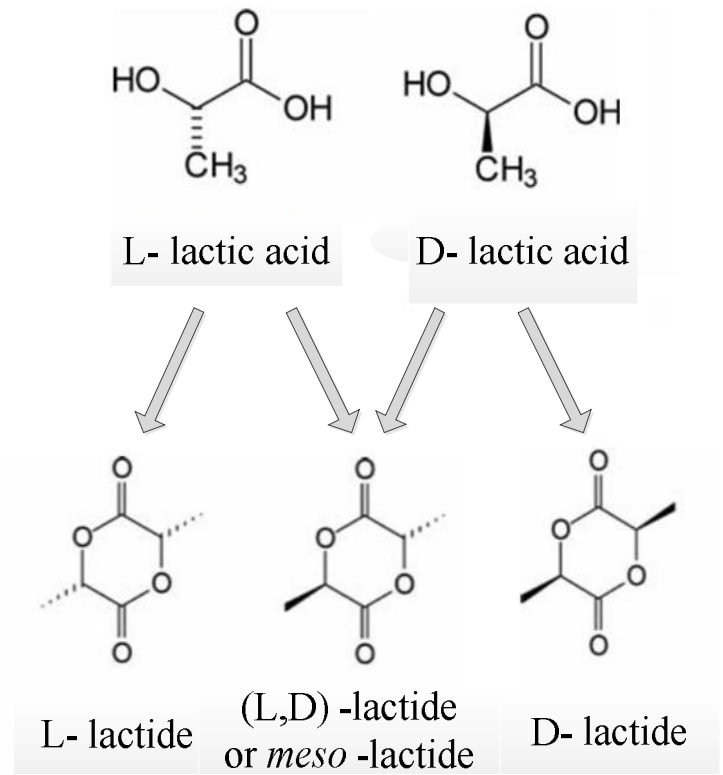

Figure 2.2. *Stereoisomers of lactic acid and lactide. Modified from (Auras et al. 2010).*

In general polymers are named after their monomer with a prefix "poly". Poly(lactic acid) is made from lactic acid monomers by direct polycondensation while polylactide is made from lactide via ring-opening polymerisation. Both of these polymers are referred to as PLA. (Södergård & Stolt 2002; Gupta & Kumar 2007.) However, nowadays PLA more often refers to polylactide, because it is preferred over poly(lactic acid) due to better mechanical properties and stereoregularity control. The homopolymer of L-lactide is named poly-L-lactide (PLLA) and a polymer composed only of D-lactide is designated as poly-D-lactide (PDLA). If both the L- and D-forms of lactide are used in the synthesis, the resulting polymer is named poly(L,D)lactide (PLDLA). The ratio of the two forms is usually indicated in the name of the polymer: for example in 96/4 or 96:4 PLDLA there are 96 weight percent of L-lactide and 4 percent of D-lactide. (Middleton & Tipton 2000; Gupta & Kumar 2007.)

2.2 Crystallinity

PDLA and PLLA are both semicrystalline polymers with a glass transition temperature of about 55 °C and a melting point of 180 °C. PLLA exhibits about 37 % crystallinity. (Middleton & Tipton 2000; Södergård & Stolt 2002; Nair & Laurencin 2007.) The crystallinity of PLA can be decreased by adding unlike monomers (for example adding D-lactide into PLLA) because they basically work as defects in the structure and disrupt

the formation of the highly organised crystals. The effects of copolymerisation are more pronounced with higher quantities of the unlike monomer. It has been observed that 72-75 % optical purity in polylactide is needed for crystallisation, but also polylactide with as low as 43 % optical purity has been crystallised using a Salen-Al-OCH_3 complex initiator. On the other hand, less than 2 % of D-lactide makes PLA highly crystalline. (Middleton & Tipton 2000; Södergård & Stolt 2002; Solarski et al. 2007.) The degree of crystallinity and orientation affect the tensile properties of the material so that the mechanical properties improve with growing organisation in the structure (Penning et al. 1993).

The crystallinity can be increased by slow cooling or drawing. PLLA can form four different kinds of crystallites depending on the crystallisation and drawing conditions. The most common α-crystallites are formed when amorphous PLLA film is drawn in temperatures above the glass-transition temperature (55 °C) with low hot-draw ratios (1-6). The α-crystallites can transfer into β-form crystallites when semicrystalline PLLA film with α-crystallites is drawn with higher hot-draw ratios (4-20) in higher temperatures (near the melting temperature of the α-form, 180 °C). Thus the products of PLLA processed by drawing consist of only α-crystallites or a mixture of α- and β-crystallites. (Eling et al. 1982; Hoogsteen et al. 1990; Sawai et al. 2002; Takahashi et al. 2004.)

The third and fourth crystallite forms are rarer and require specific conditions to form. Cartier et al. obtained the third crystallite, the γ-form, in epitaxial crystallisation of PLLA on hexamethylbenzene at 140 °C. (Cartier et al. 2000.) The fourth type of crystallites emerges only in racemic blends which have a 50/50 distribution of PLLA and PDLA. The crystallite is called a stereocomplex crystal and interestingly it exhibits a melting temperature 60 °C higher (230 °C) than the α- and β-homocrystallites. (Takasaki et al. 2003.)

2.3 Degradation

There are four terms (biodegradation, bioerosion, bioabsorption and bioresorption) to indicate that a medical device will eventually disappear in the body. In this work the definitions for the terms are used according to the usage suggested by the Consensus Conference of the European Society for Biomaterials (Williams 1987). The term “degradation” is used when the material or device degrades by chemical means resulting in the cleavage of the covalent bonds and the term “erosion” is used when there are physical changes in the material or device (e.g. changes in size, shape or mass).We are dealing with medical applications of the polymers and thus using the term “biodegradable” in its medical sense. Bioabsorption and bioresorption are used interchangeably meaning controlled degradation and complete disappearance in the body via cell metabolism.

PLA can degrade because of thermal, mechanical or chemical stress, or in the presence of enzymes, micro-organisms, irradiation or water. However, in this work we concentrate on thermal (Section 4.1.) and hydrolytic degradation. In presence of water PLA undergoes hydrolytic degradation and erodes hydrolytically via bulk erosion (homoge-

neously throughout the material). The reaction is a simple scission of the ester bond resulting in acid and alcohol groups as shown in Figure 2.3. and it can be described as reverse polycondensation. The hydrolysis of PLA does not require catalytic enzymes. (Garlotta 2002; Nair & Laurencin 2007.)

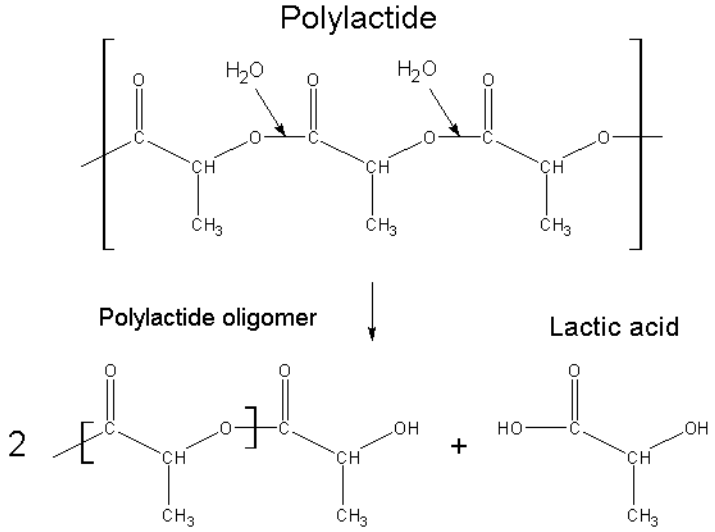

Figure 2.3. *The mechanism of hydrolytic degradation of polylactide. Modified from (Lunt 1998).*

Hydrolytic degradation is affected by chemical structure, molar mass and its distribution, purity, initiator/catalyst type, morphology, shape of the specimen, history of the polymer and the surrounding conditions of the hydrolysis. The pH of the medium has an effect on where the chain scission occurs. Alkaline conditions cause the chains of polylactide to be cut randomly whereas in acidic conditions there are more chain end scissions. This is explained by the growing amount of chain ends which leads to a higher probability of chain end scission over time. (Södergård & Stolt 2002.)

The hydrolysis rate depends on the size and shape of the sample as well as the isomer ratio and temperature of the medium (Garlotta 2002; Nair & Laurencin 2007). In general crystalline polymers degrade slower than amorphous because the well-organised structure of the crystals is denser and the degradative agents cannot get into the matrix as easily. For example semicrystalline PLLA can take any time between a few months (low molar mass film) to 60 years (oriented fibres) whereas the amorphous PLDLA degrades in 12-16 months. This makes PLDLA more attractive for drug delivery applications. (Middleton & Tipton 2000; Södergård & Stolt 2002.)

3 MELT SPINNING

Polymer fibres can be manufactured via dry, wet- and melt spinning processes. In this work we concentrate on the latter. Melt spinning is the main production method in industry due to its high suitability and cost-effectiveness for polymer fibre manufacturing at industrial scales. Melt spun fibres exhibit better mechanical and chemical properties compared to fibres obtained by other spinning methods, the process is easier to control and friendlier for the environment as it does not involve solvents. (Lim et al. 2008; Jia 2010; Zhou & Kumar 2010.)

Melt spinning processes can be divided into two subgroups; two-step melt spinning which comprises of extrusion and drawing (it can be a continuous process or the fibre can be collected from the spinneret and drawn later) and high speed melt spinning. The latter can further be divided in two according to if the fibre is collected straight from the spinneret or undergone drawing. (Ellä 2012.)

3.1 Two-step melt spinning

A schematic of a two-step melt spinning process is presented in Figure 3.1. A two-step melt spinning process comprises of melt extrusion and drawing. The solid polymer is melted in the extruder barrel and the melt is forced through a die with multiple holes called a spinneret. As the polymer jets emerge from the spinneret, they are solidified by cooling them down with air. The resulting fibre is called as-spun fibre if it is collected straight from the spinneret and not undergone further treatments. These further treatments often include drawing, which is discussed in the next section. In the end of the spinline the finished fibre is collected with a winder. (Lim et al. 2008; Jia 2010; Zhou & Kumar 2010; Tadmor & Gogos 2013.)

Drawing

Usually the as-spun fibres do not exhibit the mechanical properties desired and drawing is applied to reinforce the fibre with orientation and crystallinity. Improved crystallinity also enhances the thermal resistance of the fibre. (von Oepen & Michaeli 1992.) The drawing units apply drag force on the fibre thinning it and orienting the polymer chains. The orientation improves the fibres' mechanical properties such as tensile strength and elastic modulus. (Lim et al. 2008; Jia 2010; Zhou & Kumar 2010; Tadmor & Gogos 2013.)

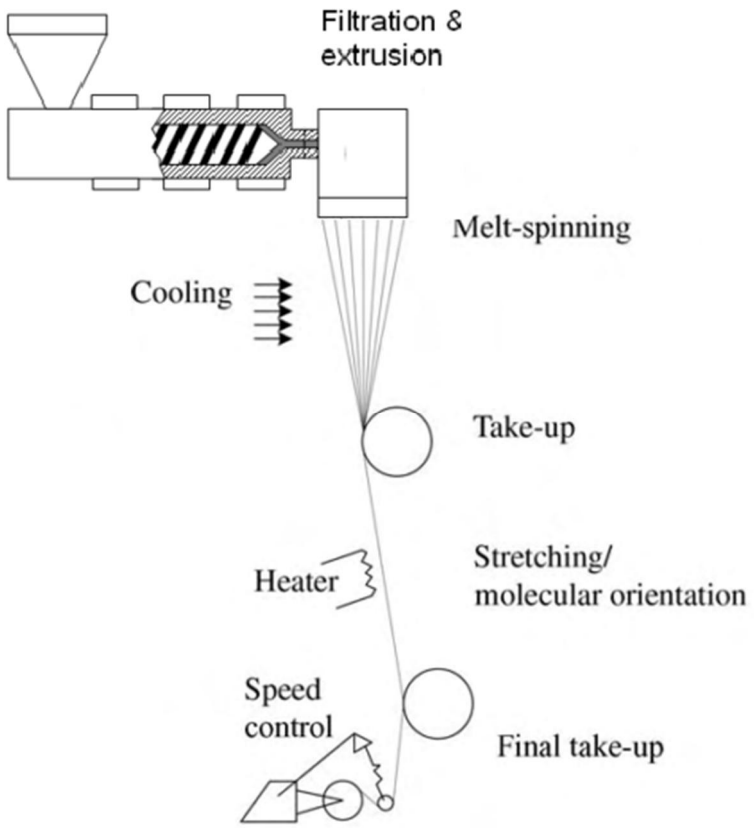

Figure 3.1. *A schematic representation of a fibre melt spinning process. Modified from (Jia 2010; Tadmor & Gogos 2013).*

Orientation means parallelisation of the polymer chains (in amorphous regions) or lamellae in a crystal (in crystalline regions) in the direction of the fibre axis. The molecular orientation develops in two stages during melt spinning: in the spinneret channel and under elongation. First the molecules of the polymer get aligned when the melt is forced through the capillary channel but this preliminary orientation unwinds after the spinneret and thus has little effect on the final structure of the fibre. The stretch force along the spinline makes the major contribution to the final molecular orientation. (Jia 2010.) The fibre orientates in a short (0.3 - 2 mm) area called the neck point. It is situated closely before the leaving point of the supply roll (when drawing as-spun fibre) or the spinneret (continuous two-step melt spinning) into the drawing zone. In this zone the non-oriented and randomly arranged polymer chains are drawn into a semi-crystalline fibre. (Gupta & Kothari 1997; Fourné 1999.)

The fibre can be drawn in ambient temperature (cold drawing) or the mechanical properties of the fibre can be further ameliorated by adding thermal treatment in the spinline (hot drawing). (Lim et al. 2008; Jia 2010; Zhou & Kumar 2010; Tadmor & Gogos 2013.) The optimum temperature for hot drawing is near the glass transition temperature of the polymer (i.e. 70 °C for dry polyethylene terephthalate). The heating in the spinline can be done by external heating or partly generated by using the inner frictional heat from drawing. Nevertheless, it has to be taken into account that the time

the fibre spends in the necking point is in the range of 10^{-4} s and the fibre has to reach the sufficient temperature for crystallisation in that time. For example when using external heating the temperatures have to be adjusted accordingly. (Gupta & Kothari 1997; Fourné 1999.)

In melt spinning besides orientation the polymer chains organise into highly organised structures, crystallites. There are two types of crystallisation; stress- or orientation-induced and temperature-induced. Stress-induced crystallisation is formed at spinning velocities higher than 2000 m/min and discussed in more detail in Section 3.2. Temperature-induced (also called quiescent) crystallisation forms at a temperature called crystallisation temperature, which for most polymers is glass transition temperature ($T_{g)}$ + melting temperature (T_m) divided by two. For example the crystallisation temperature of PLLA is around 130 °C. There is no single temperature inducing maximum crystallisation for fibre drawing because the temperature and stress both affect the crystallisation. Stress-induced crystallisation also has a crystallisation temperature, but it is likely to be different than the one for the temperature-induced crystallisation. (Cicero & Dorgan 2001; Auras et al. 2010; Battegazzore 2011.)

Crystallinity can be increased by three routes; adding a nucleation agent, plasticisers or tuning the process conditions, mainly temperature and cooling time. (Battegazzore 2011.) In medical applications nucleation agents and plasticisers do not come into question as their removal can be difficult and their remains can cause unwanted responses in the body. This leaves modifying the processing conditions as the main route for increasing fibre crystallinity.

3.1.1 Effects of drawing conditions

Hot drawing is a complex process with a number of variables which have an effect on the structure and thus the properties and appearance of the finished fibre. These parameters include for example winding speed, throughput, cooling conditions and relative humidity of the drawing line. The effects of these variables on the structure of as-spun fibres at low spinning velocities (<2000 m/min) are shown in Table 3.1. Spinning stress is defined as draw-induced stress inside the filament. (Auras et al. 2010.)

Table 3.1. *The effects of hot drawing parameters on the structure of as-spun fibres. Modified from (Auras et al. 2010).*

Parameter	Spinning stress	Filament temperature	Time spent in drawing line	Fibre orientation	Fibre crystallinity	Remarks
↑ Take-up speed	↑	↓	↓	↑	↑	
↑ Throughput	↓	↑	↑	↓	↑	Higher denier
↑ Cooling air temp.	↓	↑	↑	↓	↑	Slower cooling
↑ Cooling air speed	↑	↓	↓	↑	↓	Faster cooling
↑ Relative humidity	↑	↓	↓	↑	↓	Carries more heat

Fibre orientation and crystallinity

Controlling the molecular orientation and crystallinity of the fibre is important because they affect the fibres' final structure and properties. Crystallinity and orientation are closely linked to the tensile properties of the fibre and it has been confirmed that tensile and impact strength increase with increasing degree of orientation and crystallinity. (Grijpma et al. 2002; Jia 2010.)

Temperature has an effect on both crystallinity and orientation. Increasing the temperature increases polymer chain relaxation and thus lowers the orientation. Its effect on crystallisation is the opposite because when the temperatures are higher, the filaments take longer time to cool down and they spend a longer time near the crystallisation temperature. (Cicero et al. 2002; Gupta et al. 2007.) Brucato et al. examined the effect of cooling rate on the crystallinity of isotactic polypropylene (iPP), polyethylene terephthalate (PET) and polyamide 6 (PA 6). Thin polymer films were quenched in an experimental apparatus at very high cooling rates (up to 2000 °C/s. The samples were characterised by powder wide angle X-ray diffraction (WAXD) and density measurements. The results stated that there was one certain cooling rate for each polymer, after which there was a dramatic decrease in crystallinity. These rates were 100 °C/s for iPP, 10 °C/s for PA6 and 2 °C/s for PET. (Brucato et al. 2002.) Higher take-up speed on the other hand results in increased stress along the spinline and increases both filament orientation and crystallinity, as can be seen in Table 3.1. (Cicero et al. 2002; Gupta et al. 2007.)

Solarski et al. and Twarowska-Schmidt melt span PLA with heated draw rolls and inspected the influence of the draw roll temperature and draw ratio (the ratio of the velocities of the first and last draw roll) on fibre crystallinity. The materials they used were 96/4 PLDLA and 98.6/1.4 PLDLA, respectively. Solarski et al. noticed that low temperatures of the draw roll (80 °C) did not induce high crystallisation even with high DR:s (9-21 % with draw ratios 2-3.5), but Twarowska-Schmidt fabricated fibre with a maximum of 50.8 % of crystallinity with the same draw roll temperature and only a slightly higher draw ratio (4). The difference might yield from the higher amount of L-lactide in the material that Twarowska-Schmidt used. Solarski et al. noted that the max-

imum crystallinity (38.3 %) was formed by increasing the temperature of the draw roll to 110 °C with a draw ratio of 3.5. Twarowska-Schmidt obtained fibre with a much higher maximum crystallinity (52.1 %) with a lower draw roll temperature (90 °C) and a draw ratio of 3.39. It was concluded that the drawing caused the polymer chains to orientate, but the thermal treatment was needed for higher levels of crystallinity. (Solarski et al. 2007; Twarowska-Schmidt 2012.)

Mechanical properties of the fibre

As previously mentioned, mechanical properties (tensile strength, Young's modulus) reflect the changes in orientation of polymer chains, crystallinity and glass transition temperature, so these factors cannot be observed fully separately (Penning et al. 1993; Fambri et al. 1997). In general, higher crystallinity and orientation (higher draw ratios) result in better mechanical properties, but sufficient elongation is needed to prevent brittle behaviour. However, it should be kept in mind that drawing enhances the fibres' mechanical properties only in the direction of the fibre axis and perpendicular to the axis the properties are remarkably poorer. (Grijpma et al. 2002.)

Cicero and Dorgan examined the effects of draw ratio (DR) on mechanical properties of monofilament fibres. The material used was staple-fibre-grade 98:2 PLDLA. Their equipment consisted of two heating godets and a radiant heating zone between them. Above DR = 3 the polymer chains started to orientate partially and exhibit some strength and modulus. Drawing the fibres more resulted in better tensile strength and modulus values. In general there is a trade-off between higher modulus/lower extensibility and lower modulus/greater extensibility. This is related to the extent of orientation in the amorphous phase and has to be taken into account in processing. (Fourné 1999; Cicero & Dorgan 2001; Schmack et al. 2003.)

In the same study, Cicero and Dorgan also inspected the effect of the heater levels (50, 75 and 100 %, reflecting air temperatures of 98, 135 and 175 °C) on the tensile strength and modulus of the fibre. With DR = 5 the highest modulus (2.8 GPa) was achieved with 50 % heater level. Higher heater levels provided too much heat to increase the modulus, probably due to insufficient molecular orientation coupled with low crystallinity. Increasing the DR and the heater level to maximum (5 and 100 %) provided enough thermal and mechanical stress on the fibre resulting in maximum modulus (3.1 GPa). As conclusion; in general higher draw ratios coupled with higher heating results in better mechanical properties, but with lower heater levels the DR has to be sufficient to induce enough orientation. (Cicero & Dorgan 2001.)

Solarski et al. investigated the influence of the drawing temperature on Young's modulus of the fibres. The results were parallel with the crystallinity results. The maximum values (4.5, 5.9 and 6.66 GPa) were achieved with the highest temperatures (100-110 °C) regardless of the draw ratio, although higher draw ratios resulted in higher Young's moduli. At 120 °C the modulus decreased probably due to thermal degradation of the polymer. (Solarski et al. 2007.) Fourné et al. encountered a new phenomenon called filament flow while studying very high drawing temperatures. They observed that

with drawing temperatures significantly higher than T_g the diameter of the fibre decreased without an increase in strength. This phenomenon can be beneficial in manufacturing superfine fibres because the fibres can be first drawn to the desired diameter and improving the mechanical properties can be done later. (Fourné 1999.)

Thermal properties of the fibre

Thermal properties of the fibre (for example the glass transition temperature and the profile of the melting peak) also depend on the processing conditions and are closely coupled with crystallinity and mechanical properties. For example the glass transition temperature increases with increasing draw ratio and temperature of the draw rolls due to increased crystallisation. In glass transition temperature the polymer chains move segmentally in cooperation in the amorphous regions passing the polymer from a glassy state to a rubbery state. In semicrystalline polymers the movements in the amorphous regions are restricted by the crystallites. Higher crystallinity anchors the amorphous region more efficiently and therefore more thermal energy is required for the transition. (Cicero et al. 2002; Solarski et al. 2007.)

In a later study Solarski et al. investigated the thermal properties of the fibres and found that the temperature of the draw roll has an effect on the kind of crystallites developed during processing. The melting peak had a shoulder or a second peak at draw ratio of 2 at all draw roll temperatures (80-120 °C) but they were more distinct on higher temperatures. This shoulder or a second peak has been connected to unfinished crystals developed during the thermal characterisation. The research group did not find a link between the DR and the profile of the melting peak. (Solarski et al. 2007.)

3.1.2 Melt spinning of polylactide

Melt spinning of polylactide can be done with conventional melt spinning processes using standard equipment in a similar way with typical synthetic polymers, such as PP and PET (Perepelkin 2002). PLA fibres are also used in similar applications as most other synthetic fibres: as fabrics, knits and nonwovens in industry, agriculture and medicine. Nowadays the medical applications of polylactide fibres can be besides conventional sutures, also bone fixation devices, pharmaceuticals and tissue engineering scaffolds. (Perepelkin 2002; Gupta et al. 2007.) Many properties of PLA fibres, for example mechanical properties, are very similar to other thermoplastic fibres. The property that makes PLA fibre unique is that it is the only melt-processable fibre made from raw materials derived from annually renewable sources. (Blackburn 2005.)

Melt spinning was one of the first methods used for making PLA fibres and therefore it has been extensively studied using different processing conditions. Typically PLA fibres are spun in temperatures between 185-240 °C from materials with L/D ratios of 2-10. PLA with more D-isomer content can be processed at lower temperatures, but usually PLA with higher L-lactide content is used in fibre applications to achieve higher level of crystallinity and thermal resistance. (Lim et al. 2008; Ren 2010; Auras et al. 2010.) PLA with different melt flow indexes (MFI) are offered for different kinds of

fibrous products. For monofilament fibre production PLA with a MFI of 5 – 15 g/10 min is available, whereas for staple and continuous fibres the MFI available is 15-30 g/ 10 min and for spunbond nonwoven materials MFI = 70 – 85 g/10 min (Twarowska-Schmidt 2012). PLA can be drawn at a number of draw ratios but the usually employed range is 3:1-4:1. The optimal draw ratio depends on the type of the polymer, the orientation of the as-spun fibre and the desired tensile properties of the product. (Auras et al. 2010.)

Comprehensive data on PLA melt spinning is presented in Appendix 1. The D-lactide content in the polymers used varies between 0 and 15 per cent. As previously stated, stereoregularity of the polymer affects the crystallinity and mechanical properties of the fibre. This is why fibres made from different L/D –ratio copolymers can exhibit only a certain maximum crystallinity depending on their stereochemical properties. (Cicero et al. 2002b.) For example Cicero et al. and Solarski et al. used 96/04 PLDLA and reached maximum crystallinities of 35 and 38 % respectively while Cicero & Dorgan and Cicero et al. have fabricated fibre with maximum of 51 % crystallinity from 98/02 PLDLA (Cicero & Dorgan 2001; Cicero et al. 2002a; Cicero et al. 2002b; Solarski et al. 2007). Yuan et al. manufactured fibres from PLLA with 64 % of maximum crystallinity (Yuan et al. 2001).

Our group has mainly melt spun GMP grade PLDLA 96/4 into four-filament fibres and studied the thermal degradation of the raw material during processing and the hydrolytic degradation of the fibres after gamma irradiation (Ellä et al. 2007; Paakinaho et al. 2009; Ellä et al. 2011a; Ellä et al. 2011b; Paakinaho et al. 2011). The hydrolytic degradation of the fibres has been studied in short-term (Ellä et al. 2007; Ellä et al. 2011a) and long-term (Ellä et al. 2011b) hydrolysis series. It was found that the monomer content in the fibre generated in processing has a significant impact on the hydrolytic degradation rate of the fibre. The fibre with 1.24 % monomer lost 65 % of its strength in 9 weeks compared to 3 % loss of a fibre containing 0.17 % monomer. (Ellä et al. 2011a.) In long-term hydrolysis a fibre with low monomer content lost 65 % of its strength during 42 weeks (Ellä et al. 2011b). Also the effect of molecular weight of the raw material on the thermal degradation of the polymer has been studied. The high-molecular-weight polymers were found to degrade more in processing compared to low-molecular-weight PLA. (Paakinaho et al. 2009.)

As previously mentioned, increasing draw ratio promotes orientation and gives better mechanical properties (tensile strength and Young's modulus) for the fibre. According to Appendix 1 PLA fibre has been drawn with draw ratios of 1-20.5 producing fibres with rather good mechanical properties. The tensile strengths were in the range of 0.007-0.87 GPa the average being 0.44 GPa. The lowest values were as-spun fibre with draw ratio of 1 and PLLA drawn with a draw ratio of approx. 6 had the highest strength. The highest draw ratio (20.5) resulted in fibre with a tensile strength of 0.87 GPa. Also the drawn filament diameter has been listed in the Appendix 1. The research groups fabricated PLA fibres with filament diameters in the range of 25-500 μm. Conclusions about the effect of only the draw ratio on the filament diameter cannot exactly be drawn

as the size of the spinneret holes affects directly the diameter of the filaments, but in general with same size spinneret holes increasing the draw ratio decreases the filament diameter.

The most common problems in PLA melt spinning according to the studies collected in Appendix 1 seem to have been high degree (up to 83 % decrease in molecular weight) of thermal degradation and low collection rates (0.25-20 m/min) (Eling et al. 1982; Penning et al. 1993; Fambri et al. 1997). Solutions for these problems are discussed in the subsequent sections.

3.2 High speed melt spinning

High speed melt spinning is more attractive than conventional melt spinning because it is economically and commercially more efficient. Processes with spinning velocities exceeding 2000 m/min are considered as high speed spinning. High speed melt spinning can also be used to produce an unoriented or partially oriented pre-form of the fibre and then afterwards finalise the orientation in a hot postdrawing step. (Mezghani & Spruiell 1998; Auras et al. 2010.)

There are new variables that have to be taken into account in high speed spinning. When the spinning speed is increased, in addition to conventional factors the effects of air drag and inertial forces on the total stress in the spinline have to be considered. (Mezghani & Spruiell 1998; Auras et al. 2010.) The increasing stress in the spinline causes a new type of phenomenon called stress-induced crystallisation. Stress-induced crystallisation is most effective in processes where orientation is possible and the stress is applied in temperatures approximately 10 °C over the glass transition temperature followed by a heat-setting period (Lunt 1998). The amount of crystallinity acquired by orientation depends on the stereochemical purity of the polymer, mode of stretching (is it sequential or simultaneous), strain rate, draw ratio, temperature and annealing conditions. (Lim et al. 2008.)

Strain-induced crystallisation makes the orientated and partly crystallised polymer chains turn into a rubber-like structure. The material also starts to show stress-hardening behaviour which locks the structure and inhibits further changes. When the polymer is highly strained, its apparent elongational viscosity first decreases due to thinning and then rises sharply after the strain hardening phenomenon takes place. At higher spinning velocities all of these changes happen to a greater extent and faster. The apparent viscosity does not change in this way at lower velocities. Higher spinning velocities, lower throughput and lower extrusion temperatures result in higher necking and more orientation and crystallinity. As the spinning speed rises, the neck moves closer to the spinneret and the fibre spends less time in the necking region. For example when the spinning speed is 5500-6500 m/min, the necking length is 8-10 cm and at these velocities the fibre spends only about 5 ms in the necking region. (Takasaki et al. 2003; Auras et al. 2010.) Takasaki et al. studied the steepness of the necking region in high speed spinning

of racemic PLA. Their main results were that lower throughput and lower spinning temperatures resulted in steeper neck-like deformation. (Takasaki et al. 2003.)

High speed melt spinning of polylactide

High speed melt spinning has been introduced to increase the take-up rates of PLA fibre to meet industrial demands. While there were numerous studies on melt spinning PLA at low velocities, only a few research groups have melt spun PLA fibre on high velocities. Data on high speed melt spinning of PLA is presented in Table 3.2. It can be seen from the table that PLA can be melt spun at take-up velocities up to 10 000 m/min and a draw ratio up to six. The high speed melt spun fibres exhibit good mechanical properties with maximum tensile strength of 0.55 GPa and Young's modulus of 7. PLA fibre as fine as 12 μm in filament diameter and up to 47 % of crystallinity has been drawn.

Table 3.2. *Previous studies on high speed melt spinning of polylactide.*

Reference	Material	Initial Mw (kDa)	Filament count / drawn filament diameter (μm)	Take-up speed (km/min) / draw ratio	Thermal degradation (%)	Drawn fibre crystallinity (%)	Tensile strength / Young's modulus (GPa)
(Mezghani & Spruiell 1998)	P(L/meso)LA 92/8	212	4-fil / 12–73	0,1 - 5 / ?	23	47	0.38 / 3.6-6
(Schmack et al. 1999)	P(L/meso)LA 92/8	164	12-fil / ?	1-5 / 4-6	31	0-24	0.198-0.46 / 3.1-6.3
(Schmack et al. 2001a)	P(L/meso)LA 92/8	207	12-fil / ?	0.2-5 / 4-6	13	0-23.9	0.198-0.46 / 3.1-6.3
(Schmack et al. 2003)	PLDLA, D-content 1, 3, 5, 8	205, 305, 365, 405, 410	12-fil / ?	2-5 / ?	?	0-40	? / 3.5-7
(Takasaki et al. 2003a)	PLDLA 98.5/1.5, 91.9/8.1, 83.6/16.4	?	Monofil. / 20-70	1-10 / ?	?	0-47	0.1-0.55/ 2-6
Takasaki et al. 2003b	PLDLA 98.5/1.5 and a 50/50 blend of PLLA and PDLA (r-PLA)	?	Monofil. / r-PLA 25-80, PLLA 25-70	1-10 / ?	?	5-38	0.1-0.580 / 2-6

When comparing to the data on low-speed melt spun PLA in Appendix 1, the most notable difference is the low degree of thermal degradation. In high speed melt spinning

of PLA the highest degree of thermal degradation is only 31 % whereas in conventional melt spinning the corresponding value is 83 %. As the thermal degradation mostly occurs in the extruder and the drawing process does not affect the degree of thermal degradation occurred in the extruder, the difference seems to yield mainly from material properties and/or increased throughput required by high speed spinning. All the data on the thermal degradation in Table 3.2. is of P(L/meso)LA to which there is no corresponding data on Appendix 1. The lower molecular weights of the raw materials in Table 3.2. (164-410 kDa) than in Appendix 1 (19-600 kDa) can partly explain the low degree of degradation. With an increased throughput the time the polymer spends in the extruder (residence time) is shorter. This gives the polymer less time to degrade in the extruder and reduces the overall thermal degradation. Increased screw speed can also affect similarly. (Ellä et al. 2011a)

The highest take-up speed or draw ratio often did not lead to the best mechanical properties. Mezghani et al. produced PLLA fibre with take-up speeds ranging from 100-5000 m/min. They found that the maximum orientation corresponding to tensile strength and modulus of 385 MPa and 6 GPa, respectively, was achieved at take-up velocities of 2000-3000 m/min. (Mezghani & Spruiell 1998.) Schmack et al. melt span P(L/meso)LA 92/8 fibres with draw ratios up to 6. They observed the orientation maximum at a slightly higher take-up speed of 3500 m/min. (Schmack et al. 2001b.)

The degree of crystallisation depends on the spinning speed also in high speed spinning. Mezghani et al. noticed that the onset speed for stress-induced crystallisation was 2100 m/min. Above 3000 m/min the crystallinity decreased because the cooling increased more than the crystallinity kinetics could compensate. At these velocities it is likely that the diameter of the fibres starts to fluctuate more. (Mezghani & Spruiell 1998.) Interestingly, Schmack et al. did not notice stress-induced crystallisation below 3500 m/min, although the material the two groups used was very similar (Schmack et al. 2001b).

4 THERMAL DEGRADATION OF POLYMERS

Polymers are exposed to rough conditions during processing. High-molecular-weight materials require elevated temperatures and high pressures to make them flow through small orifices in melt processing. These circumstances also make thermal degradation a common problem in polymer processing, for example in injection moulding or extrusion. The degradation products can be considered as impurities which reduce the melt viscosity and elasticity of the polymer resulting in a final product with poorer mechanical properties and quality. (Lim et al. 2008; Rajan et al. 2010.) When medical devices are in question, higher quality and predictable properties and degradation behaviour of the processed material are even more important. Especially the hydrolytic degradation rate in the physical environment has to be predictable. Thermal degradation is known to accelerate the hydrolytic degradation of biodegradable polymers because the degradation products act as catalysts for the hydrolysis reaction. Minimising thermal degradation is an important issue because the magnitude of the catalysis effect is hard to predict and it often also excessively accelerates the hydrolytic degradation rate resulting in quicker degradation than planned. (Paakinaho et al. 2009; Ellä et al. 2011a.)

During processing the polymer chains are cut due to high temperatures, mechanical forces or chemical degradation. Mechanical degradation refers to scission of polymer chains caused by mechanical stress; shear stress, elongational stress or combination of the two. Mechanical degradation basically never occurs alone, but is combined with thermal degradation because of the high temperature of the melt. The shear forces can also cause the temperature to rise uncontrollably locally, especially in the areas where the polymer deforms with a non-uniform rate. Chemical degradation occurs as a result of chemicals reacting with the polymer. These chemicals can be for example acids, bases, solvents or reactive gases. (Rajan et al. 2010.)

Often it is hard to distinguish which type of degradation causes for example the molecular weight loss. However, the effects of a certain factor can be in some cases minimised. For example drying the raw material thoroughly and preventing moisture getting into contact with the polymer during processing minimises the hydrolytic degradation of polymers with hydrosensitive bonds. (Middleton & Tipton 2000.) Drying can be done as vacuum drying or by using a resorption circulating air dryer. Because of the heat sensitivity of the polymers, the drying temperature has to be chosen carefully. For example, if amorphous polymers are dried in temperatures over their glass transition temperature, the granules may fuse together. As a consequence most amorphous polymers should not be dried in temperatures above room temperature. There are some additional techniques to prevent the moisture entering the fabrication process. It is

recommended to pack the material in small quantities so that the material is used up quickly after opening the package to avoid absorption of the moisture over time. Running nitrogen or dried air atmosphere in the hopper or material inlet also prevents moisture entering the system. (Middleton & Tipton 2000.) This work focuses on thermal degradation of polylactide and on the effects of the processing conditions on the degree of degradation induced by elevated temperatures.

4.1 Thermal degradation of polylactide

Thermal degradation of PLA seems to be a very complex process which involves various different non-radical and radical mechanisms. These can include 1) inter- and intramolecular transesterifications, 2) pyrolytic elimination, 3) oxidative degradation, 4) hydrolysis, 5) radical reactions and 6) zipper-like depolymerisation. (Jamshidi et al. 1988; Kopinke et al. 1996; Södergård & Stolt 2002; Carrasco et al. 2010.) Non-radical reactions of PLA are presented in Figure 4.1. including intramolecular transesterification (NR1), its corresponding inverse reaction (NR2), a reaction with the same principle resulting in acetaldehyde and carbon monoxide (NR3) and a cyclic transition (NR4). McNeill and Leiper as well as Jamshidi et al. proposed that PLA degrades mainly by a nonradical backbiting ester interchange reaction which involves the hydroxyl end groups. This reaction is presented in Figure 4.1. as NR1, with R=H. They studied the effect of blocking –OH end groups by acetylation, which was showed to reduce thermal degradation of PLA. (McNeill & Leiper 1985, cited in Kopinke et al. 1996; Jamshidi et al. 1988.) Kopinke et al. proposed that in temperatures above 200 °C, PLA degrades mainly by intramolecular transesterification, *cis*-elimination which results in acrylic acid acrylic oligomers and fragmentation releasing acetaldehyde and CO_2. (Kopinke et al. 1996.)

1) Inter- and intramolecular transesterifications are typical for condensation polymers in temperatures near their melting points. In the case of polylactide, it has been concluded that the degradation is mostly caused by intramolecular transesterification. The reaction is referred as NR1 in Figure 4.1. and it leads to longer chains to be cut into lactic acid (n = 0), lactide (n ≥ 1) or cyclic oligomers of lactic acid and lactide. As intramolecular transesterification involves only one molecule, intermolecular transesterification occurs between two ester molecules exchanging their radicals. Both of these reactions have been shown to have their reverse reactions happening at the same time. Simultaneously as lactic acid and lactide are formed, they are recombining into the linear polyesters through insertion reactions. Inter- and intramolecular transesterifications are most rapid in the melt, but they do also happen below the melting temperatures. (Jamshidi et al. 1988; Wachsen et al. 1997; Södergård & Stolt 2002; Nicolae et al. 2008; Carrasco et al. 2010.) Thermal decomposing can also be referred to as pyrolysis. ***2) Pyrolytic elimination*** on the other hand is a reaction leading to formation of molecules with acrylic end groups, but it is considered as a less important side reaction. (Wachsen et al. 1997; Nicolae et al. 2008; Carrasco et al. 2010.)

3) Oxidative degradation leading to random chain scission occurs if PLA is processed in air atmosphere. The already minor effect of oxidative degradation is usually minimised by processing PLA under atmospheres with other gases, usually inert nitrogen. (Nicolae et al. 2008; Rasselet et al. 2014.) On the other hand oxygen can have a slightly stabilizing effect on PLLA during the first minutes of melt processing. This happens only if there are traces of catalytic tin, because the oxygen deactivates the remaining catalyst and therefore prevents depolymerisation caused by it. Catalytic tin is used in tin(II) 2-ethylhexanoate catalyzed ROP. (Södergård & Stolt 2002.)

4) Thermohydrolysis is moisture-induced degradation in elevated temperatures and it happens as a competitive reaction when there is moisture in the melt. The mechanism is bulk hydrolysis including the autocatalytic degradation phenomenon likewise as in ambient and body temperatures. Thermohydrolysis differs from conventional hydrolysis in crystalline residue formation. In temperatures above 170 °C hydrolytic degradation does not leave crystalline residue regions of PLLA because the melting temperature became lower than the degradation temperature, in other words the polymer melt before it could form crystalline residues. (Tsuji et al. 2008.) The autocatalytic degradation phenomenon is also present in the melt. The degree or moisture absorbance depends on the crystallinity of the polymer. Semicrystalline PLLA absorbs water only some per cents of its weight whereas amorphous PLDLA is more permissive to water. (Södergård & Stolt 2002; Nicolae et al. 2008.) The efficacy of drying the polymer before processing to reduce moisture-induced degradation is further discussed in the following section.

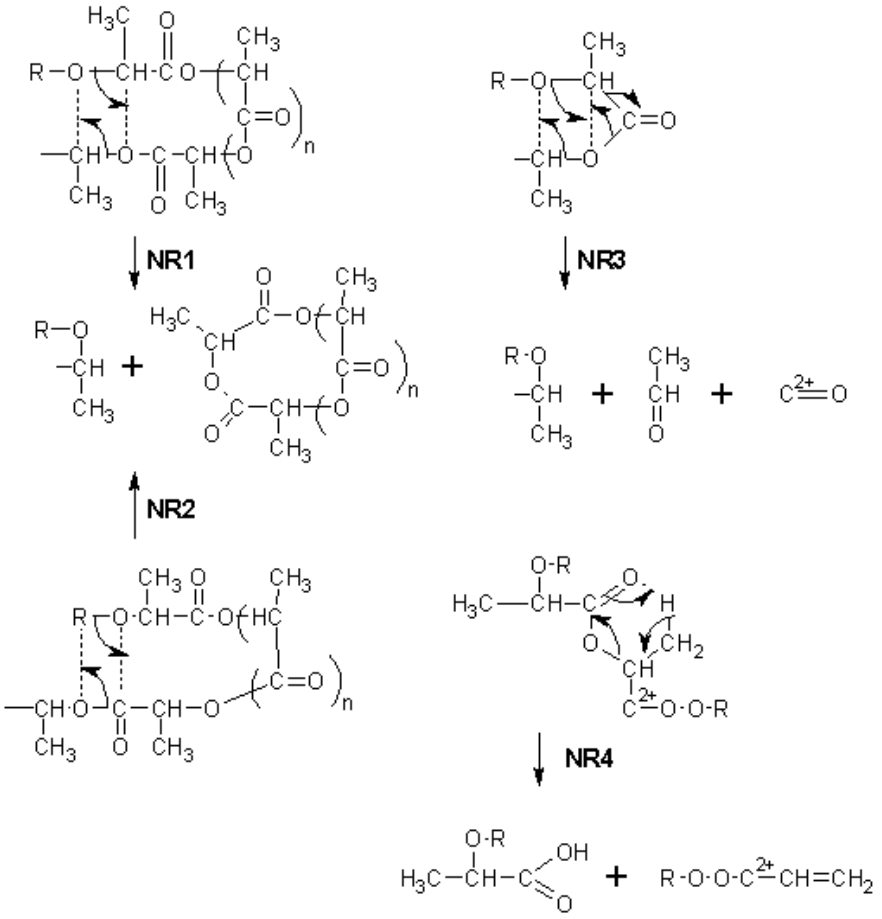

Figure 4.1. *Non-radical mechanisms of thermal degradation of polylactide. Modified from (Kopinke et al. 1996).*

5) Radical reactions have to be taken into account only when the processing temperatures rise above 250 °C (Kopinke et al. 1996; Wachsen et al. 1997; Carrasco et al. 2010). The radical degradation reactions of PLA can start either with an acyl-oxygen or alkyl-oxygen homolysis depending on which C-O bond in the polymer backbone is cut by the heat. The resulting acyl-, oxy-, carbonyl- and carbon macroradicals can decompose further by splitting off smaller fragments such as CO, CO_2, acetaldehyde and methyl ketene. Some of the decomposing products, for example the carbon-radical can cyclise into lactide by an addition-elimination mechanism, whereas the acyl- and carboxyl radicals are mainly expected to decompose. CO_2 on the other hand can be used as a marker of radical reactions as it will not decompose. (Kopinke et al. 1996.) If PLA is exposed to temperatures above 325-375 °C it completely thermally decomposes. The exact decomposing temperature depends on the materials processing history. (Carrasco et al. 2010.)

Many factors, including time, temperature, moisture, molecular weight, atmosphere, residual metal catalysts and other impurities have an effect on thermal degradation of polylactide. (Aoyagi et al. 2002; Garlotta 2002; Meng et al. 2012.) ***6) Catalysts and/or traces of them*** have been found to drastically decrease the degradation tempera-

ture, accelerate the degradation and cause zipper-like depolymerisation. They can also cause viscosity and rheological changes, fuming during processing and poor mechanical properties in the final product. (Cam & Marucci 1997; Garlotta 2002; Aoyagi et al. 2002 Södergård & Stolt 2002.) Cam et al. studied the effect of different metal catalysts on the decomposition temperature of PLLA. They found out that even low amounts (1-2 wt-%) of tin, zinc, aluminium and iron decrease the thermal decomposition temperature by 50, 60, 70 and 110 degrees, respectively. (Cam & Marucci 1997.) The factors with low molecular weight, for example moisture and monomers and oligomers produced by hydrolysis, can be removed by preheating. However, the possible degradation of the polymer during preheating also has to be taken into account. (Cam & Marucci 1997; Aoyagi et al. 2002.) Cam et al. pre-treated PLLA in nitrogen atmosphere at 150 C for 60 minutes which was sufficient for removing the low molecular weight compounds but did not affect the thermal stability of the material. (Cam & Marucci 1997.)

Thermal degradation of PLA, especially the catalyst and impurities-induced degradation, can be minimised with purifying, compounding or chemically treating the polymer. GMP grade polymers are treated with high level purification, but commercial grade polymers can also be chemically treated or compounded to a composite. (Södergård & Näsman 1996; Wachsen et al. 1997.) There have also been studies promoting the importance of purifying the polymer. Fan et al. stated that removing the residual catalyst tin by carefully purifying the polymer is more efficient in bringing up the degradation temperature than treating the polymer chemically with blocking the hydroxyl end groups (Fan et al. 2004).

There are ways to improve the thermal resistance which can be used also for GMP grade PLA. Perhaps the most used way is to use PLDLA instead of the homopolymers PLLA and PDLA. For example Tsuji and Fukui successfully enhanced the thermal stability of pure PLLA and PDLA films by making 50/50 PLDLA film. The activation energy for thermal degradation of the PLDLA film was 82-110 kJ/mol higher compared with pure L-lactide or D-lactide polymer films. (Tsuji et al. 2012.) The degree of thermal degradation can also be reduced by choosing a polymer with slightly lower molecular weight. It has been concluded that polymers with higher molecular weight degrade more, because the longer the chains are the more they can be cut. (Paakinaho et al. 2009.)

4.2 Effects of processing conditions

PLA can be processed into a variety of products (for example rods, fibres and moulded parts) for example by extrusion and injection moulding (Middleton & Tipton 2000). However, the processing window of PLA is very narrow, because the polymer is very sensitive to heat and has been noticed to undergo extreme thermal degradation in melt processing. (Penning et al. 1993; Södergård & Stolt 2002; Ellä et al. 2011a.) Degradation of PLA during processing can occur due to thermal or mechanical stress, contact with oxygen and also by hydrolysis. Careful selection of the processing parameters is

crucial in order to minimise the degradation. The most important parameters in melt extrusion are processing temperature, residence time, shear force, moisture content and atmosphere. (Södergård & Stolt 2002; Ellä et al. 2011a.)

Processing temperature and residence time

PLA is usually processed in temperatures between 200 and 250 °C depending on its molecular weight (Shalaby & Johnson 1994). It has been concluded that higher processing temperatures and longer residence times degrade polylactide more. The higher the temperature is, the more the polymer chains are cut producing monomers and dimers that further accelerate the degradation. Higher temperatures also provide more energy for the reactions and the movements of the molecules. In general high-viscosity PLA require higher temperatures which results in more degradation whereas lower temperatures suffice for melting PLA with a lower viscosity. (von Oepen & Michaeli 1992; Taubner & Shishoo 2001; Wang et al. 2008; Ellä et al. 2011a.)

Screw speed and residence time

Ellä et al. investigated the effects of processing parameters on thermal degradation of 96:4 PLDLA in melt spinning. The monomer content in the polymer was used as an indicator of the degree of thermal degradation. (Ellä et al. 2011a.) Wang et al. studied thermal degradation of poly-L-lactide during extrusion. They identified thermal degradation of PLLA as discolouring and monitored it on-line with an ultraviolet-visible light (UV-vis) spectrometer. The results were confirmed with an off-line molar mass measurement. (Wang et al. 2008.) The combined effect of increased residence time and higher shear stress clearly degraded the polymer more but the effect of one factor was difficult to distinguish. When the screw speed was higher, it introduced more shear stress on the polymer but the residence time decreased. At lower screw speeds the shear stress was lower but residence time longer. In general increasing the screw speed resulted in decreased degradation despite the increase of the shear stress. The residence time was found to have a greater effect on the degradation and thus the effects of shear stress did not show clearly. However, the effect of residence time was less pronounced at low processing temperatures and the effects of shear stress more pronounced at elevated temperatures. (von Oepen & Michaeli 1992; Wang et al. 2008; Ellä et al. 2011a.)

Moisture content

Since PLA is a polymer susceptible for hydrolytic degradation, the polymer has to be carefully dried before processing to minimize moisture-induced degradation during processing (Södergård & Stolt 2002; Nicolae et al. 2008; Signori et al. 2009; Ren 2010; Ellä et al. 2011a). For example Taubner and Shishoo noticed higher amount of thermal degradation when processing PLLA with 0.3 wt- % moisture content compared to dry material (Taubner & Shishoo 2001).

Interestingly, there are also studies stating that they found no difference in the degree of thermal degradation between dried and undried material (Jamshidi et al. 1988;

Södergård & Näsman 1994). Natureworks LLC, a supplier of commercial grade PLA, recommends that PLA resins should be dried below 50 ppm (0.005 wt- %) moisture content before extrusion. However, the material should be dried as well as possible to minimise hydrolytic degradation during processing. (PLA Meltblown Process Guide 2005.)

PLA is normally dried in the temperature range of 80-100 °C. The time required for drying is dependent on the temperature. For example for semicrystalline pellets in 100 °C the drying half time of 0.6 hours is sufficient whereas in 40 °C the required half time is 4.3 hours. Amorphous pellets should not be dried over the T_g (60 °C), because otherwise the pellets may stick together bridging and blocking the feeder. Semicrystalline polymers can be dried at higher temperatures. (Lim et al. 2008.) In choosing the drying temperature and duration, more efficient drying is achieved with higher temperatures rather than long drying times. It has also been noted that drying under 0.02 % causes the polymer to excessively absorb moisture. (von Oepen & Michaeli 1992.) Dried PLA resin absorbs critical levels of moisture in 10 minutes when exposed to air and therefore the contact with air has to be minimised after drying (PLA Meltblown Process Guide 2005).

The effect of moisture on degradation of PLA seems to depend on the processing temperature. At temperatures below 230 °C the degradation by moisture is more pronounced than at higher temperatures, because the degradation by heat becomes dominant in temperatures over 230 °C. Also the vaporisation of moisture in high temperatures has its role. (von Oepen & Michaeli 1992.)

Processing atmosphere

As previously stated, oxygen can also cause degradation of polylactide. It has been noted that processing PLA in inert atmospheres, usually nitrogen, decreases thermal degradation. (Liu et al. 2006; Signori et al. 2009; Ellä et al. 2011a; Rasselet et al. 2014.) Interestingly, Signori et al. found that using nitrogen atmosphere in processing of PLA had a greater effect in minimising degradation than careful drying (Signori et al. 2009).

5 REAL-TIME MONITORING OF MELT EXTRUSION

Melt extrusion is one of the most widely used processing technologies in the plastic, food and rubber industry. It is defined as a process where raw material is melted and mixed with a rotating screw and pumped through a die under controlled conditions resulting in a product with a fixed cross section. (Crowley & Zhang 2007.)

Monitoring the extrusion parameters and the quality of the product is crucial for successful production. Many parameters are measured outside the production environment in laboratory with separate analysing equipment causing a time lag and extra effort. This can also generate a great amount of scrap because the time between collecting the sample and adjusting the processing conditions might be long. (Mould et al. 2011.) Real-time monitoring systems have been developed to overcome these problems. Measuring in real time allows continuous flow of information of the production process without sampling and separate analysing equipment. The measurement techniques applicable to polymer melts include rheometric, optical, ultrasonic, electrical and spectroscopic methods. Real-time measurements can be used to measure flow properties, polymer structure, morphology and composition, additive concentration, dimensions, appearance and colour of the polymer and also the consistency of the production. (Coates et al. 2003; Wang et al. 2008.)

The process analytical techniques can be divided to off-line, at-line, on-line and in-line measurements. Conventional ***off-line*** measuring means taking the samples from the process stream and transporting them to a separate analysing equipment (Saerens et al. 2014). The ***at-line*** method consists of a dedicated measuring instrument installed in close proximity to the process line. In ***on-line*** measurements a small sampling stream is isolated from the process flow line, transported to the analyser and in some cases returned to the process stream. On-line measurements can be divided into two subgroups; intermittent methods where a portion of the sample stream is injected into the analysing instrument and continuous methods where the sample flows continuously through the analyser. (Callis et al. 1987; Coates et al. 2003.)

The advantages of on-line applications include easier calibration, cleaning and maintaining, simpler adaptation to different equipment and good temperature control. Nevertheless it has to be confirmed that these devices minimise the time lag between sample collection and measurement and that the morphology changes in the material are minimised during sampling and measuring. These systems can also conduct measurements along the axis of the extruder. Normally the morphology or chemical reaction of a certain polymer system will have achieved steady-state or been completed well before

the die, which rises a need for measuring in multiple points along the extruder barrel. (Mould et al. 2011.)

In-line analysis means conducting the measurements directly in the process flow line, which enables quick sampling and measuring. The sensors used in-line can be divided to invasive or non-invasive ones depending on whether they are in contact with the sample flow or not. (Alig et al. 2010; Saerens et al. 2014.) There are classical, spectroscopic, scattering and imaging in-line methods, as can been seen in Figure 5.1. The classical methods acquire information on the process state (pressure, temperature) and material properties (viscosity, conductivity), the spectroscopic methods (e.g. infrared, Raman) measure for example the composition of the polymer melt (e.g. molecular weight, filler content/distribution) and scattering and imaging methods (e.g. X-ray scattering, optical microscopy) are used mainly for monitoring morphology and structure of the material.

There have been in-line sensors for conventional parameters such as barrel and die temperature and melt pressure for a long time, but these parameters give only a weak estimation of the flow and heat transition conditions. As the demands for quality and monitoring rise, new in-line sensors are needed for monitoring other parameters. (Alig et al. 2010; Mould et al. 2011 Saerens et al. 2014.) Although these kind of measuring systems are relatively new, there have been many studies of their use, some of which have been gathered in Appendix 2. The table gives a good overview of process analytic techniques used in polymer extrusion as well as their limitations.

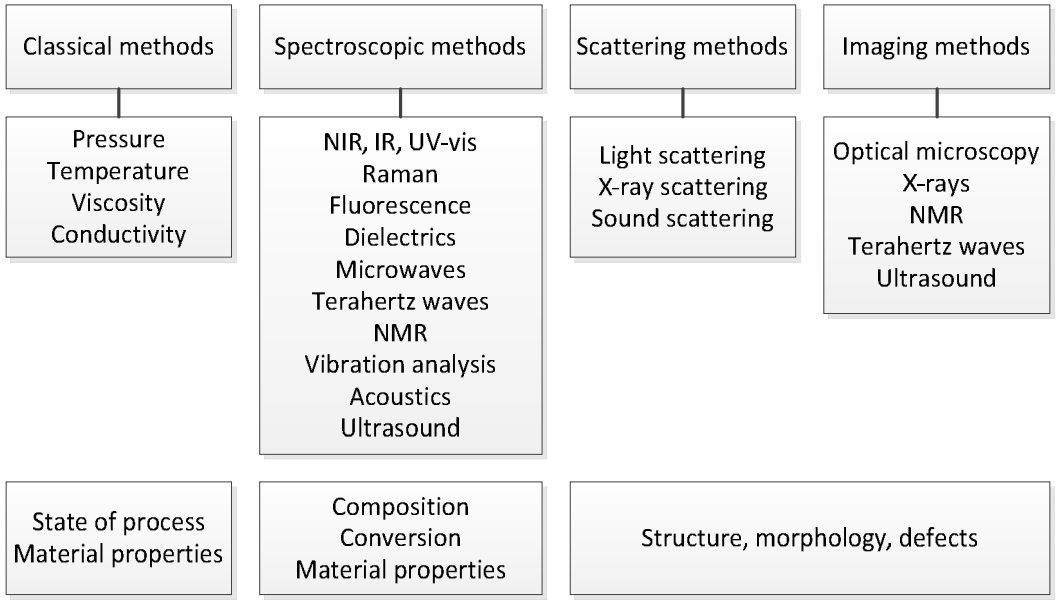

Figure 5.1. *In-line methods for real-time monitoring of polymer processing. Modified from (Alig et al. 2010).*

In this work the emphasis is on on-line and in-line methods for monitoring the thermal degradation during polymer extrusion and on particle size and distribution monitoring in composites. Our collaborator FOS Messtechnik GmbH is a German enterprise

developing and manufacturing fibre optical sensors and sensor-related technologies. Its main products include fibre optical pressure sensors, fibre optics, IR-temperature sensors and optical probes for general purposes and spectral analysis. (Innovative Sensors 2008) In this section we also evaluate the suitability of the sensors manufactured by FOS for the applications mentioned.

5.1 Traditional parameters

Traditionally barrel and die temperatures, feed rate or throughput, torque and drive amperage, melt temperature, melt pressure, screw speed and in some cases melt viscosity have been monitored in-line. There have been real-time sensors for these parameters for a long time and they have developed to be quicker, more robust and more accurate. (Saerens et al. 2014.) In this work we concentrate on melt temperature and melt pressure because of their importance and the great advances in the measuring techniques. Measuring melt viscosity is discussed in the next section.

5.1.1 Melt temperature

Melt temperature is one of the most important variables in polymer extrusion as it directly influences the polymer viscosity, density and degradation kinetics as well as product quality. As previously mentioned, usually during extrusion the temperature of the melt is not uniform throughout the melt; there can be temperature peaks caused by the shear forces generated by the rotating screw. These temperature peaks make accurate melt temperature measuring challenging. Conventionally temperature has been measured with a thermocouple which is flush mounted at the extruder die wall. It has been shown that these sensors are actually measuring the temperature of the metal wall and not the melt. There is a need for sensors capable of detecting fast temperature changes in complex applications with extra heat sources, e. g. shear forces in extrusion. The detection of the temperature peaks is especially important when the processed polymer is sensitive to heat as higher temperatures will induce excessive degradation. (Shen et al. 1992, see Vera-Sorroche et al. 2013; Bur et al. 2004; Innovative Sensors 2008; Rajan et al. 2010.)

Measuring the temperature in various points in the melt gives a better insight in the real temperature in the melt. One multi-point temperature measurement solution is a thermocouple mesh. It is a grid made of a small diameter thermocouple wires to minimise the disturbance of the melt and response times. An electromotive force is created at each grid junction and it can be correlated with the local melt temperatures. Thermocouple wire grid –based sensors have been used for example for monitoring melt temperature profiles and temperature variation. (Brown et al. 2004; Kelly et al. 2006.) Unfortunately this kind of sensor suits research rather than production environments as it is very fragile, complex and has disruptive effects on the melt and output (Abeykoon et al. 2011; Vera-Sorroche et al. 2013).

There is also a multi-point temperature measuring method based on fluorescence. Temperature sensitive fluorescent dye is added to the melt and the fluorescence emitted is monitored by optical fibre sensors. The temperature at different points is derived from changes in the fluorescence spectrum. As the dye is flowing with the melt, this method gives accurate temperature values representing the resin properties. However, in some polymer-fluorescent systems the changes in the spectrum induced by temperature and pressure are hard to distinguish from each other. (Bur et al. 2001; Bur et al. 2004; Bur & Roth 2004.) This kind of temperature monitoring systems cannot be used in implantable medical devices as the fluorescent dye could cause unwanted tissue response.

FOS provides a melt thermometer based on infrared radiation, IRTHERM 2003. The infrared technology also measures the temperature of the bulk melt. The heat of the plastic melt radiates through a very wear-resistant sapphire window to the sensor. A detector in the sensor connection head converts the radiation into an electrical signal. The IRTHERM sensor uses contactless detection, which is much quicker than the physical contact –method, which is used by the conventional sensors. The response time of the sensor is very short, less than 20 ms. (Innovative Sensors 2008.)

5.1.2 Melt pressure

Stable melt quality leads to consistent product quality. In industry melt pressure at the screw tip is considered as the most important indicator of melt quality. The screw speed, melt temperature, screw geometry and the material being processed affect the melt pressure. The melt pressure also gives an idea of the viscosity of the polymer melt and of the amount of material in the extruder. Unstable melt pressure results in fluctuating throughput and inconsistent product quality and dimensions. (Deng et al. 2013; Gao et al. 2014.) Conventionally the pressure sensors have been liquid-filled, which has restricted the thickness of the measuring membrane thus leading to membrane destruction in for example extrusion. The high shear forces in extrusion causes the process to be demanding for monitoring equipment. Another problem of conventional sensors is that the measuring ends of the sensors create dead space. FOS provides pressure sensors overcoming many of these problems. The EDS2 sensor has a flat measuring end to remove the dead space. There is no transmission liquid in the sensors, which enables the use of ten times thicker and more resistant membrane compared to the conventional sensors. The sensor can be used simultaneously to monitor temperature and pressure. The pressure range for the sensors is from 0-50 bars to 0-3000 bars. (Innovative Sensors 2008.) Also when processing polymers for medical applications, using liquid (often mercury) filled pressure sensors creates a risk of damaging the membrane and contaminating the product.

FOS also provides a miniature pressure sensor with a frontend membrane diameter of only 1.5 / 3 mm. A single optical quartz fibre connects the sensor head to an optoelectronic amplifier. The working principles of the two sensors are similar. The sensors use a light-based contactless measurement of membrane deformations caused by pressure. Behind the pressure membrane is a mirror, which is lit by an optical fibre. The

position of the mirror and thus the distance between the mirror and the fibre changes with outside pressure. Depending on the position of the mirror, varying amounts of light is reflected back to the fibre and guided to an optoelectronic detection device. The difference between the amount and intensity of the transmitted and received light is measured and processed into pressure values. The measuring is done with high resolution, because the greater thickness of the membranes causes the maximum deformations to be very small, only about 10 μm. In addition to conventional pressure measuring, also dynamic pressures up to 50 kHz can be measured with FOS pressure sensors. (Innovative Sensors 2008.)

5.2 Thermal degradation

Monitoring thermal degradation of the polymer during processing gives valuable information on the effects of the processing parameters on the thermal degradation in real time. In general thermal degradation can be seen as changes in colour, molecular weight or viscosity. The degree of thermal degradation is evaluated in real time mainly by using spectroscopic methods to detect the changes in colour or molar mass and also by measuring the viscosity of the melt with rheometers. (Rajan et al. 2010.)

As previously mentioned, moisture can cause thermal degradation during processing. FOS has developed a sensor called Hydro-Master which can aid in moisture sensitive plastics processing. The highly sensitive electrochemical probe of the sensor can be used for measuring on-line the residual moisture of raw materials. (Innovative Sensors 2008.)

5.2.1 Colour

In some cases the thermal degradation of a polymer can be seen as changes in colour. UV-vis spectroscopy is very sensitive to colour changes in the polymer melt, which makes it a promising tool for real-time monitoring of thermal degradation. The degradation of the material can be seen as the change of the UV-absorption edge to longer wavelength regions. Absorption in wavelengths below 400 nm can be visually recognised as yellow colour of the polymer. (Alig et al. 2010.) UV-vis spectroscopy is non-destructive, simple and straightforward technique and can also detect other chemical changes in the polymer, for example the formation of new groups in PLLA. It has a much lower detection limit compared to near infrared (NIR) and Raman spectroscopy. However, this method has its drawbacks. The spectra require proper pre-processing and chemometric analysis. In certain wavelengths the absorption of the optical fibres which are connecting the UV-vis spectrometer to the probes become dominant and cover more important absorption values. This leads to a large error in interpreting the results. In analysis state a reference UV-vis spectrum is subtracted from the measured spectrum leaving only the spectrum with thermal degradation. (Wang et al. 2008; Saerens et al. 2014.)

Wang et al. (Wang et al. 2008) applied UV-vis spectroscopy to monitor in-line the colour changes of PLLA during extrusion. The measurements were carried out by using a special measurement slit die, which was flange connected to the extruder. A UV-vis probe was fitted to the melt channel of the slit die and the probe was connected to the spectrometer via optical fibres. UV-vis spectroscopy revealed to be a functional and non-destructive tool for real-time monitoring the thermal degradation of PLLA. (Wang et al. 2008.)

FOS provides a sensor for measuring colour changes on-line during extrusion, Color-Master X. The sensor operates in visible light wavelengths, 0.4 – 0.9 μm. The measuring principle is based on spectroscopy; a broad band light source illuminates the plastic melt and the melt transmits or reflects the light back. The spectral intensity of the light is measured and according to that information the light is modified. In addition to measuring changes in colour, Color-Master is also capable of determining the chemical "fingerprint" specific to a material. The sensor can be applied to direct on-line high resolution melt-colour measurement, masterbatch production and processing, detection of lot variations, permanent quality control, detecting impurities and contaminations and continuous process control. FOS also has a general sensor which can measure ultraviolet, visible and near-infrared radiation. Optimelt X can detect changes in colour, humidity, additives, fillers and contamination. The melt degradation, oxidation, turbidity, schlieren, index of refraction and particle distribution of the melt can be monitored with the sensor. (Innovative Sensors 2008.)

5.2.2 Monomer content

The extent of thermal degradation of a biodegradable polymer during processing can also be evaluated by measuring in-line the monomer content generated in extrusion. Mainly optical spectroscopic methods (Raman, infrared, near-infrared, ultraviolet-visible, fluorescence) are used to monitor the chemical composition of the melt. Optical spectroscopic sensors are capable of generating the "spectroscopic fingerprint" of a molecule from where information about the structure and properties of the molecules (for example the monomer content) can be extracted. The methods use light of different wavelengths and create an absorbance spectrum of the materials. Some of the methods (for example infrared and UV-vis) can be used either in reflection of transmission mode. This means that the light either bounces off (reflection probe) or goes through the extruding material (transmission probe). The transmission mode is usually favoured for transparent materials because the reflectance spectrum contains more noise. (Fischer et al. 1997; Alig et al. 2010; Saerens et al. 2014.) In the following sections the different optical spectroscopy methods for in-line monitoring the chemical composition of the melt are introduced.

Infrared spectroscopy

Infrared (IR) -spectroscopy has been used for polymer processing monitoring for decades and it was the first optical spectroscopic method to be studied for extrusion moni-

toring. (Alig et al. 2010.) The illumination of the sample with a broad band source of radiation in the IR region of the electromagnetic spectrum (wavenumber range 12 000 – 400 cm^{-1}) causes vibrational excitation. (Coates et al. 2003.) The IR photon collides with the molecule giving it the photon's energy which turns into vibrational energy. With this energy the molecule is elevated at the frequency of vibrational resonance. The IR absorption comes from direct resonance between the IR radiation frequency and the vibrational frequency of molecular vibration. (Lewis & Edwards 2001.) The mid-IR range from 4000 to 400 cm^{-1} contains fundamental vibrations, whereas the near-IR (NIR) range is from 12 000 to 4000 cm^{-1}, where are the overtone and combination band features. The vibrations of bonds with large dipole moments, such as oxygen–hydrogen and carbon–hydrogen bonds, are strongly IR active. (Coates et al. 2003.) However, IR spectroscopy has its drawbacks. In in-line measurements the IR radiation can penetrate only to the depth of about 1.5 μm and in a viscous material the exchange of a layer this thin takes time. Mid-range infrared spectroscopy also requires expensive and easily damaged optical fibre technology. (Alig et al. 2010.)

IR spectrometer can detect only one frequency of radiation, whereas Fourier Transform Infrared (FTIR) spectroscopy allows all frequencies to be detected simultaneously. In addition it applies a Fourier transform to convert the raw data into the actual spectrum. This makes FTIR much quicker, more accurate and provides measurement with a better resolution compared to dispersive IR instruments. In addition FTIR is non-destructive and does not require sample preparation or the use of solvents or consumables. (Wilson & Poole 2009; Alig et al. 2010.)

Fourier transform can also be used in near-IR region, in which case the instrument is called Fourier Transform Near Infrared (FT-NIR) spectrometer. The absorbance of FT-NIR is low, which allows measurements to be made from long distances through traditionally infrared-opaque material. It can measure component concentrations and strict physical properties, such as average particle size. (Hirsch 2010.) However, NIR spectrum has fewer details than an IR spectrum. NIR can detect mainly C-H, O-H and N-H bonds and the spectra contain broad, notably overlapping peaks and combination bands which makes the analysis of the spectra challenging. Also quantitative analysis is more difficult with NIR spectrum. (Alig et al. 2010; Saerens et al. 2014.)

Although FTIR spectrometry is a suitable tool for monitoring chemical composition of the melt, it has its drawbacks. If the melt monitored is strongly absorbing the radiation, the path length has to be 50 μm for the measurement, which restricts the use of FTIR only for on-line setups with a bypass. The viscous melt fills the bypass and the narrow measurement cell which causes delay in the measurement. (Alig et al. 2010.) This problem has been addressed with a combination system of FTIR with an attenuated total reflection (ATR) probe. This system eliminates the ultra-narrow path length cells and their attendant difficulties with blockage from particle matter in the sample and interference fringes. This system is mainly used for liquids but is suitable also for multiphase systems, for example emulsions (Callis et al. 1987). The ATR probe withstands

high pressures and temperatures, but high melt viscosity of the polymer melt is a problem for this system (Callis et al. 1987; Alig et al. 2010).

FTIR has already been used for monitoring PLA degradation. Chen et al. used offline FTIR to study the thermal degradation products of packaging grade PLA during thermogravimetric analysis. (Chen et al. 2012.) The method was proven suitable for the offline application, which suggests that the tool might be usable also for real-time measurements. FOS also has an optical probe for in-line control of polymer processing which uses NIR spectroscopy. The probe has a pressure proof optical window and it withstands high pressure and wear. It can perform optical measurements in either reflection or transmission mode. (Innovative Sensors 2008.)

Raman spectroscopy

Raman scattering is inelastic scattering of light. While IR absorption is a one-photon event, Raman scattering involves two photons. When monochromatic light encounters a molecule it is possible that the optical oscillation interacts with the molecular vibrations of the electron cloud of the molecule. The interaction makes an electron to excite from the valence band to the conduction energy band by absorbing a photon. The excited electron is scattered by emitting (or absorbing) phonons and then relaxes back to the valence band by emitting a photon. The radiation emitted by the scattered photon (light) is sensed as Raman scattering. (McCreery 2000; Lewis & Edwards 2001; Dresselhaus et al. 2005.) The advantages of Raman spectroscopy include the portability of the instrumentation, usability with fibre-optic coupling and stability also in humid atmosphere. However, Raman spectroscopy is more complex than IR-spectroscopy both experimentally and theoretically and the normalisation of the spectra is particularly challenging in in-line measurements. (Coates et al. 2003; Gururajan & Ogale 2009.)

Twin-screw extruders are typically starve-fed which creates voids in the barrel. This poses challenges for Raman spectroscopy as the distance between the measured material and the sensor varies. This variation creates variability in the spectra and has to be filtered out. Raman spectroscopy is complementary with NIR spectroscopy. Depending on the material monitored, one technique will be more suitable than the other. For example fluorescence and colour of the material influence Raman spectra and cause a high background signal. These difficulties can however be partly overcome by changing the type of laser. (Saerens et al. 2014.)

Nuclear magnetic resonance spectroscopy

Nuclear magnetic resonance (NMR) is one of the most suitable methods for the characterisation of polymers. It bases on magnetic properties of the atomic nucleus. In an NMR probe there are two permanent magnets which create a static magnetic field. The atomic nucleuses that spin in the field are excited by an external radio-frequency field and emit a radio-frequency signal that contains information on for example the molecular structure where the atoms are. (Gottwald & Scheler 2005.) NMR can also be used to detect crystallinity and particle size (Crowley & Zhang 2007). NMR is non-destructive,

does not require direct contact with the sample and can measure also optically opaque materials. The measurements can be carried out from arbitrary distances since the penetration depth does not depend on the polymer sample but the probe has to be near the sample to ensure a strong signal. The main drawback of NMR is its low sensitivity which creates a need for an extended experiment time for signal accumulation. (Gottwald & Scheler 2005.)

Surface NMR mainly provides information on molecular mobility via relaxation times which can be related to temperature, composition and homogeneity of the melt. The main advantages of the surface NMR in comparison with other NMR systems include small size of the equipment and low cost of the probes. There are two main difficulties in adaptation of the surface NMR to extrusion monitoring; the high temperatures and the ferromagnetic materials. Changing the temperature distracts the rf-resonance by putting it out of tune and changes the field strength of the magnet material. Additional problems include the ferromagnetic parts in the extruder which deform the static field and the considerable mechanical forces between the extruder and the NMR probe which pose challenges for mounting the probe. (Gottwald & Scheler 2005.)

The applications of NMR in real-time monitoring are still few and far between. Gottwald and Scheler applied in-line surface-NMR spectroscopy for measuring relaxation times of soft polyvinyl chloride sheet. The NMR probe they had designed withstood the harsh conditions although the melt was in direct contact with its surface and the detected signal was clearly distinguishable from the background signal. The authors plan to design an extruder part for mounting a NMR probe capable of monitoring in-line any NMR-detectable parameter, rheological information and component composition. (Gottwald & Scheler 2005.)

5.2.3 Melt viscosity

Melt viscosity is considered as the best indicator of melt quality in polymer processing as it is directly connected to the dimensions, appearance and the functional properties of the extruded product (Chen et al. 2003; McAfee & Thompson 2007). It can be used as a measure of the molecular weight of the polymer and thus it also gives information on the thermal degradation of the material. Viscosity can be defined as the measure of "the resistance of a material to flow" and is derived from the ratio of shear rate and shear stress as

$$\eta = \frac{\tau}{\gamma} \tag{1}$$

where η represents the viscosity, τ is the shear stress and γ the shear rate. Shear stress can be determined from the pressure drop along a channel in a slit die or a capillary and the shear rate can be calculated from the volumetric flow rate through the die. (Liu et al. 2012; Deng et al. 2013.)

Currently there are four types of melt viscosity measuring techniques; off-line laboratory capillary rheometer, on-line side-stream slit, capillary or rotational rheometer, torsional rheometer and in-line slit or capillary rheometer. The laboratory rheometer provides the most accurate results but is also the most time-requiring. The other rheometers measure on/in-line but the side-stream rheometer is the slowest having a measurement delay of several minutes. (Chen et al. 2003; Deng et al. 2013.)

Generally the on-line rheometer separates a portion from the melt with a gear pump to a capillary or a slit in a bypass for measuring. The viscosity is derived from the pressure drop in the capillary or slit channel. After the measurement the melt merges with the main stream. The main problem of the side-stream system aside its long measurement lag is that the melt in the side stream does not always represent the bulk flow. (McAfee & McNally 2006; Mould et al. 2011; Liu et al. 2012.) To have a more complete understanding of what happens inside the extruder barrel, on-line rotational rheometers can be used to monitor viscosity in multiple points along the axis of the extruder. However, the advantages of sampling along the axis do not overcome the limitations of on-line measurements. (Covas et al. 2008 Mould et al. 2011.)

In-line rheometers are particularly attractive as they are using the whole material flow for sampling which removes the problem of unrepresentative sample flow. In the extruder setup they are located between the screw and the die. In-line rheometers can also be divided in slit die and capillary rheometers. The in-line slit die rheometer is an extruder die with a small rectangular flow channel with a high width-to-height ratio. The pressure drop along the melt channel is measured and in constant temperature the viscosity of the melt can be derived from the pressure difference. (McAfee & McNally 2006; Mould et al. 2011; Liu et al. 2012; Deng et al. 2013.) For example FOS provides an in-line viscosity measurement set called Viscomaster X with two miniature pressure sensors (diameter 3 mm) and a thermometer. The system monitors the viscosity of the melt continuously and gives an alarm signal if pre-set limits are exceeded. (Innovative Sensors 2008.)

The in-line slit rheometer is the most promising melt viscosity measurement system as it is mounted directly in the process stream and it can measure in real time. (McAfee & McNally 2006; Mould et al. 2011; Liu et al. 2012; Deng et al. 2013.) Additionally, when the width to height ratio of the slit is over 10, the polymer flow can be considered unidimensional and no edge corrections are needed (Silva et al. 2015). However, the die cross-sections have to be small for accurate pressure difference measurements and maintaining the temperature stable but they introduce a problem of limiting mass production. This is why slit dies are more suitable for research purposes rather than high-scale industrial production. (McAfee & McNally 2006; Mould et al. 2011; Liu et al. 2012; Deng et al. 2013.) There have also been attempts for using a larger cross-section, but these studies did not contain reference measurements with off-line methods which left the accuracy of the measurements unclear (Chiu & Lin 1998; Chiu & Pong 1999; Chiu & Pong 2001, cited in McAfee & McNally 2006).

To improve the measurements with the slit die, hole-pressure and exit pressure – methods have been developed. In the hole-pressure method the elastic functions are calculated from the difference in pressure drop between a flush-mounted transducer and a recess transducer. These two devices are fixed opposite to each other. In the exit pressure method the same variables are calculated from the excess pressure drop related to the atmospheric pressure at the exit of the die. These methods can be used with slit rheometers and applied in-line. However, the exit pressure method is less reliable due to errors in the extrapolation of at least three pressure readings to the exit. Recently Teixeira et al. investigated the practical utility limits of hole-pressure method, namely its error sources and sensitivity of the results. They used a small-scale modular slit die to measure viscosity in-line in silicon oil, polyethylene and polystyrene melts. The method was proven suitable for shear viscosity, but the required level of accuracy called for oversampling techniques and the method was found out to be sensitive to even low (5 °C) temperature changes. (Teixeira et al. 2013.) The torsional rheometer measures the torque required to rotate a disk or a bob at a certain speed. It measures fairly accurately and in real time, but is expensive and restricts the flow of the melt. (Deng et al. 2013.)

Despite all the attempts for developing a reliable and precise device for rheological real-time monitoring, all of the above mentioned methods have limitations. The main disadvantages of in-line rheometers include reducing the output rate of the product, the special care in design they require and their high cost. The on-line and off-line systems suffer mainly from long measurement lags. Due to these problems in real-time viscosity measuring, alternative methods for determining melt viscosity based on modelling techniques have been proposed. The data produced by present sensors is used to calculate and evaluate the viscosity of the melt. These values can be for example screw rotation speed and amperage, melt temperature, geometric dimensions of the extruder and material constants. (Chen et al. 2003; Mould et al. 2011.)

These approaches, also called “soft sensor” methods, remove the need of throughput-limiting and expensive physical sensors. Modelling saves money but the models are as accurate as physical measurements. Deng et al. developed a mathematical method for monitoring the energy usage profile along the extruder. In determining the viscosity this soft sensor approach was found out to be a satisfactory alternative for the slit-die rheometer. (Deng et al. 2013.) Liu et al. developed an approach which involves a nonlinear finite impulse response model with adaptable linear parameters. It estimates the viscosity of the melt based on the process inputs. The output of this model is fed to another model where on-line measured barrel pressure is predicted. The system uses the difference between the predicted and measured pressure as a feedback signal to correct the viscosity estimate. The system was found to have a root mean square percentage error of less than 1 % and thus suitable for real-time monitoring of polymer viscosity. (Liu et al. 2010; Liu et al. 2012.)

The ‘soft sensor’ systems require tuning of many parameters and they lack understanding of the process. To overcome these problems, systems using ‘grey box’ modelling have been reported. These models use prior knowledge of the system to make pre-

dictions and empirical techniques to refine the predictions combined with intelligent algorithms, for example fuzzy logic. However, these methods are only on the modelling state and there are no reports on applying these models to real-time monitoring systems. (McAfee 2007; Nguyen et al. 2014.)

5.3 Filler dispersion and particle size

The final properties of compounded polymer products, including mechanical modulus, stiffness, toughness and scratch resistance, depend strongly on filler dispersion, particle size and size distribution. This makes morphology control of these products desirable already during manufacturing. Traditionally monitoring particle size has been done with in-line, off-line and at-line turbidity measurements at a single wavelength. In data analysis stage, the measured turbidity is compared to simulated turbidity data. The difficulty of turbidity measurements is that they need additional sample information such as the number of particles or the number density of particles. (Alig et al. 2010.)

Optical spectroscopy techniques (Raman, IR, NIR, UV-vis and fluorescence, of which the two firstly mentioned sensors are shown in Figure 5.2.) can trace even very small quantities of additives in polymers. For example NIR spectroscopy is sensitive to the degree of dispersion, but UV-vis spectroscopy can detect smaller particles. Since the spectroscopic techniques extract a spectrum containing chemical and morphological information, particle size is indirectly derivable information. Therefore chemometric models have been developed for analysis. In case of heterogeneous materials, for example a compounded polymer, the matrix and the filler give different light scattering spectra. The analysis of the background curve gives direct information on average particle size and number density, but for quantitative analysis the background curve has to be separated from the "chemical information". (Alig et al. 2010.)

Barbas et al. monitored the dispersion and particle size of clay fillers in PP/clay nanocomposites with NIR spectroscopy. The group compared NIR in in-line diffuse reflectance mode and on-line transmission mode. Off-line FTIR measurements were used as reference data. Both reflectance and transmission methods were found to perform high-quality measurements. The diffuse reflectance probes are nowadays available with standard Dynisco mounting threads, which make their fixing considerably simpler. However, the spectra may be affected by the rotation of the screw elements or large particulates of the filler acting as reflectors (depending of the type of the filler) or by voids created by only partly-filled screws. The authors propose using several reflectance probes positioned along the screw axis for more complete monitoring of the extrusion event. (Barbas et al. 2013.) Barnes et al. used in-line transmission FT-NIR to measure the filler concentration in polyethylene/magnesium hydroxide –system. After treating the raw data with chemometric methods and a calibration model, accurate values of filler content were acquired. (Barnes et al. 2007.)

In composite systems with over 40 % filling of relatively large, micron-size (1-10 μm) particles the samples are usually too opaque for optical transmission measurements.

The reflection measurements are possible in principle, but the multiple scattering due to high concentration of large particles blurs the wavelength dependency. The much larger wavelength of ultrasonic waves makes the ***ultrasonic spectroscopy*** much more suitable for systems with a high degree of filling. An ultrasonic sensor is shown in Figure 5.2. In addition to spectroscopic techniques, ultrasonic spectroscopy is one of the classical methods for in-line control. It is appealing because the measurements are not limited to transparent materials, the equipment is relatively inexpensive, it directly measures mechanical properties in the melt and the sensors are highly robust against abrasion and high pressure. Ultrasonic spectroscopy can be used for in-line monitoring of size distribution, particle size and dispersion. (Alig et al. 2005; Alig et al. 2010.)

Figure 5.2. *Raman, Near Infrared (NIR) and ultrasonic (US) sensors. A measurement slit die is partially shown on the left side. Modified from (Alig et al. 2010).*

Alig et al. measured two concentrations of Irganox in PP with on-line NIR, Raman and ultrasonic spectroscopy and conducted a comparison of these methods. All three methods showed that they are suitable for detecting additive levels in polymers on-line during melt processing. They all turned out to be accurate, but NIR and ultrasonic spectroscopy were identified as the cheapest methods. (Alig et al. 2005.)

In addition to the methods mentioned above, ***terahertz spectroscopy*** has been used for filler content measurements. Terahertz frequencies, also called as far-infrared region, are broadly defined as 0.1-30 THz. The low-energy excitations in electronic materials, low-frequency vibrational modes of condensed phase media as well as vibrational and rotational transitions in molecules manifest themselves on this spectral range. (Dexheimer 2008.) The refractive index of the melt can be calculated from the time required by the terahertz pulse to propagate through the melt. A linear relation between this time and the volumetric additive content of a polymer-filler compound can be established. Terahertz spectroscopy system is very complex and expensive, but it can measure additive content and melt density fairly reliably. (Saerens et al. 2014.)

When conductive fillers are used, ***dielectric spectroscopy*** can measure morphological properties of the compound system. Dielectric spectroscopy generates an electric field across the melt and measures the resulting alternating current. Dielectric sensors can be used for example to measure in-line the permittivity and capacitance as well as physical and chemical structure of organic materials by measuring their dielectric properties, viscosity, melt composition, filler concentration and comonomer content. Filler concentration can be derived from measurements of permittivity contrast between the polymer and the filler or changes on conductivity of the composite. (Saerens et al. 2014.)

6 REAL-TIME MONITORING OF HOT DRAWING

Melt spinning of fibres is a continuous process with new variables to measure in real time compared to extrusion. For example coefficient of variation, fibre diameter and temperature are time-consuming to measure separately from the production line. Real-time systems enable a better control over the process and the quality of the fibre produced. However, the nonplanar geometry, small size, high velocity and thus vibration pose challenges for real-time measurements in melt spinning.

6.1 Fibre diameter and coefficient of variation

The coefficient of variation (CV) is defined as the mass variation per unit length or the diameter variation of fibres. CV is the most important evenness characteristic in textile processing and quality control. The irregularities in fibres often cause the fibre to break in the subsequent processing steps after extrusion, for example spinning and knitting. CV influences strongly the weight, strength and productivity of fibres, which are directly lied to the cost and quality of the product. As a consequence one of the most important ways to improve product quality is to monitor the fibre CV. (Huang & Tang 2007; Ibrahim et al. 2012.)

Conventionally the fibre CV has been measured with pressure rollers, air flow, radiation, photoelectric elements, capacity, microwave and image processing (Huang & Tang 2007). The nowadays used sensors for measuring fibre CV can be divided into three groups; instruments using capacitance, optics, or a combination of the two. The principles of the capacitive and optical systems are presented in Figure 6.1. In capacitive devices there is an alternating electrical voltage between two metal plates (C in Figure 6.1a). A fibre (Y in Figure 6.1a) entering the capacitor electrical field alters the capacity by an amount that is proportional to the thickness of the fibre. This method assumes that the mass density and the dielectric polarisation intensity are uniform along the fibre. The capacitive system is sensitive to fibre shape, dielectric constant of the material and moisture content. (Sparavigna et al. 2004; Ibrahim et al. 2012.)

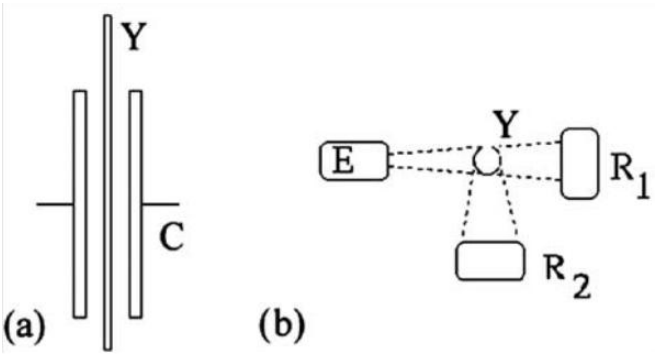

Figure 6.1. *Principles of capacitive and optical diameter measurement instruments (Sparavigna et al. 2004).*

The main elements of an optical instrument include a light source (E in Figure 6.1b) and photodiodes (R_1 and R_2 in Figure 6.1b). The light sources can emit for example infra-red, visible light or laser beam. Photodiodes function as receivers; they generate a potential difference or change their electrical resistance when exposed to light. A fibre brought to the light field partly absorbs the light and partly reflects it. There can be one receiver detecting the shadow that the fibre generates (R_1 in Figure 6.1b) and another one measuring the reflected light (R_2 in Fig. 6.1b). The shadow method can be used for measuring the width or diameter of the fibre. However, the optical sensors tend to be sensitive to environmental temperature, humidity and light. (Vondra 2003; Sparavigna et al. 2004.) Optical methods assume that the cross-sectional shape of the fibre is round which can cause problems in some applications. Yet, optical sensors have some advantages over capacitive sensors; in addition to all the variables that capacitive sensors can measure, optical sensors can also detect the yarn shape, hairiness and the presence of foreign fibres. (Sparavigna et al. 2004.)

There are many commercial testers for real-time diameter and CV measurement. One example of the manufacturers is Zumbach Electronic AG located in Switzerland. The company offers non-contact diameter measuring devices based on laser technology (ODAC) and light emitting diode (LED) shadow method (MSD). ODAC comes with built-in processors to processing the raw data and it can also detect for example faults in fibres, ovality and position. MSD can measure diameter and ovality on-line precisely and inexpensively. (Laser measurement devices 2014.) There has been also a similar approach in research. Tsai and Chu developed a photoelectric sensor for measuring the fibre CV and diameter on-line. The device was found able to function regardless of fibre movements and vibration, and temperature and humidity had no effect on its performance. Nonetheless, the LED in the sensor had a short life and the sensor was found to be sensitive to environmental light. (Tsai & Chu 1996.)

Many of the real-time monitoring sensors have problems with environmental humidity or light, high temperatures, the movements of the fibre or non-round cross-sectional shape of the fibre. A more accurate and robust device seems to be the one developed by Huang and Tang. The system was an optical instrument with four pairs of

infra-red emitters and receivers and its functionality was compared to a commercial tester. The multiple pairs of emitters and receives reduced the effects of the non-regular shape of the fibre and the environmental temperature and humidity. Additionally the device proved to be as accurate as the commercial tester, suitable for on-line measurements, inexpensive and the convenient as the signal was transmitted to a computer in a common way. The processing runs were conducted with cotton and polyester fibres. (Huang & Tang 2007.)

Microscopes and high speed cameras can also be used for measuring diameter and CV in real time. De Rovére & Shambaugh studied measuring fibre diameter on-line with high speed flash photography and microscopy. The images acquired were viewed under a microscope with a micrometer eyepiece. A fine wire of a known diameter was photographed simultaneously with the spinline for reference. The images were taken from many different angles with the assistance of a traverse system. This eliminated the problem of fibres with non-circular cross-sections. However, the measured fibre diameters tended to be higher than the ones obtained from off-line measurements because of the blurred edges in the fibres. (De Rovére & Shambaugh 2001.) Measurement systems firstly intended to measure other variables can also be used to measure fibre diameter. For example infrared cameras can be used for measuring fibre temperature and diameter simultaneously and the diameter can be measured indirectly with fibre speed measurements by calculating the diameter from the speed data. (Golzar et al. 2004.)

Optical real-time methods for measuring fibre diameter have also been applied to high speed melt spinning. Kikutani et al. suggested a diameter measurement system with three diameter monitors. The device is able to measure the movement of diameter profiles based on the back-illumination principle. The system was studied in high speed spinning of PET and was accurate in measuring diameters of less than 50 to 135 μm with a spinline velocity of 5 000 m/min. (Kikutani et al. 1999; Takasaki et al. 2003.)

6.2 Other variables

Aside from measuring the above mentioned parameters, also fibre temperature, velocity, acceleration and structure development (orientation, crystallinity and birefringence) can be measured in real time. Measuring the fibre temperature and cooling profile gives insight in the crystallisation development. There are contact and noncontact methods for measuring fibre temperature. The most important contact methods are based on a thermocouple measuring the temperature of the melt before solidification. Its main limitation is the perturbation of the fibre forming zone. (Golzar et al. 2004.) Noncontact methods can be used on-line and are based on the infrared radiation hot fibres emit which can be detected by specialised detectors, such as radiation thermometers (also called pyrometers) (Bresee & Ko 2003; Bendada & Lamontagne 2004) or infrared cameras (also called infrared thermography) (Bansal & Shambaugh 1998; Lin et al. 2001; Marla et al. 2009). The cameras are used to measure temperature variations on the surface of the fibres. However, the space resolution of the infrared cameras is limited

and the emissivity of the fibres can behave complexly which poses challenges for infrared measurements. Additionally, the radiation that the polymer emits is not evenly distributed in the infrared spectrum due to semi-transparency of the fibres. (Bendada & Lamontagne 2004.)

X-ray scattering, especially combined use of small angle x-ray scattering (SAXS) and wide angle x-ray scattering (WAXS) can obtain structural information of different length scales simultaneously. Cui et al. used simultaneous WAXS and SAXS for studying structure development in melt spinning. However, the system could not detect a structural feature larger than 20 nm because the distance between the sample and the detectors was small and the beam stop was large. The relationship between the external processing conditions and the structural evolution can be understood with this system. (Cui et al. 2014.) Birefringence is refraction of the crystallised and amorphous phases, indicating crystallinity. Polarising microscopes or crossed polarisers can be used to monitor birefringence on-line. (Bansal & Shambaugh 1998; Kikutani et al. 1999; Marla et al. 2009.) Fibre velocity and acceleration can be monitored on-line with a laser Doppler velocimetry or rapid framing cameras (Bansal & Shambaugh 1998; Bresee & Ko 2003).

EXPERIMENTAL PART

7 RESEARCH METHODS AND MATERIALS

The polylactide fibre in this work was manufactured using two different melt spinning set-ups, a conventional melt spinning line and an updated drawing line with real-time monitoring. The fibre manufactured with the conventional spinning line was characterised in terms of hydrolytic degradation study comprising of mechanical and thermal testing as well as molecular weight and viscosity measurements. In this set-up the melt pressure, temperature, motor load and temperatures of the extruder zones were monitored in real time.

Another set-up was identified for scaling up the production of the 4-filament fibre and also for researching new possibilities in real-time monitoring. Two separate processing trial series were performed. The first was for initial testing of the set-up with a packaging grade material and the second for more comprehensive testing using a GMP grade material. The objective of the trials was to find parameters in the new set-up to produce fibre having similar properties as the fibre produced in the conventional set-up. The fibres manufactured in the trials were examined for mechanical properties and viscosity. The experimental part of the work was conducted in the Biomaterials and Tissue Engineering group in the Department of Electronics and Communications Engineering in Tampere University of Technology.

7.1 Materials

Three different polylactides were used in this study. One batch of GMP grade poly(L/D)lactide 96/4 (Purasorb product line, Purac Biochem bv, Gorinchem, The Netherlands) was used for the manufacture of the fibre using the conventional melt-spinning line and another batch for the trials with the real-time monitoring set-up. Packaging grade polylactide Revode 190 manufactured by Zhejiang Hisun Chemical Co., Ltd. (Zhejiang, China) was used for the initial trials with the real-time monitoring set-up. The data on the materials is presented in Table 7.1.

Table 7.1. *Material data. The value marked with an asterisk was measured in Tampere University of Technology.*

	GMP grade material for *in vitro* studies	Packaging grade material for initial real-time monitoring trials	GMP grade material for real-time monitoring trials
Manufacturer	Purac Biochem bv	Zhejiang Hisun Chemical	Purac Biochem bv
Ratio L/D (%)	96/4	?	96/4
Batch number	1003000889	L130	1401002864
Inherent viscosity (dl/g)	3.49	1.59*	3.62
Form	Granule	Granule	Granule

Purac Biochem bv was selected as the supplier of the GMP grade materials as they take part in the project as collaborators and we have previously done extensive work with their materials. The packaging grade polylactide was a kind gift from Queen's University Belfast.

7.2 The conventional set-up

The fibre for the *in vitro* testing was manufactured using a single-screw micro-extruder (Gimac TR Ø12 L/D 24:1 B.V.O) provided by Gimac di Maccagnan Giorgio (Castronno, Italy). Further details of the extruder are gathered in Table 7.2. The temperatures of the heating zones were adjusted according to the values in Table 7.3. The screw speed was set between 9 and 10. Filter pack with a single large hole was used in the extrusion and the 4-filament fibre exiting the die was cooled down with air.

Table 7.2. *The properties of the single-screw extruder used in the conventional set-up.*

Extruder	Gimac TR Ø12 L/D 24:1 B.V.O.
Screw diameter (mm)	12
Screw L/D ratio	24:1
Number of heating zones	6
Filter pack	one large hole
Nozzle	4 x Ø 0.4 mm

Table 7.3*. The extrusion temperatures used in the manufacture of the fibre for* in vitro *testing.*

Heating zone number	Temperature (°C)
1	185
2	200
3	215
4	228
5	240
6	280

The fibre was drawn with a drawing line comprised of fibre guides, three drawing units, four ovens and a winder. The drawing line configuration is presented in Figure 7.1. and the temperatures of the ovens and the velocities of the drawing units are shown in Table 7.4. The velocities were measured with a tachometer.

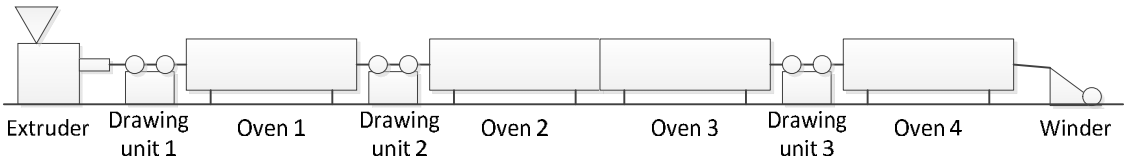

Figure 7.1. *Schematic drawing of the configuration of the conventional melt spinning line.*

Table 7.4. *The drawing parameters in the conventional set-up used in the manufacture of the fibre for* in vitro *testing.*

Oven 1	100 °C
Oven 2	120 °C
Oven 3	110 °C
Oven 4	115 °C
Drawing unit 1	13 m/min
Drawing unit 2	25 m/min
Drawing unit 3	57 m/min
Draw ratio	4.4

Before processing the polymer was dried in glass bottles in a vacuum. The vacuum was heated at a rate of 1 °C/min and the polymer was kept in 100 °C for 16 hours after which it was let to cool down to room temperature. The dry granules were taken out of the vacuum under nitrogen atmosphere and poured into the feeder one 100 g bottle at a time. The feeder and the extruder hopper were under inert nitrogen atmosphere (with a flow rate of 1 l/min). The feeder was custom made at TUT.

Only traditional sensors were used in the conventional set-up. The melt pressure and temperature were measured in-line with a conventional pressure and temperature sensor (model TPT 463-7.5M-6/18, Dynisco Instruments, Franklin, Massachusetts, USA). Also the motor current and the temperatures of the heating zones were monitored in real time.

7.3 The real-time monitoring set-up

A new melt spinning set-up was identified to study upscaling of the production of the 4-filament fibre with real-time monitoring. The new set-up was constructed of a co-rotating twin-screw extruder (Mini ZE 20*11.5 D, Neste Oy, Porvoo, Finland) and four high speed spinning plants (MONO2, DUO1, DUO2 and MONO3) manufactured by Fourné Polymertechnik GmbH (Alfter, Germany). The configuration of the equipment used in these trials is presented in Figure 7.2. and the properties of the extruder in Table 7.5. The MONO drawing units have only one godet as DUO units consist of a godet

pair. MONO1 unit also exists but was not used because it is much smaller in height and would have required violent guiding of the fibre or a table for which there was not enough space. The distance from the wall closest to the die of the first drawing unit (MONO2) from the die was 90 cm and the distance between the outer walls of MONO2 and DUO1 was 40 cm. The rest of the spaces between the drawing units were both 50 cm. The speed of the winder was always kept 3 m/min above the speed of the last godet and the transversal movement was 25 ds/min in all the trials.

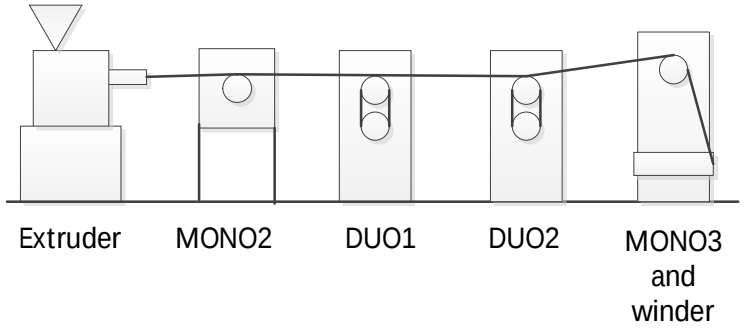

Figure 7.2*. Schematic drawing of the configuration of the updated melt spinning line.*

Table 7.5. *Properties of the twin-screw extruder used in the real-time monitoring set-up.*

Extruder	Neste Mini ZE 20*11.5 D
Number of heating resistors	4
Nozzle	4 x Ø 1 mm

The screw speed was kept in the minimum (92 rpm) and the fibre was cooled down with air. The cooling of the feeding zone was kept in 8 °C with a cooler (model FL300, Julabo GmbH, Seelbach, Germany). The polymer was dried according to the same protocol as in the trial with the conventional set-up.

7.3.1 Real-time monitoring

More advanced real-time monitoring methods were applied in the updated set-up compared to the conventional one introduced in the previous section. The main goal of the real-time monitoring was to measure in-line the shear viscosity and monomer content of the melt. A slit die was designed for this purpose in cooperation with Institute of Technology Sligo. A schematic illustration of the slit die is presented in Figure 7.3. The slit die was made of two halves to facilitate the cleaning of the part and to ensure that the sensors would be flush mounted with the melt channel as precisely as possible.

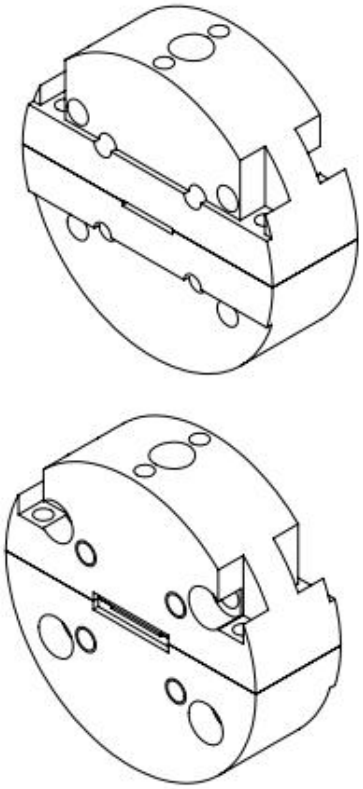

Figure 7.3. *The design of the slit die used in the real-time monitoring set-up.*

The slit die has a narrow melt channel (width/height ratio of 20:1) with six places for sensors. The sensor openings can be seen at the top of the die. Across the die on the bottom there is a similar set of holes. The smaller openings are for special miniature pressure and temperature sensors provided by FOS Messtechnik GmbH (Schacht-Audorf, Germany). The models were EDS 3000 F and ETS 3000 1K, respectively. The larger openings are designed for measuring the melt temperature and pressure with the conventional equipment and in a later stage for spectroscopic sensors for monomer content measurements. The slit die with all the sensors is presented in Figure 7.4. The readings from the conventional sensors could be used as a reference for the data given by the miniature sensors.

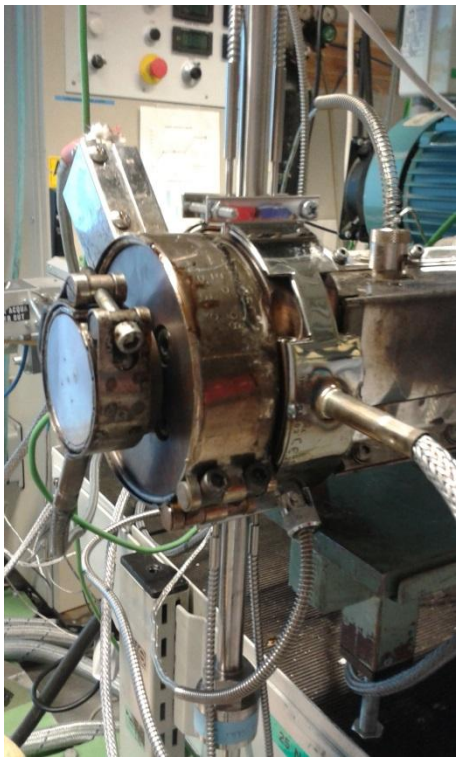

Figure 7.4. *The slit die with miniature melt pressure and temperature sensors and two conventional melt pressure transducers with thermocouple.*

The shear viscosity will be obtained by defining the pressure drop along the melt channel of the slit die and calculating with the help of throughput data, dimensions of the melt channel in the slit die and density data of the material. The monomer content in the melt is going to be obtained from a NIR spectrum. However, the focus in this study was to upscale the fibre manufacturing process and to study the processing parameters with the updated set-up. The determination of the shear viscosity or the monomer content of the melt was not the scope of this study.

7.3.2 Trials with the packaging grade polylactide

Several processing trials were carried out with the packaging grade polylactide. Various processing conditions were studied and the extrusion parameters are gathered in Table 7.6. The feeder used in the initial trials was the same custom made feeder that was used for the processing trial with the conventional set-up. The feed rate was calculated from the measured rotation speed of the feeding screw based to a figure drawn from feeding tests.

Table 7.6. *The extrusion parameters used in the trials with the packaging grade polylactide.*

Parameter	Range studied
Temperature of the extruder zone 1 (°C)	160–165
Temperature of the extruder zone 2 (°C)	170–175
Temperature of the extruder zone 3 (°C)	180–185
Temperature of the extruder zone 4 (°C)	200–205
Feed rate (g/h)	310–430

Different drawing parameters were also examined. The drawing parameters studied are shown in Table 7.7. The names MONO1, DUO1, etc. refer to the drawing units used in the trials. The number of the rounds on the godets describes how many times the fibre had been guided around the godet or a godet pair.

Table 7.7. *The studied drawing parameters in the trials with packaging grade polylactide.*

Godet	Velocity (m/min)	Temperature (°C)	Number of rounds
MONO2	50	73–75	3-4
DUO1	60–75	78–80	3-6
DUO2	90–100	75–80	3-5
MONO3	92–102	-	1
Winder	95–105	-	-

In addition to the parameters listed in the table the angle between the two godets in DUO drawing units was adjusted. The angle was measured as distance between the edge of the right side (as seen from the front) of the lower godet of the godet pair and the front wall of the drawing unit. The distance varied between 9.5 and 11.3 mm.

7.3.3 Trials with the GMP grade polylactide

After studying the processing parameters with the bulk quality material a few processing trials were conducted with a GMP grade polylactide. In these trials a new gravimetric feeder (Model K-SFS-24, Coperion K-Tron (Schweiz) GmbH, Niederlenz, Switzerland) was used. The used extrusion parameters are gathered in Table 7.8. and the parameters of the drawing line in Table 7.9.

Table 7.8. *The studied extrusion parameters in the trials with the GMP grade polylactide.*

Extruder zone	Temperature (°C)
1	210–217
2	220–227
3	245–254
4	265–274

Table 7.9. *The studied drawing parameters in the trials with the GMP grade polylactide.*

Godet	Velocity (m/min)	Temperature (°C)	Number of rounds
MONO2	50–60	85–95	4–5
DUO1	90–100	90–105	6–7
DUO2	130–150	85–100	4–5
MONO3	132–152	-	1
Winder	135–155	-	-

The feed rate was kept constant at 300 g/h and the filter pack with small holes was used in all of the trials. The angle between the godet pairs was kept constant at 11.3 mm.

8 CHARACTERISATION METHODS

The fibres manufactured using the real-time monitoring set-up were characterized in terms of mechanical properties and viscosity measurements. In addition the hydrolytic degradation properties of the fibres produced with the conventional set-up were examined. The mechanical and thermal properties as well as molecular weight and viscosity of these fibres were studied.

8.1 Hydrolytic degradation studies

The *in vitro* degradation properties of the fibres manufactured with the conventional set-up were determined by hydrolysis studies. Two different fibres were studied: gamma irradiated and non-irradiated fibre from a conventional multifilament processing run. The gamma irradiation of the samples was carried out with a minimum dose of 25 kGy (BBF Sterilisationsservice GmbH, Kernen, Germany).

The fibres were incubated for 0, 1, 2, 3, 4, 6, 8, 12, 16, 20, 24, 28, 32, 36, 42 and 48 weeks. The samples (24 cm) were tied in both ends and 5 parallel samples were carefully twisted together and put into test tubes with 30 ml of buffer solution. The buffer solution used was phosphate buffered saline (PBS) solution with a composition presented in Table 8.1. The pH of the solution was adjusted to 7.4. The test tubes were placed in 37 °C in a static incubator. To make sure that the pH level was maintained approximately the same the buffer solution was changed and the pH values were measured fortnightly with a Mettler Toledo SevenMulti pH-meter (Mettler-Toledo International Inc., Greifensee, Switzerland).

Table 8.1*. The composition of PBS used in the* in vitro *study.*

Reagent	Amount (g/l)	Concentration (mol/l)
Na_2HPO_4	3.54	0.0249
$NaH_2PO_4*H_2O$	0.76	0.0055
NaCl	5.90	0.1009

The mechanical, chemical and thermal properties of the samples were tested after the hydrolysis. After the tensile tests the samples were dried in fume cupboard for a few days and then put into the vacuum for a week before further testing.

8.2 Molecular weight

The weight-average molecular weight (M_w) and number-average molecular weight (M_n) of the samples were determined with gel permeation chromatography (GPC). The polydispersity index (PDI) was calculated from the results using equation (2).

$$PDI = \frac{M_w}{M_n} \tag{2}$$

The sample (7.3-7.6 mg) was dissolved in high-performance liquid chromatography quality chloroform (5 ml) overnight. The next day the samples were filtered through a membrane filter with a pore size of 0.45 µm. The measurements were performed with a modular system (Shimadzu Corporation, Kyoto, Japan) comprising of LC-20AD pump, RID-20A detector and Shodex KF-206 M polystyrene gel columns (Waters Corporation, Milford, Massachusetts, USA). The samples were measured at 40 °C using chloroform as an eluent with a flow rate of 1 ml/min. Calibration was performed using low polydispersity polystyrene standards and Mark-Houwink parameters for PS ($\alpha = 0.73$, $K = 1.12 \cdot 10^{-4}$) and PLA ($\alpha = 0.73$, $K = 5.45 \cdot 10^{-4}$). The injection volume of the samples was 100 µl.

The molecular weight characterisation was performed only in the hydrolysis study – part of the work. The samples were collected at pre-determined times at 0, 1, 8, 16, 24, 28 and 36 weeks. The number of the parallel samples was two.

8.3 Viscosity

The inherent viscosity (i.v.) measurements were conducted in Ubbelohde 0c capillary viscometer tubes (Schott-Instruments, Mainz, Germany) with an automatic viscometer (LAUDA, Lauda-Königshofen, Germany). The sample (20 ± 0.8 mg) was weighed and dissolved overnight in 20 ml of chloroform. The measurements were carried out in room temperature (25 °C).

The inherent viscosity measurements were used in the real-time monitoring trials to evaluate the effect of the extrusion temperatures on the thermal degradation of the material. The samples were collecting samples from the nozzle and the number of parallel samples was three. In the hydrolysis study the samples were collected at 0, 6, 12, 20, 24, 28 and 36 weeks and two parallel samples were prepared.

8.4 Thermal properties

The thermal analysis was performed only on the samples in the hydrolysis study. The thermal properties, especially the glass transition temperature (T_g), melting temperature (T_m) and crystallinity of the samples were determined by a differential scanning calorimeter (DSC) TAinstruments Q1000 (TAinstruments, New Castle, DE, USA) The

samples were collected at pre-determined times at 0, 1, 8, 16, 24, 28 and 36 weeks and the number of the parallel samples was two.

Only intact material i.e. not knotted parts or the parts deformed in tensile testing were used. Standard aluminum sample pans were used. The fibre was rolled into small balls of 5 mg (± 2 mg) in weight. The pans were closed with an encapsulating press. The method used contained two heating cycles from 0 to 200 °C at a rate of 20 °C/min. The crystallinities (X_c) of the samples were calculated from the melting enthalpies of the samples using the value of 100 % crystalline PLLA (93.7 J/g) according to equation (3):

$$\frac{\Delta H_{melting}}{93.7\ J/g} \times 100\ \% \tag{3}$$

, where the $\Delta H_{melting}$ refers to the melting enthalpy obtained from the melting peak in the DSC thermogram. The T_m and X_c were determined from the first heating cycle and the T_g from the second heating cycle.

8.5 Mechanical properties

The mechanical testing was conducted with an Instron 4411 material testing machine (Instron Ltd, High Wycombe, England) in room temperature. The parameters of the tensile testing are presented in Table 8.2.

Table 8.2. *The parameters of the tensile testing.*

Load cell	500 N
Gauge length	50 mm
Crosshead speed	30 mm/min

The diameters of the filaments were measured with a micrometer (N = 20) and the cross-sectional areas of each filament were calculated separately (the cross-sections were assumed circular). These areas were then added up in order to obtain the whole cross-sectional area of the 4-ply multifilament fibre. The tensile strength of the samples was determined using the equation (4):

$$\sigma = \frac{F}{A} \tag{4}$$

, where σ (N/mm^2 = MPa) is the tensile strength, F (N) is the tensile force and A (mm^2) is the cross-sectional area of the fibre.

The mechanical properties of the fibres from the real-time monitoring trials were tested to relate the results with the processing parameters. All the fibres from the trials were mechanically tested and the number of parallel samples was 2-5.

In the hydrolysis series the tensile properties of the samples were measured at every time point. Before testing the samples were taken out from the buffer solution and rinsed with distilled water. The average of the cross-sectional areas of the samples up to 4 weeks of hydrolysis was calculated and this value was used in calculating the tensile strength for the rest of the samples. The zero week samples were tested for mechanical properties both wet and dry. The wet zero samples were immersed in the buffer solution for 1 hour before tensile testing. All the samples from the hydrolysis series were tested wet. The number of parallel samples was 3-5.

9 RESULTS AND DISCUSSION

The results of this work are presented in two sections. The first part is divided in two subparts; the initial trials using packaging grade PLA and trials with GMP grade PLA. The extrusion and drawing parameters are presented alongside the results of the characterisation of the resulting fibres. In the second section the results of the hydrolytic degradation studies are discussed covering the effects of hydrolysis on mechanical and thermal properties, molecular weight and viscosity of the fibres produced using the conventional set-up.

9.1 Trials with the packaging grade polylactide

The initial trials with the real-time monitoring set-up were conducted with packaging grade PLA mainly due to the high cost of the GMP grade PLA. Six processing runs were conducted to find a relationship between the processing conditions and the filament diameter as well as the mechanical properties of the fibre with the updated set-up. Using the slit die in fibre manufacturing would provide benefits by giving real-time information on the thermal degradation (decrease in shear viscosity and increase in monomer content) of the material. In this part we examine the optimization of the processing parameters through the trials.

9.1.1 Trial 1

The objectives of the first trial with the packaging grade material were to see how the slit die would affect the quality of the melt and to obtain fibre for mechanical testing. With the mechanical testing results the mechanical properties of the fibre could be connected with the extrusion and drawing parameters. The extrusion parameters used in the first trial with the slit die are presented in Table 9.1. The temperatures in the extruder and the feed rate had already been optimised for the packaging grade material in earlier trials using the twin-screw extruder without the slit die.

As already mentioned, one of the objectives of this trial was to see if adding the slit die to the set-up would require changes in the extrusion parameters, mainly the extrusion temperatures. The narrow melt channel in the slit die is a new kind of small orifice which might require higher temperatures to make the polymer flow smoothly through it. However, the extrusion temperatures did not require changes which probably means that the material was already melted enough to pass the slit.

The filter pack with large holes was chosen for the trial because we expected it to make the material flow more homogenous compared to the filter pack with a single

large hole. In the earlier trials there had been a problem of large fluctuation in the filament diameters. The choice of the filter pack was also addressed to sort out this problem.

Table 9.1. *The extrusion parameters in trial 1.*

Extrusion temperatures (°C)	Filter pack	Feed rate (g/h)
160, 170, 180, 200	With large holes	317

Four spools were manufactured in the first trial. The drawing parameters and the mechanical testing results of all the spools are presented in Table 9.2. The drawing velocities are presented so that the first value is the godet closest to the nozzle and the last is the winder. The temperatures are presented in a similar way, but the last godet was not heated. The two godets in the DUO units were kept at a same temperature even though it would have been possible to adjust their temperatures separately. The fibre was always wrapped once around the last godet.

The ultimate goal was to obtain 4-filament fibre with a filament diameter of 90 µm or less with as high tensile strength as possible and with moderate strain (20-60 %). The target values were drawn from the minimum limits enabling usual textile post-processing methods. There are no exact requirements for the mechanical properties as they could not be reached with the packaging grade material. The most promising results were obtained with the first spool. It had the highest ultimate tensile strength and the lowest filament diameter. The velocities of the drawing units were lowered in the spools 3 and 4 and the change can be seen in the diameters, although the difference between spool 2 and 4 is not remarkable. The ultimate tensile strength also decreased by ~ 20 MPa in average with the decrease of the drawing speeds.

The draw ratio used in the trial is also exhibited in Table 9.2. It was calculated as the ratio of the velocities of the winder and the first draw roll. The draw ratio of approximately 2 seems low compared to the draw ratios usually employed for PLA (3-4, Auras et al. 2010).

Table 9.2. *The studied parameters and the properties of the fibres in trial 1. In tensile test n=5, unless otherwise stated. * n=4, ** n=3.*

Spool	Drawing velocities (m/min)	Draw ratio	Drawing temperatures (°C)	Rounds on the godets	Average filament diameter (μm)	Load on max. Load (N)	Ultimate tensile strength (MPa)	Strain on max. Load (%)
1	50, 70, 100, 102, 105	2.1	75, 80, 80	3, 3, 4	92 ± 15	4.4 ± 0.2	172 ± 25	46 ± 4
2	50, 70, 100, 102, 105	2.1	75, 80, 75	3, 3, 3	98 ± 32	4 ± 0.2*	150 ± 23*	43 ± 21*
3	50, 60, 90, 92, 95	1.9	75, 80, 75	3, 3, 3	107 ± 25	4.4 ± 0.8**	147 ± 15**	76 ± 20**
4	50, 60, 90, 92, 95	1.9	75, 80, 80	3, 3, 3	100 ± 25	3.4 ± 0.3**	132 ± 7**	30 ± 6**

The strain in the spool 1 was also at an acceptable level, because high strain (>50 %) would mean that the fibre could have been drawn more. The high strain of spool 3 (76 %) indicates that the temperatures and velocities of the drawing line was not enough. As already mentioned in the theoretical background –part, generally higher temperatures and velocities enable orientation and crystallisation of the fibre resulting in better mechanical properties. It can also be noted that the combination of highest temperatures and velocities in the drawing line resulted in best tensile properties and also desired filament diameter (spool 1). None of the fibres produced in this trial exhibited stress whitening which means that they were not extensively drawn.

The rounds around the godets also have an impact on the diameter and the properties of the fibre. It was expected that the more there are rounds around the godet the more the fibre is drawn and the longer it is under thermal treatment. This leads to thinner fibre with better mechanical properties. It seems that increasing number of rounds on the godets thins the fibre and also enhances its tensile properties. The first spool had better mechanical properties compared to the other spools and it had four rounds around the last godet pair while the other spools had 3 rounds around all godets. However, it has to be kept in mind that the difference of one round could be too small to have an effect that could be seen in the properties of the fibre. In addition, there was no spool with the exact same drawing velocities and temperatures to be compared with the spool 1.

In places one curly filament much thinner than the others could be found. The formation of this kind of filament is a sign of the fibre being stretched too much or unevenly. The velocities of the drawing units can be too high or the filament is getting stuck

under the other filaments when exiting a godet and getting drawn more than other filaments. This can be avoided by adjusting the angle of the two godets in the godet pairs, which was done from the next trial onwards. A larger angle between the godets increases the spaces between the rounds of the fibre. One possible reason can be also that there are melt streams with different thicknesses exiting the nozzle. The filter pack has an effect on the melt flow and thus different filter packs should be studied. The slit die also has its effect on the melt flow and might cause whirls in the melt ending up in uneven extrusion of the material through the nozzle.

As can be seen in Table 9.2. the standard deviations of the filament diameters are relatively large (24.5 µm in average) which is for example a quarter of a 100 µm diameter. The fluctuations in the filament diameter affect the quality of the textile products made from the fibre. Factors causing fluctuation of diameter can be for example the filter pack. A filter pack with multiple holes will homogenise the melt flowing through it and force it to mix. The fluctuation can also derive from unsteady feeding of the material in the hopper. This is a likely cause because the feeder is known not to have a variable feeding rate. The feeder also probably has a greater impact in filament diameter fluctuation than the choice of the filter pack.

9.1.2 Trial 2

The goal of the second trial was to investigate the effect of a different filter pack on the flow of the melt and the properties of the resulting fibre and also study the effect of changing the feed rate and the adjusted angle of the DUO units. The parameters which were kept constant throughout the trial are presented in Table 9.3. The temperatures of the extruder zones were slightly higher than in the first trial. The temperatures were increased because we wanted to make sure that the polymer is molten enough and study the effect of the higher temperatures on the thermal degradation of the material. In addition with the change of the temperature values we could provide more comprehensive pressure data for the shear viscosity calculations. The rounds on the godets were kept constant because finding the right velocities and temperatures for the godets was the focus of this trial.

Table 9.3. *The fixed parameters in trial 2.*

Extrusion temperatures (°C)	Filter pack	Drawing velocities (m/min)	Draw ratio	Rounds on the godets	Godet angle (mm)
165, 175, 185, 205	With a single large hole	50, 70, 90, 92, 95	1.9	3, 3, 3	9.6

The best mechanical properties in the first trial were obtained with the highest velocities of the drawing units (speed of the last drawing unit 102 m/min) and thus these velocities were chosen as starting velocities for this trial. However, the drawing produced some curly filaments despite that the angle of the godet pairs was now adjusted so that the filaments would not overlap. After noticing the curly filaments the velocities of the godets were decreased to avoid stretching the fibre too much. The angle between the godets might still also have to be increased in the next trial to ensure that the fibres run freely on the godets.

The studied parameters and the properties of the fibres are presented in Table 9.4. The drawing temperatures in the beginning of the trial were the same as in the previous one. Nevertheless, the combination of these temperatures with the decreased velocities caused the fibre to stick on the godets. This problem was solved by decreasing the temperatures of the godets. The last godet pair seemed to break the fibre repeatedly and after the second spool its temperature was further decreased to 70 °C.

Table 9.4. *The studied parameters and the properties of the fibres in trial 2. In tensile test n=3.*

Spool	Feed rate (g/h)	Drawing temperatures (°C)	Average filament diameter (μm)	Load on max. Load (N)	Ultimate tensile strength (MPa)	Strain on max. Load (%)
1	330	75, 75, 80	116 ± 29	4 ± 0.4	107 ± 14	79 ± 7
2	330	75, 75, 80	127 ± 41	4.2 ± 0.3	104 ± 18	56 ± 15
3	350	75, 75, 70	126 ± 28	4.7 ± 0.1	93 ± 4	78 ± 28

Three spools were manufactured in the second trial. As we can see in Table 9.4., the filaments were much thicker and exhibited much poorer tensile properties than in the first trial. This is because not as high velocities and temperatures of the drawing units could be employed. The high strain values obtained indicate that the fibres could have been drawn more. Also the feed rate was increased after the second spool because the melt pressure was low. This change generally results in thicker fibre. The feed rate was increased because the melt pressure was low (approx. 400 psi). The drawing parameters should have been increased proportionally, but the fibre could not stand the drawing. One possible reason for this could have been higher temperatures of the extruder zones which could have indicated more thermal degradation or simply wrong combinations of velocities and temperatures on the godets.

The fluctuation of the diameters were even higher (32.8 μm in average) than in the first trial. This could mean that the fluctuation is generally smaller with thinner filaments. The change of the filter pack seemed not to have the desired impact. However, it could be anticipated that a filter pack with multiple holes would homogenise the melt more than a filter pack with only one large hole. The increased feed rate could also cause more fluctuations in the feeding of the material and thus to the average diameter values.

9.1.3 Trial 3

The fixed parameters for the Trial 3 are shown in Table 9.5. The temperatures of the extruder zones were chosen to be between the values of the two last trials again to provide variable measurement data for viscosity estimation. The parameters which were varied in the trial and the results of the mechanical testing of the fibres are presented in Table 9.6. The feed rate was optimised so that the melt pressure would be around 500-600 psi, which has proven to be a good range in terms of fibre quality.

Table 9.5. *The fixed parameters in trial 3.*

Extrusion temperatures (°C)	Filter pack	Godet angle (mm)
162, 172, 182, 202	With large holes	9.5

Six spools were manufactured in this trial. The velocities of the drawing units were first kept the same as in the previous trial and increased after the first spool was manufactured. Slightly higher drawing temperatures were studied compared to the previous trial because it was anticipated that with higher temperatures the fibres could be drawn more. The average diameters of the filaments were between the diameter values obtained in the previous two trials and the fibres were mechanically better than in the second trial but still poorer than in the first trial. The achieved strain values indicate that the parameters are getting closer to the optimum drawing parameters.

Table 9.6. *The studied parameters and the properties of the fibres in trial 3. In tensile test n=5, until otherwise stated. * n=4, ** n=3. *** n=2.*

Spool	Feed rate (g/h)	Drawing velocities (m/min)	Draw ratio	Drawing temperatures (°C)	Rounds on the godets	Average diameter (μm)	Load on max. Load (N)	Ultimate tensile strength (MPa)	Strain on max. Load (%)
1	354	50, 70, 90, 92, 95	1.9	75, 80, 78	3, 3, 4	104	3.8 ± 0.2**	131 ± 34**	51 ± 11**
2	354	50, 75, 100, 102, 105	2.1	75, 80, 78	3, 3, 3	114	4.6 ± 0.4*	133 ± 31*	47 ± 10*
3	376	50, 75, 100, 102, 105	2.1	75, 80, 78	3, 3, 3	108	4.6 ± 0.4*	140 ± 36*	53 ± 10*
4	376	50, 75, 100, 102, 105	2.1	75, 80, 78	4, 4, 4	105	4.7 ± 1.7***	154 ± 23***	50 ± 23***
5	376	50, 75, 100, 102, 105	2.1	75, 78, 78	4, 4, 4	123	5 ± 0.6*	139 ± 43*	48 ± 26*
6	376	50, 75, 100, 102, 105	2.1	73, 78, 78	4, 4, 4	119	4.9 ± 0.8	109 ± 27	85 ± 26

In this trial we had a chance to study the effect of the rounds around the godets on the properties of the fibre. For example the spool number 4 had the same drawing parameters than spool 3 but there were one round more around each godet compared to spool 3. Spool 4 had an average diameter of 3 μm lower than spool 3 and its ultimate tensile strength was 14 MPa higher. This would indicate that increasing the number of rounds would result in thinner fibre with better mechanical properties. However, it has to be taken account that the number of parallel samples of spool 4 is only two which reduces the reliability of the result.

However, the fibre in the spools 5 and 6 was wrapped around the godets for one round more than the spool 3. The average filament diameter of spool 5 was 15 μm higher compared to spool 3. The spool 6 had the lowest ultimate tensile strength and the corresponding value of spool 5 was approximately the same as spool 3. Hence, no conclusions from the effect of the rounds around the godet can be drawn. However, the reason can be that one round more around the godets is not a difference big enough to

be reflected in the properties of the fibre. The effect of the number of the rounds should be studied with more notable differences.

The filter pack used in this trial was the same as in the first trial and it could be anticipated that it would decrease the diameter fluctuation. However, the average diameter fluctuation was 31.5 μm in this trial, which is very similar compared to the previous trial where a filter pack with a single large hole was used. It seems that the choice of the filter pack does not have a large impact on the variation of the filament diameters. Probably the unsteady feeding causes the large fluctuation.

9.1.4 Trial 4

The objective of the trial was to repeat the spool 1 of the first trial, which is the best spool produced so far. The extruder temperatures as well as the velocities and temperatures of the drawing units were kept the same throughout the trial and presented in Table 9.7. The extruder temperatures were close to the temperatures used in the first trial, but the nozzle temperature was 2 degrees higher. The temperature of the nozzle was increased to produce fibre with a smoother surface. The filter pack was chosen to be the same as in the previous trial. The drawing temperatures and velocities were the same as for the first spool of Trial 1 except the temperature of the last godet pair which had to be reduced to 78 °C because the fibre was sticking on the godet.

Table 9.7. *The fixed parameters in trial 4.*

Extrusion temperatures (°C)	Filter pack	Drawing velocities (m/min)	Draw ratio	Drawing temperatures (°C)	Godet angle (mm)
160, 170, 180, 202	With large holes	50, 70, 100, 102, 105	2.1	75, 80, 78	11.15 (DUO1), 11.23 (DUO2)

The feed rate and the rounds on the godets were varied in the trial. These parameters, the average filament diameters and the mechanical properties of the fibres are shown in Table 9.8. The feed rate was increased to 370 g/h after 2 spools because the melt pressure was below 500 psi and also to produce different pressure data with the real-time monitoring system for the viscosity calculations.

As previously mentioned, one goal of this trial was to repeat the spool 1 from Trial 1. The spool 1 in this trial is closest to that spool in terms of processing conditions but the spool 2 has more similar mechanical properties. The average filament diameter of spool 2 was almost identical but the ultimate tensile strength was approximately 20 MPa lower. It is hard to repeat the trials as the conditions slightly vary each day, for example the humidity of the air and atmospheric temperature. We also did not have exactly the same extrusion conditions as in the first trial because the melt behaved differently and the fibre was sticking on the last godet which it did not do in the first trial. There are

also always some unknown factors affecting the behaviour of the material in melt processing.

Table 9.8. *The studied parameters and the properties of the fibres in trial 4. (In tensile testing n=5, until otherwise stated). * n=4, ** n=3.*

Spool	Feed rate (g/h)	Rounds on the godets	Average diameter (μm)	Load on max. Load (N)	Ultimate tensile strength (MPa)	Strain on max. Load (%)
1	309	3, 3, 3	95 ± 21	3.8 ± 0.3*	136 ± 29*	62 ± 21*
2	309	4, 5, 3	90 ± 27	3.9 ± 0.9	153 ± 30	53 ± 31
3	370	3, 3, 3	118 ± 31**	5.2 ± 0.7**	134 ± 23**	64 ± 21**
4	370	3, 3, 3	111 ± 21	5.0 ± 0.1	125 ± 12	69 ± 30
5	370	3, 3, 3	125 ± 33*	5.0 ± 0.2*	117 ± 25*	97 ± 31*

The spool 2 had more rounds around the godets than the other spools. In this trial it seems to have a slightly thinning effect on the fibre and seems to have given it somewhat better mechanical properties. However, if we look at spools 3, 4 and 5 which have been manufactured using the exact same parameters, their average diameter ranges from 111 to 125 μm, which shows a rather large fluctuation. Also their ultimate tensile strength varies between 117 and 134 MPa and the strain from 64 to 97 %. This shows that even with the exact same parameters in the same processing day the properties of the fibres differ greatly. This could be caused by the unsteadiness of the feeding of the material. If the melt leaving the spinneret is inhomogeneous, so will be the quality of the fibre. However, the average diameter fluctuation is 26.6 μm which is similar, but surprisingly slightly lower than in the three previous trials.

There was also another problem that occurred during mechanical testing. In some samples one of the filaments was much thicker than the other ones and exhibited significantly lower tensile properties by breaking without any mentionable force during testing. The possible explanations for this are uneven feeding and the possible effect of the slit die to the melt.

The thermal degradation of the material during processing in these extrusion temperatures was characterised by measuring the change in inherent viscosity of samples collected from the nozzle compared to the viscosity of the raw material. The results are shown in Table 9.9.

Table 9.9. *The effects of processing on the inherent viscosity of packaging grade PLA in trial 4 (n=3).*

Sample	Inherent viscosity (dl/g)
Raw material	1.59 ± 0.02
After extrusion in 160, 170, 180, 202 °C	1.55 ± 0.08
Decrease in inherent viscosity	0.04
In per cents	2.52

The decrease in inherent viscosity is only 0.04 dl/g, which suggests that the material has hardly degraded at all during processing. This means that the temperatures used in the trial were good for minimising the thermal degradation of the material. Of course, when we are talking about packaging grade materials, more gentle processing temperatures can be used which results in less thermal degradation.

9.1.5 Trial 5

This trial's objective was mainly to provide measurement data for the viscosity calculations. For this purpose the focus was in varying the feed rate of the material and not the drawing parameters. The temperatures of the extruder and the drawing parameters are presented in Table 9.10. The extrusion temperatures were increased again in order to provide different pressure data.

Table 9.10. *The fixed parameters in trial 5.*

Extrusion temperatures (°C)	Filter pack	Drawing velocities (°C)	Draw ratio	Drawing temperatures (°C)	Godet angle (mm)
165, 175, 185, 205	With large holes	50, 70, 100, 102, 105	2.1	75, 80, 78	11.3

As previously mentioned, the feed rate was varied throughout the trial as can be seen in Table 9.11, where also the results of the mechanical testing of the fibres are presented. Surprisingly, the diameters of the filaments do not vary as much as would be expected. The difference in the feeding rate was approximately 130 g/h, but the difference in diameters is only 7 µm. Furthermore, the spools 2 and 3 have the same diameter value despite the supposed 60 g/h difference in the feed rate. It could be again that be-

cause of the feeder the diameters of the filaments fluctuate a lot. The average fluctuation of the diameter is 26.8 μm, which is the same magnitude as in the previous trials.

Table 9.11. *The studied parameters and the properties of the fibres in trial 5. (In tensile test n=5).*

Spool	Feed rate (g/h)	Rounds on the godets	Average diameter (μm)	Load on max. Load (N)	Ultimate tensile strength (MPa)	Strain on max. Load (%)
1	306	3, 3, 3	98 ± 23	3.7 ± 0.5	137 ± 9	68 ± 12
2	365	3, 3, 3	105 ± 25	4.8 ± 0.7	147 ± 37	72 ± 21
3	434	3, 3, 3	105 ± 39	4.4 ± 1.2	136 ± 56	35 ± 25
4	306	4, 3, 5	93 ± 26	3.4 ± 0.4	136 ± 34	55 ± 7
5	306	4, 5, 3	91 ± 21	3.5 ± 0.2	142 ± 41	60 ± 27

Later in the trial the number of the rounds around the godets was again experimented. The spool 4 had 4, 3 and 5 rounds around the godets and the spool 5 had 4, 5 and 3 rounds. The number of the rounds seems not to have a great impact on the diameter or the tensile strength of the fibres. Altogether the fibres produced in this trial seem better than in the other trials after the first one. Notably, the spool 6 has a satisfactory diameter and relatively good tensile strength. However, the problem of the single thicker filament persisted in the fibres produced in this trial.

The thermal degradation of the material was studied also in this trial as the temperatures employed were higher than in the previous trial. The results are gathered in Table 9.12.

Table 9.12. *The effects of processing on the inherent viscosity of packaging grade PLA in trial 5 (n=3).*

Sample	Inherent viscosity (dl/g)
Raw material	1.59 ± 0.02
After extrusion in 165, 175, 185, 205 °C	1.58 ± 0.02
Decrease in inherent viscosity	0.01
In per cents	0.6

The decrease of the inherent viscosity would have been anticipated to be more than with the 5 degrees lower extrusion temperatures. Surprisingly the difference is even smaller. This indicates that there is hardly any thermal degradation occurring in the extruder. At this point the result of the raw material could be questioned but the measurements were redone with the same results.

9.1.6 Trial 6

The objective of the sixth trial was to repeat Trial 5 because there was much noise in the pressure measurement data. This is why the extrusion temperatures, filter pack, drawing velocities and temperatures and the angle between the godets were kept the same from the last trial (Table 9.10). The feed rate and the rounds on the godets were varied and the mechanical testing results of the fibres can be seen in Table 9.13.

Table 9.13. *The studied parameters and the properties of the fibres in trial 6. (In tensile test n=5).*

Spool	Feed rate (g/h)	Rounds on the godets	Average diameter (μm)	Load on max. Load (N)	Ultimate tensile strength (MPa)	Strain on max. Load (%)
1	310	4, 5, 3	86 ± 29	3.8 ± 0.6	173 ± 50	71 ± 5
2	434	4, 6, 4	103 ± 26	5.8 ± 0.8	174 ± 45	87 ± 53

Only two spools were produced in the trial as the main goal was to get measurement data. However, both of the spools exhibited fairly good tensile properties and the first spool was acceptable also in terms of filament diameter. The high strain values (71 and 87 %) indicate that there could have been still more drawing. Both of the spools had more rounds around the godets (4, 5, 3 and 4, 6, 4) than most of the spools in the earlier trials. This time it seems to have been beneficial. The average diameter variation (27.5 μm) is roughly the same as in the previous trial.

In general in the trials with the packaging grade polylactide the effect of the drawing velocities could be seen by comparing the fibres within the first and third trial. In the first trial increasing the drawing velocity by 10 m/min in the two last godets seems to produce thinner fibres with better mechanical properties, but in the third trial the same increase between spools 1 and 2 produces fibre with very similar properties (131 and 133 MPa). Actually, the average filament diameter of the spool 2 with higher drawing velocities is 10 μm thicker compared to spool 1. It has to be taken into account that spool 1 of the third trial had one round more around the last godet pair which might have had a slight effect on the filament diameter.

We can also compare the spool 3 of the third trial with the spools 3-6 of the trial 4 and the spool 2 of trial 5 to get an idea of the effect of the drawing velocity on the fibre properties. The spool 2 of the trial 5 had a 5 m/min lower velocity on the second godet pair compared to the other spools. This has no effect on the draw ratio which is the ratio of the velocities of the winder and the first godet. The average filament diameters of the spools with lower velocities vary from 105 to 125 μm and the value for the spool 3 of trial 3 is 108 μm. The corresponding values for ultimate tensile strength are 117-147 MPa and 140 MPa. Only the spool 2 of the trial 5 has a lower filament diameter and higher tensile strength than the spool 3 of the trial 3. It has to be noted that the feed rate in the trial 5 has been slightly lower compared to the other spools mentioned here. This might cause the fibre to be thinner and mechanically relatively stronger. We can conclude that in general higher drawing velocities produce thinner fibre with better mechanical properties.

We can see the effect of the drawing temperatures in the trials 1, 2 and 3. The temperature of the last godet pair in the spool 1 of trial 1 was 5 °C higher compared to the spool 2 of the same trial. The spool 1 also had one round more around the last godet pair but it probably had only a negligible effect on the properties of the fibre. The spool 2 had 5 μm higher average filament diameter and 22 MPa lower tensile strength, which suggests that higher temperatures on the godets would enable more drawing. Comparing the spools 3 and 4 from the same trial shows the same result in regard of the filament diameter but surprisingly the ultimate tensile strength has been higher with the lower temperatures. On the other hand, the decrease of 2 °C in the first godet between spools 5 and 6 in trial 3 has resulted in 4 μm thinner fibre with 30 MPa lower tensile strength. Thus, no reliable conclusions can be drawn from the effect of the drawing parameters on the properties of the fibre. More trials are required where only the parameter studied is varied and all the others are kept constant. Unfortunately, no reliable conclusions could be drawn from the effect of the filter pack or of the number of the rounds around the godets either.

9.2 Trials with the GMP grade polylactide

After studying the effects of the processing parameters on the properties of the fibre the trials with the GMP grade polylactide were started. The ultimate goal of these trials was to produce fibre that could be treated with widely used textile post-processing methods and find the optimum parameters for this. In order to reduce the fluctuation in the filament diameters and improve the quality of the fibre, a new gravimetric feeder was introduced.

9.2.1 Trial 1

The extrusion temperatures were optimised in the beginning of the trial and after that kept constant along the feed rate. Different temperatures and velocities of the drawing units were studied, but all the spools were manufactured using the fixed parameters in-

troduced in Table 9.14. Higher temperatures on the godets caused sticking of the fibre and higher velocities made the fibre exhibit stress whitening, breaking of the fibre on the godets and filament breaks on the spools.

When comparing the extrusion temperatures and the drawing parameters in Table 9.14. to the corresponding values in the earlier set of trials, it can be noticed that much higher temperatures and velocities were employed. This difference yields from the material properties (Table 7.1.) as the highly purified medical grade material has a much higher melting temperature and glass transition range. In addition we are not aware of the composition of L- and D- enantiomers in the packaging grade material but the GMP grade material is known to have 96 w-% of L-lactide, which makes its behaviour very close to pure PLLA homopolymer. The GMP grade material is more crystalline than the packaging grade polylactide which allows it to stand higher extrusion temperatures, more drawing and heat treating in higher temperatures.

Table 9.14. *The fixed parameters in trial 1.*

Extrusion temperatures (°C)	Filter pack	Feed rate (g/h)	Drawing temperatures (°C)	Drawing velocities (m/min)	Draw ratio	Godet angle (mm)
215, 225, 252, 272	With small holes	300	85, 90, 85	50, 90, 130, 132, 135	2.7	11.3

The starting temperatures of the extrusion zones were based on earlier trials with a GMP grade material with a similar set-up without the slit die. The temperatures were first chosen to be lower (210, 220, 245 and 265) because increasing the temperatures during the trial is quicker than waiting for the massive metal parts to cool down. Also finding the right temperatures from low temperatures up minimises the thermal degradation and there is a lower risk of choosing too high temperatures. The right temperatures were chosen based on the melt quality; the melt exiting the nozzle should be transparent and flow nicely. In addition the surface of the cooled extrudate should be smooth (there should not be signs of melt fracture).

The filter pack with small holes was chosen to maximise the homogenisation of the melt in the extruder. The feed rate was chosen to correspond to the feed rate of the first spool of the first packaging grade trial because that spool exhibited the best mechanical properties and a good filament diameter value. A lower feed rate probably would not fill the screw enough and a higher rate would result in too thick fibre. The angle between the godet pairs was optimised already in the packaging grade trials and we saw no reason to change it.

There were four spools manufactured in this trial, but the last two of them contained so little fibre that the spools were decided to leave without mechanical testing. The fibre on those spools also exhibited stress whitening. The results of the mechanical testing of

the first two spools are gathered in Table 9.15. Here the demanded mechanical properties and filament diameters are added below the table because now with the GMP grade material the required values can actually be compared with the results obtained from these trials. The results that are on the acceptable level can be seen with a green background. The first spool is already acceptable in terms of the diameter and strain, but the tensile strength still needs further optimisation. However, the limit for the ultimate tensile strength is only 20 MPa away although it would be better to obtain fibre with more superior properties and not only just above the acceptance limit.

The ultimate tensile strength of the samples is low also when comparing to 4-filament fibre which has been produced using a similar material (PLDLA 96/4, i.v. 5.48 dl/g) with the conventional set-up. The non-irradiated fibre produced with a medium screw speed (7 rpm) and the lowest nozzle temperature (277 °C) is chosen for comparison, because the filament diameter of these fibres is closest to the fibres in the this work. The ultimate tensile strength of the chosen reference fibre is approximately 430 MPa. The strain on the other hand is slightly below 40 % which is very close to the average value of the results in this work. (Ellä et al. 2011a.)

Table 9.15. *The studied parameters and the properties of the fibres in trial 1. (In tensile test n=5).*

Spool	Rounds on the godets	Average filament diameter (μm)	Load on max. Load (N)	Ultimate tensile strength (MPa)	Strain on max. Load (%)
1	4, 6, 4	82 ± 16	6.1 ± 0.9	296 ± 73	36 ± 6
2	5, 7, 5	96 ± 16	6.4 ± 0.6	219 ± 44	54 ± 10
Goal	-	75–90	> 8	> 320	25–45

Because no exact conclusions could have been drawn from the effect of the rounds around the godets, the experiments continued in this trial. The first spool was manufactured with 4, 6 and 4 rounds while the second spool was made using one round more on each drawing unit. This time adding the rounds made the fibre thicker and deteriorated the mechanical properties. All other drawing parameters were kept at the same level, so the difference did not yield from changing the other parameters. Also the strain value of the second spool was higher compared to the first one, which actually indicates that there was less draw on the fibre. However, as could be seen from the strain results of the *in vitro* studies the reliability of them is slightly questionable.

There was still notable fluctuation in the filament diameter (16 μm in average) but the deviation was significantly smaller compared to most of the packaging grade fibre (15-42 μm). It should be noted that the deviation is very similar to the best spool (spool 1 in the first trial) of the packaging grade trials. The smaller fluctuation yields probably

from the change of the feeder into a new, much more accurately feeding gravimetric device. Also the use of the filter pack into one with small holes probably has made the melt slightly more homogenous and to exit the nozzle in a more constant manner.

The extent of thermal degradation was also studied in the GMP grade trials. The inherent viscosity results are presented in Table 9.16.

Table 9.16. *The effects of processing on the inherent viscosity of PLDLA 96/4 in trial 1 (n=3).*

Sample	Inherent viscosity (dl/g)
Raw material	3.63 ± 0.08
After extrusion	2.52 ± 0.02
Decrease in inherent viscosity	1.11
In per cents	30.6

The decrease of inherent viscosity is much higher in the medical grade material than compared to the packaging grade material. Naturally, the higher extrusion temperatures create more thermal stress on the material during processing but also the higher molecular weight of the start material affect the degree of degradation. Materials with higher molecular weight degrade more during processing, as is already mentioned in the theoretical background section. The lower molecular weight makes the material to better resist the shear forces in the extruder. PLDLA with same L/D –ratio and a higher initial inherent viscosity (4.8 dl/g) experienced similar thermal degradation (34 % drop in i.v.) during melt processing in similar extrusion conditions (the temperatures in the extruder were 200-268 °C). In comparison, the same material with an initial i.v. of 2.2 dl/g did not show any thermal degradation in temperatures of 170-240 °C. (Paakinaho et al. 2009.) Although, these results show also the effect of drawing as the viscosity values were measured from fibre samples.

9.2.2 Trial 2

The main goal of the second trial with the GMP grade material was to enhance the mechanical properties of the fibres by increasing the drawing velocities and the temperatures on the godets. The fixed parameters of the trial are presented in Table 9.17. The extrusion temperatures were optimised already in the first run although the temperature of the nozzle was increased by two degrees because the fibre slightly exhibited melt fracturing. The filter pack with small holes was proven to be the best choice. The number of the rounds on the godets of the first spool of the last trial was chosen as the rounds in this trial because that spool exhibited better properties than the second one.

Table 9.17. *The fixed parameters in trial 2.*

Extrusion temperatures (°C)	Filter pack	Feed rate (g/h)	Rounds on the godets	Godet angle (mm)
215, 225, 252, 274	With small holes	300	4, 6, 4	11.3

The drawing parameters were changed in this trial in order to obtain better mechanical properties to the fibre. These parameters and the results of the tensile testing are gathered in Table 9.18. The velocities of the drawing units as well as the temperatures of the godets were increased. The winding speed in the first spool was accidently left at 145 m/min which resulted in similar draw ratios in spools 1-3 even though the velocities of the godets in the drawing line were varied.

Table 9.18*. The studied parameters and the properties of the fibres in trial 2. (In tensile test n=5).*

Spool	Drawing velocities (m/min)	Draw ratio	Drawing temperatures (°C)	Average diameter (μm)	Load on max. Load (N)	Ultimate tensile strength (MPa)	Strain on max. Load (%)
1	50, 90, 130, 132, 145	2.9	90, 95, 90	82 ± 13	4.8 ± 0.8	224 ± 37	29 ± 7
2	50, 95, 140, 142, 145	2.9	90, 95, 90	91 ± 10	6.3 ± 0.4	245 ± 49	49 ± 3
3	50, 95, 140, 142, 145	2.9	90, 100, 95	85 ± 20	5.2 ± 0.8	245 ± 43	33 ± 6
4	60, 100, 150, 152, 155	2.58	92, 105, 100	100 ± 30	5.3 ± 1.0	218 ± 44	57 ± 9
Goal	-			75–90	> 8	> 320	25–45

Again the results in acceptable limits are shown against a light green background. We can see that two spools (numbers 1 and 3) reached the requirements in filament diameter and strain. However, the problem of insufficient mechanical properties still persists. Against the expectations the highest drawing velocities and highest temperatures on the godets did not result in thinner and stronger fibre but in thicker and weaker fibre. Maybe the key here is the draw ratio and not the absolute drawing velocities. Higher draw ratios should be studied and if it seems that the fibre cannot stand the drawing, the feed rate should be increased proportionally. Nevertheless, the strain values of the

spools 1 and 3 indicate that not much more strain could be applied so the processing window here could be quite narrow.

The temperatures of the godets seem slightly low for the material to be sticking on them. The sticking might also be caused by the static electricity that these materials exhibit. This should be confirmed by testing higher temperatures on the godets. Also the exact place where the stress whitening occurs should be identified. The speed of the fibre might be too high for this to be done visually, but the fibres could be guided on a godet and let it accumulate for a while and afterwards try to inspect the fibre for signs of stress whitening.

The variation in the filament diameter in this trial was 18.25 µm in average which is slightly more than in the previous trial but again much lower than in the trials with the custom made feeder and the packaging grade polylactide. The difference can be explained by trial-to-trial variation.

The effect of the extrusion temperatures on the i.v. of the extrudates was studied also on this trial, because the temperature of the nozzle was slightly increased from the previous trial. The results can be seen in Table 9.19.

Table 9.19. *The effects of processing on the inherent viscosity of PLDLA 96/4 in trial 2 (n=3).*

Sample	Inherent viscosity (dl/g)
Raw material	3.63 ± 0.08
After extrusion	2.47 ± 0.03
Decrease in inherent viscosity	1.16
In per cents	32.0

It would be anticipated that the change of 2 degrees on the nozzle would not have a great impact on the thermal degradation of the material, especially kept in mind that the material spends a very short time in the nozzle. And indeed, the decreases in i.v. in this and the previous trial are the same magnitude. The drop is only 0.05 dl/g (1.38 %) higher than in the previous trial and taking on account that the standard deviation of the raw material samples alone is higher than the difference in the average values, this is not a significant difference.

9.3 Hydrolytic degradation studies

In order to predict how a material will perform once implanted, the situation is simulated in laboratory by exposing the material to a hydrolytic environment with pH buffering properties. This way it is possible to determine the point of time when the material's

properties start to deteriorate and the rate of the degradation. In this study the fibres' mechanical performance and the changes in thermal properties, molecular weight and viscosity were examined along the hydrolysis studies. The degradation studies of the fibre produced with the conventional set-up were performed as a reference for future *in vitro* trials of the fibre manufactured with the real-time monitoring set-up.

9.3.1 Molecular weight

As a biodegradable polymer, PLA degrades in the presence of water by simple scission of the ester bonds in the polymer chains. This can be seen as decreasing molecular weight, as it is the direct measure of the polymer chain length. The decrease of molecular weight of non-irradiated and irradiated fibre can be seen in Figure 9.1. Both weight-average and number-average molecular weights are plotted in the same figure and the results are given in relative values compared to a 0-week sample. The calculated values of the GPC measurements can be found in Appendix 3. The M_w of the non-irradiated fibre decreased fairly steadily to 47 % (89 300 Da) from the initial value of non-hydrolysed fibre (184 800 Da) in 36 weeks. The number-average molecular weights of the same fibre were significantly lower; in 36 weeks the M_w dropped to 54 % (44 500 Da) compared to the initial molecular weight (81 200 Da).

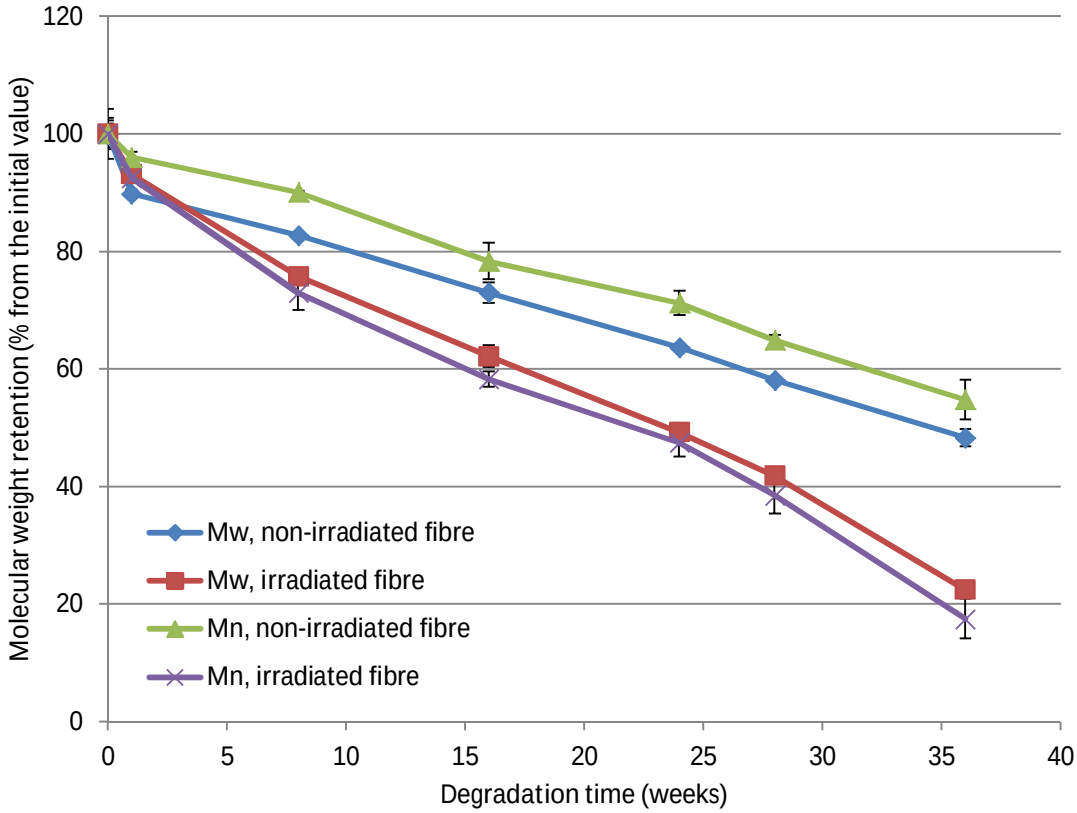

Figure 9.1. *Weight-average and number-average molecular weight retention of irradiated and non-irradiated fibre samples during hydrolytic degradation studies (n=2).*

The M_w of the fibre was reduced to 23 % (41 800 Da) of the initial value with gamma irradiation. The irradiation dropped the M_n of the fibre slightly less, to 26 % (20 800

Da) compared to the non-irradiated sample. In the hydrolysis the irradiated fibre degraded more rapidly than the non-irradiated fibre; M_w decreased 78 % (to 9 400 Da) after 36 weeks. Also the M_n of the irradiated fibre was reduced quicker than the M_w, but the difference was smaller than with the non-irradiated fibre. The M_n of the irradiated material was reduced to 17 % (3 600 Da) after 36 weeks in hydrolysis.

The degradation rate is similar or slightly quicker in comparison to earlier studies which are presented in Table 9.20 (Ellä et al. 2007; Paakinaho et al. 2009; Ellä et al. 2011b). The material examined in all of these studies is gamma irradiated 4-ply PLDLA 96/4 fibre. As we can see in Table 9.20, in (Paakinaho et al. 2009) two materials with different initial inherent viscosities have been studied. The initial i.v. of the material in the current study falls between the two grades of PLA used in the study by Paakinaho et al. The reported M_w decreases in that study were 59 % and 7 % of the material with initial i.v. of 4.8 and 2.18, respectively. In this study the corresponding drop in 24 weeks is ~ 50 %. The fibre degraded at a slightly higher rate than in (Ellä et al. 2007), where the M_w drop was ~ 27 % in 20 weeks (the corresponding result in this study would be 44 %). The fibre in this study had ~6 000 Da higher initial molecular weight, which might explain why it degraded at a slightly higher rate. It also degraded slightly quicker than the fibre in (Ellä et al. 2011b), where the fibre experienced a M_w and M_n drop of ~70 % in 36 weeks. It has to be borne in mind that each patch of fibre is processed using slightly different processing conditions and the properties of the fibres may differ and thus the different fibre patches cannot be directly compared.

Table 9.20. *The comparison of molecular weight decrease during hydrolytic degradation between earlier studies and the current study. The values marked with an asterisk are estimated from a figure.*

Study	Initial i.v. of the raw material (dl/g)	Initial Mw of the fibre (Da)	Mw of the fibre after degradation (Da)	Decrease in Mw (%)	Degradation time (weeks)
Ellä et al. 2007	5.48	35 500	25 800	27	20
Current study	3.49	41 800	23 300	44	20
Paakinaho et al. 2009	4.8	29 000*	12 000*	59	24
Paakinaho et al. 2009	2.18	28 000*	26 000*	7	24
Current study	3.49	41 800	20 600	49	24
Ellä et al. 2011b	5.47	32 000*	10 000*	69	36
Current study	3.49	41 800	9400	78	36

The polydispersity index (PDI) of the samples was calculated from the molecular weight results. The index reflects the width of the molecular weight distribution; a higher number indicates a wide distribution of different length chains and a low value refers

to a narrow distribution with similar length polymer chains (for example GPC standards typically have a low PDI). The relative PDI results of the non-irradiated and irradiated fibres are plotted in Figure 9.2. The PDI of the non-irradiated fibre decreased 12 % from the initial value (2.3) in 36 weeks whereas the PDI of the irradiated fibre increased 30 % (to 2.61) from the initial value (2.0) in 36 weeks. Most of the increase occurs within the last 10 weeks of the incubation period. The PDI of the non-irradiated fibre remains at a fairly constant level, although a slight decrease can be interpreted from the graph.

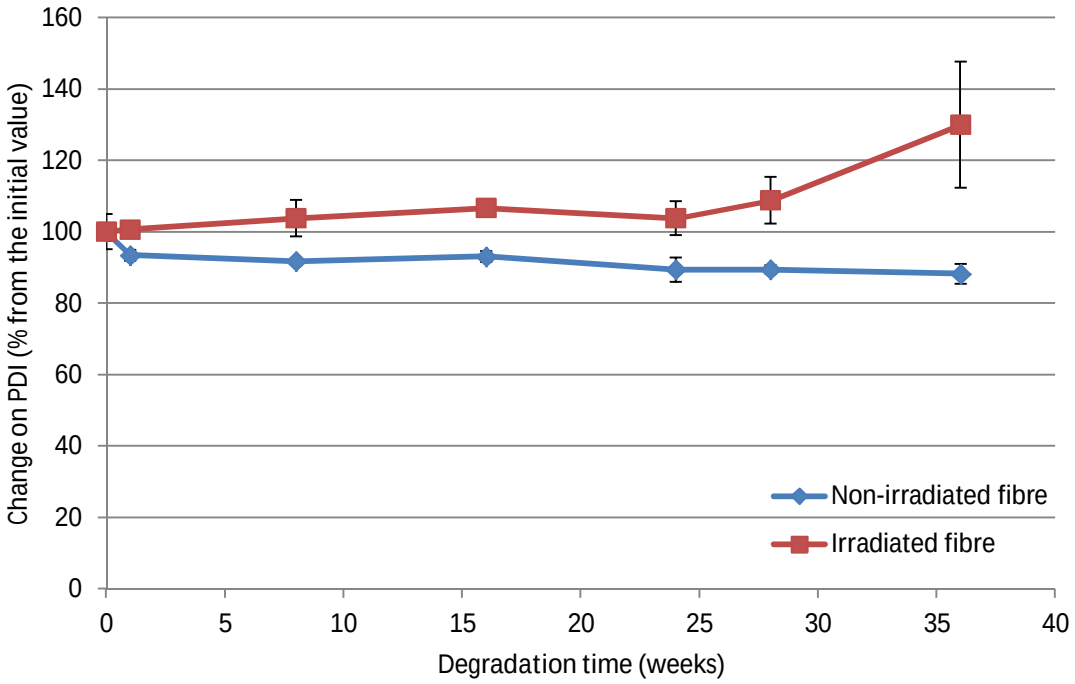

Figure 9.2. *Changes in polydispersity index of irradiated and non-irradiated fibre samples during hydrolytic degradation studies (n=2).*

As the fibre degrades in the aqueous medium and the polymer chains are cut, polymer chains of different length are created and the molecular weight distribution widens. This is exactly what happens in the irradiated fibre similarly than in (Ellä et al. 2011b) (the PDI increases from ~1.7 to ~1.8 over 36 weeks *in vitro*). Interestingly, in (Ellä et al. 2007) the PDI of the fibre dropped from 1.79 to 1.69 in 20 weeks.

The gamma irradiation diminished the PDI from 2.3 to 2.0. Probably the irradiation cut the chains to a more similar length. The same phenomenon was seen in (Paakinaho et al. 2009), where the differences in the initial molecular weights were evened out with gamma irradiation. It seems that the treatment results in certain molecular weight and PDI.

9.3.2 Inherent viscosity

The changes in the inherent viscosity of the material reflect the changes in the molecular weight as a dissolved sample with shorter chains flows faster (e.g. has a lower i.v.). The

relative i.v. results of the fibres are presented in Figure 9.3. and the absolute values are gathered in Table 9.21. A constant decrease in the i.v. was seen during the incubation period for both non-irradiated and irradiated fibre.

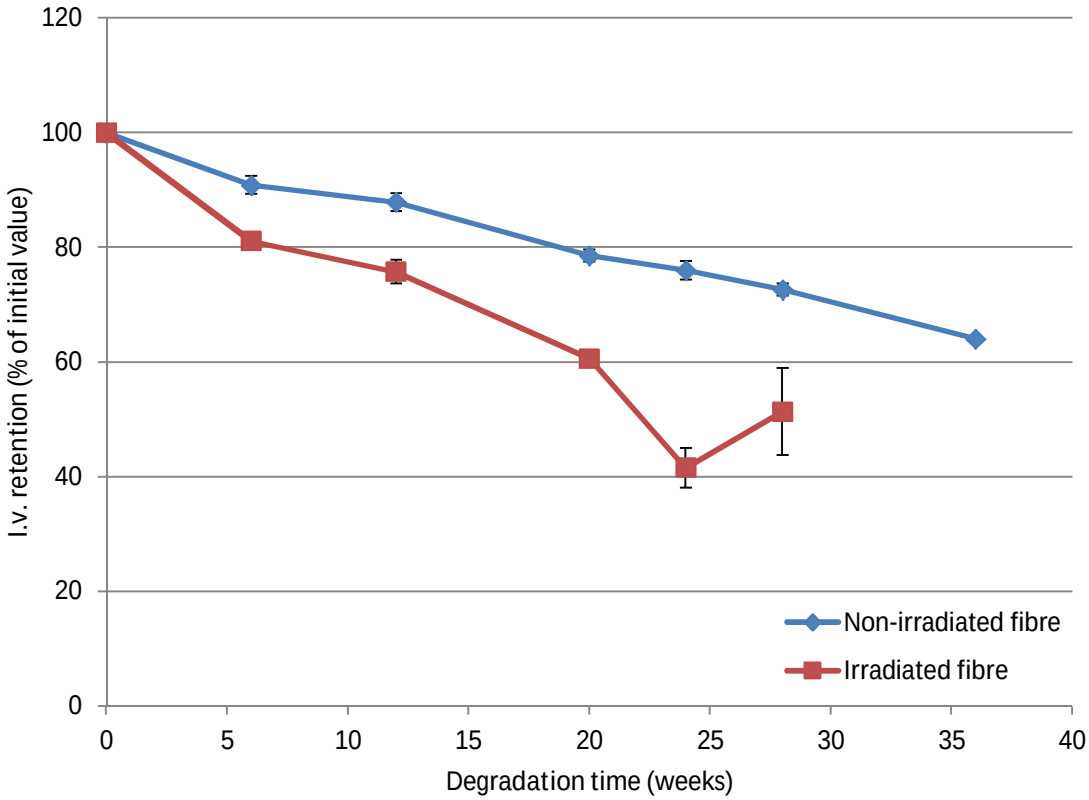

Figure 9.3. *Inherent viscosity retention of irradiated and non-irradiated fibres during hydrolytic degradation studies (n=2).*

Table 9.21. *Inherent viscosity data of the irradiated and non-irradiated fibres during hydrolytic degradation studies (n=2).*

Hydrolysis week	Sterility	I.v. (dl/g)	S. D.
0	no	2.69	0.04
6	no	2.44	0.04
12	no	2.36	0.04
20	no	2.11	0.03
24	no	2.04	0.04
28	no	1.95	0.03
36	no	1.72	0.01
0	yes	1.02	0.06
6	yes	0.83	0.01
12	yes	0.78	0.02
20	yes	0.62	0.00
24	yes	0.43	0.04
28	yes	0.53	0.08

The i.v. of the non-irradiated fibre dropped 36 % in 36 weeks and the irradiated fibre lost 49 % of its initial i.v. in 28 weeks. The degradation rate is in line with (Ellä et al. 2011a), where the i.v. decreased 50 % in 28 weeks.

9.3.3 Thermal properties

Measuring the thermal properties gives a different insight in the degradation of the material. Usually a decrease in material's molecular weight is related to a decrease in both its melting temperature and the glass transition temperature. Also the shape of the melting endotherm can change along the degradation period. The DSC results are gathered in Appendix 4. The melting temperature of the non-irradiated fibre decreased 3 degrees during the 36 weeks of incubation. Surprisingly the change with the irradiated fibre was smaller, only 0.5 °C. Similar behaviour was observed in (Ellä et al. 2007), where a decrease of only 0.6 °C was noticed with irradiated fibre.

The shapes of the melting endotherms differed in both gamma irradiated and non-irradiated samples. Example thermograms from the beginning, mid-way and end of the hydrolysis series of both, non-irradiated and irradiated samples are plotted in Figure 9.4. and Figure 9.5., respectively. The melting peak of the non-irradiated fibre seems to get larger and narrower as the degradation progresses. The melting behaviour of the irradiated fibre seems to be the opposite: the peaks widen and get shallower with the degradation. This probably indicates an increase in the crystallinity when the increased amount of crystals requires more energy. This makes the melting peak larger. The melting temperatures have been analysed from the first heating cycle which better reflects the real state of the material during the hydrolysis.

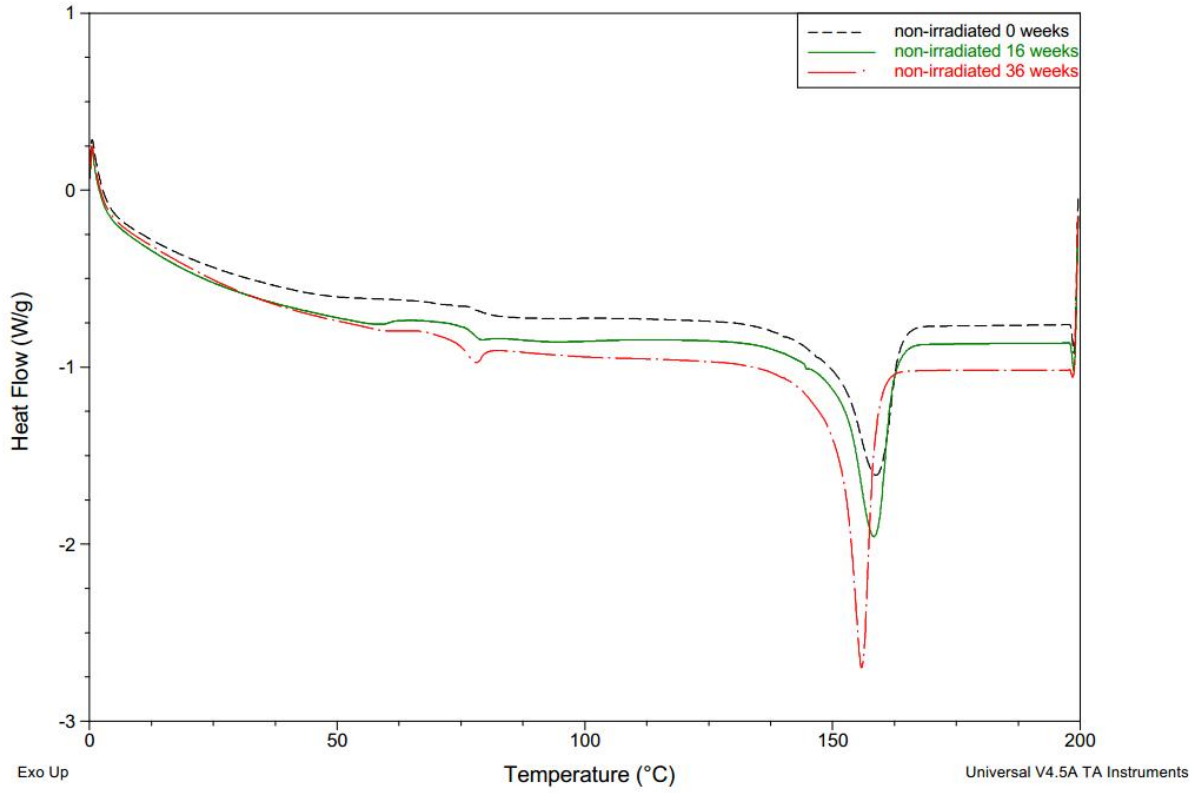

Figure 9.4. *Example DSC thermograms of the first heating cycle of the non-irradiated fibre during hydrolytic degradation studies.*

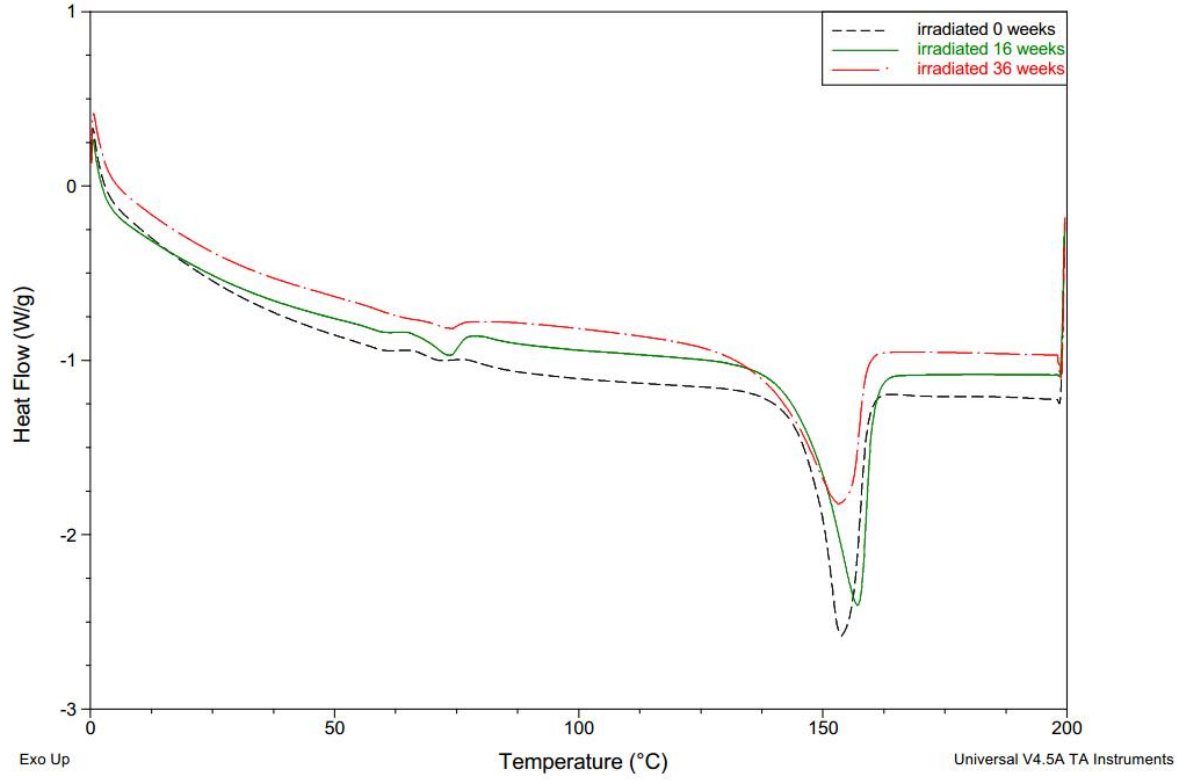

Figure 9.5. *Example DSC thermograms of the first heating cycle of the irradiated fibre during hydrolytic degradation studies.*

For comparison, the thermograms from the second heating cycle are presented in Figure 9.6. The second heating cycle shows the properties or the material itself, as all the thermal history has been removed in the first heating cycle. The graphs concerning the non-irradiated fibre show only a very slight change in the size of the melting peak. Probably the cooling cycle has induced a very small amount of crystallinity in the samples, because due to shorter polymer chains the crystallisation happens easier. In the thermograms of the irradiated samples a clear cold crystallisation and an increasing bimodal melting peak can be observed. The cold crystallisation is induced because the cooling rate in the DSC is not slow enough for the crystals to form. In the second heating when the material gets enough energy the polymer chains are organised into crystals which melt almost immediately after forming. Also a steady increase in the area of the cold crystallisation peak can be observed. As mentioned earlier, the hydrolytic degradation has made the molecular mass distribution wider which enables crystallisation.

A clearly increasing bimodality can be observed from the thermograms of the irradiated samples. The bimodality indicates that there can be two different types of crystals formed which melt in different temperatures. The cooling cycle can also introduce some imperfect crystallites which cause the second melting peak. A similar kind of bimodality has been detected also for example in (Kellomäki et al. 2000) with PLDLA 96/4 plates.

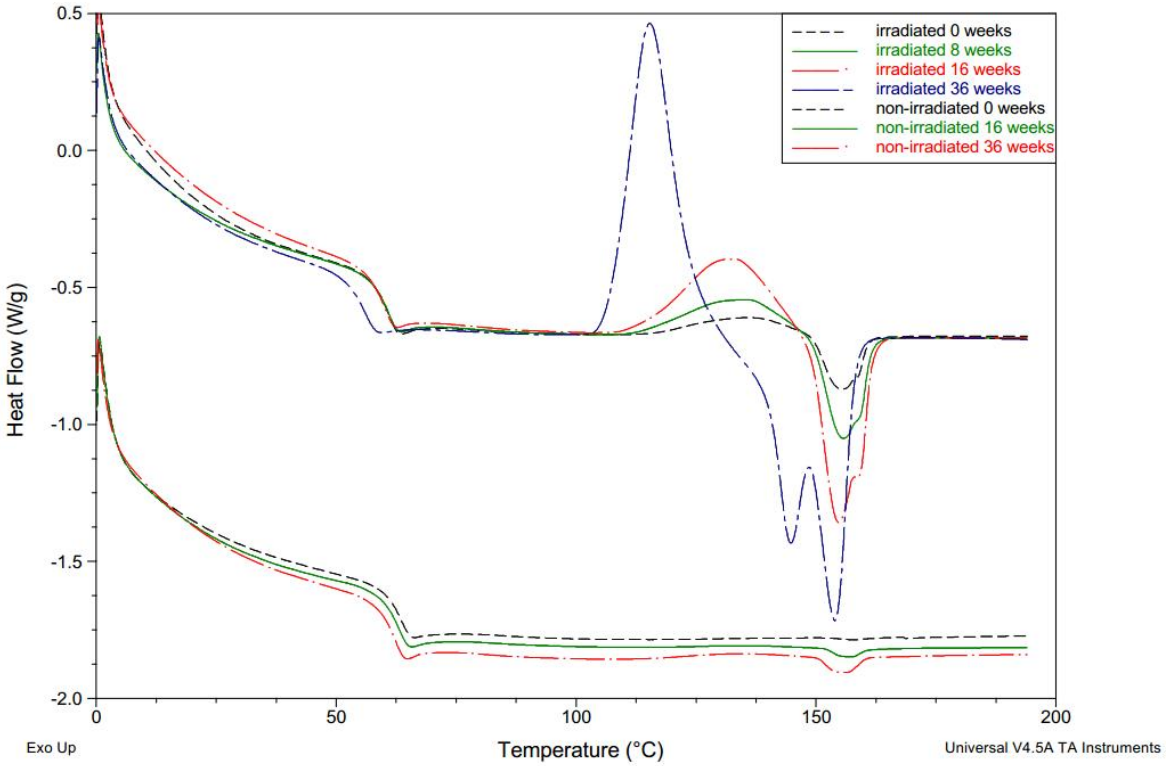

Figure 9.6. *Example DSC thermograms from the second heating cycle of irradiated and non-irradiated fibres during hydrolytic degradation.*

The results on the effects of the hydrolytic degradation on the glass transition temperature are plotted in Figure 9.7. No remarkable changes were detected in the case of the non-irradiated fibre but the glass transition temperature of the irradiated fibre decreased by 5 °C in 36 weeks. This was expected as degraded material requires less energy to transit from a glassy state to a rubbery state in heating. The results are in line with the reported study (Ellä et al. 2007), where a drop of 1.6 °C was reported in 20 weeks of incubation.

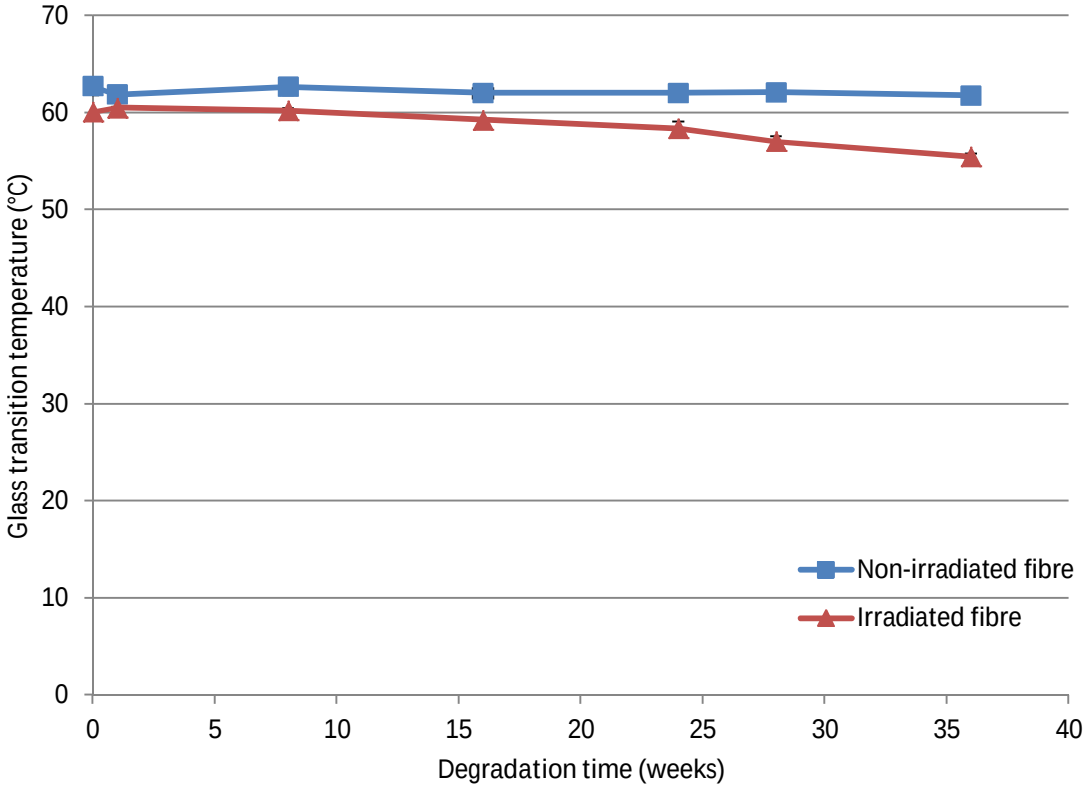

Figure 9.7. *The glass transition temperature of irradiated and non-irradiated fibres during hydrolytic degradation (n=2).*

The crystallinity of the studied fibres is presented in Figure 9.8. It can be noted that the initial values of the non-irradiated and the irradiated fibres differ by 11 %. The gamma irradiation seems to have increased the crystallinity of the fibres. During the hydrolysis the crystallinity of the irradiated fibre is increased by an additional 2 % while the crystallinity of the non-irradiated fibre is 6 % higher after 36 weeks. PLA is a semi-crystalline polymer where the amorphous regions degrade first leaving the crystalline parts intact. In addition dissolving of the amorphous regions provides more space for the chains to organise as new crystallites, inducing higher crystallinity.

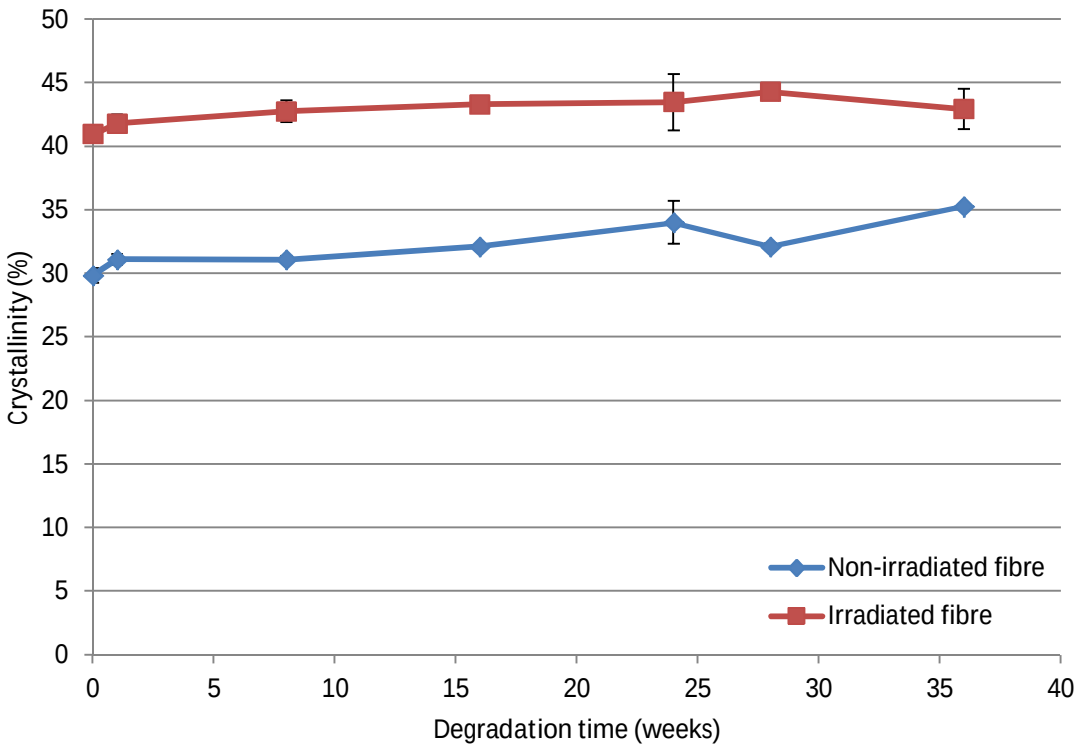

Figure 9.8. *Changes in crystallinity of the irradiated and non-irradiated fibres during hydrolytic degradation (n=2).*

The crystallinity of the irradiated material increased less compared to (Ellä et al. 2007) where the crystallinity of the fibre has increased ~ 22 % in 20 weeks. However, the initial crystallinity has been higher in the current study.

9.3.4 Mechanical properties

The mechanical properties (tensile strength, load and strain at max. load) of the fibres were measured at each time point of the hydrolysis. The relative tensile test results are plotted in Figure 9.9. and the absolute values can be found in Appendix 5. The tensile strength is the most important tool for evaluating the mechanical performance of the fibre *in vitro* and *in vivo*, because it is related to the cross-sectional area of the sample.

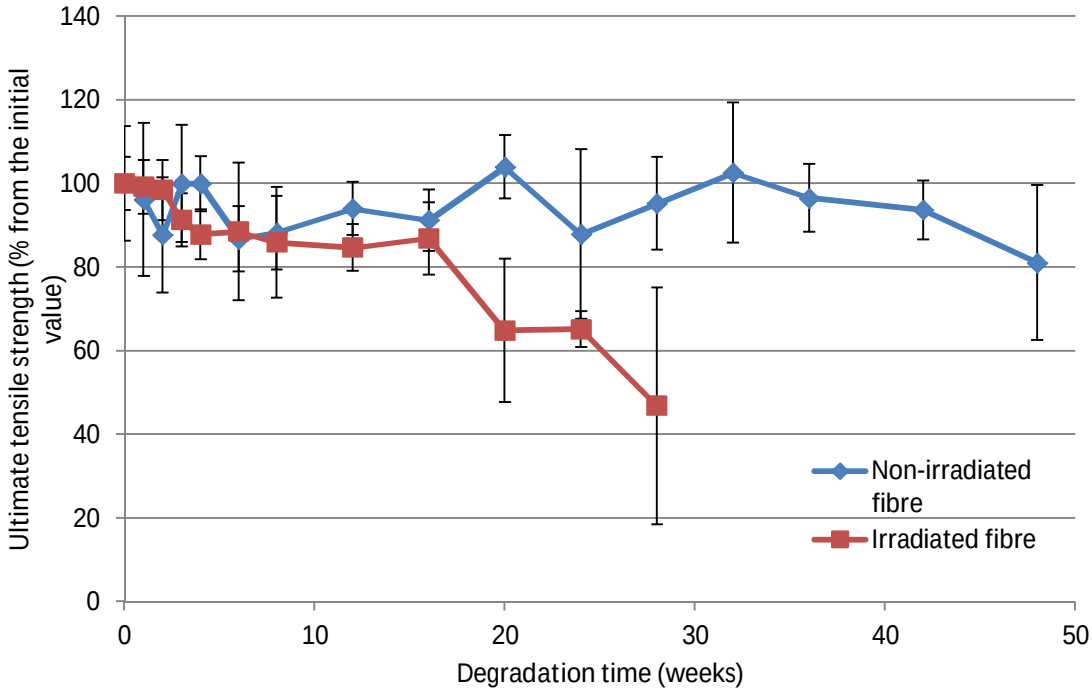

Figure 9.10. *Ultimate tensile strength retention of irradiated and non-irradiated fibres during hydrolytic degradation studies (n=3-5).*

The non-irradiated fibre exhibits no statistically significant changes during the whole incubation period. The average tensile strength at 48 weeks is 81 % (306 MPa) of its initial tensile strength (378 MPa).

The gamma irradiated fibre showed a much more dramatic decrease in tensile strength. Its tensile strength dropped by 53 % (to 114 MPa) of the initial strength (243 MPa) in 28 weeks, after which the fibre was too degraded to be tested. However, it can be said that the fibre retained its mechanical performance until 16 weeks because no statistically significant changes can be seen before that. The hydrolytic degradation rate is very similar to the reported study (Ellä et al. 2007) where the fibre retained 66 % of its tensile strength for 20 weeks, whereas the corresponding value in this study is 65 %. The decrease in the tensile strength of the fibre is related to the molecular weight decrease of the polymer as shorter chains exhibit poorer mechanical properties. Indeed, the deterioration of the mechanical properties relates well with the decrease in molecular weights.

The changes in strain properties of the fibre at maximum load can indirectly give an idea of the crystallinity of the material. If there are more crystals in the material, it behaves more rigidly and shows brittle behaviour (e.g. lower strain). The strain results of the degradation studies are shown in Figure 9.11. The standard variations are large, which gives an insight to the reliability of these results. However, the strain of the non-irradiated fibre seemed to have an overall upward trend until 48 weeks when the increase was 141 % (56 %). Only 18 % of the initial strain was left after 28 weeks. In (Ellä et al. 2007) the strain increased from 26 % to 36 % in 20 weeks. It would be anticipated that the increasing crystallinity of the material seen in the DSC results would lead

to decreasing strain values. This is how the irradiated fibre behaves but with the non-irradiated fibre there is a statistically significant increase of 20 %.

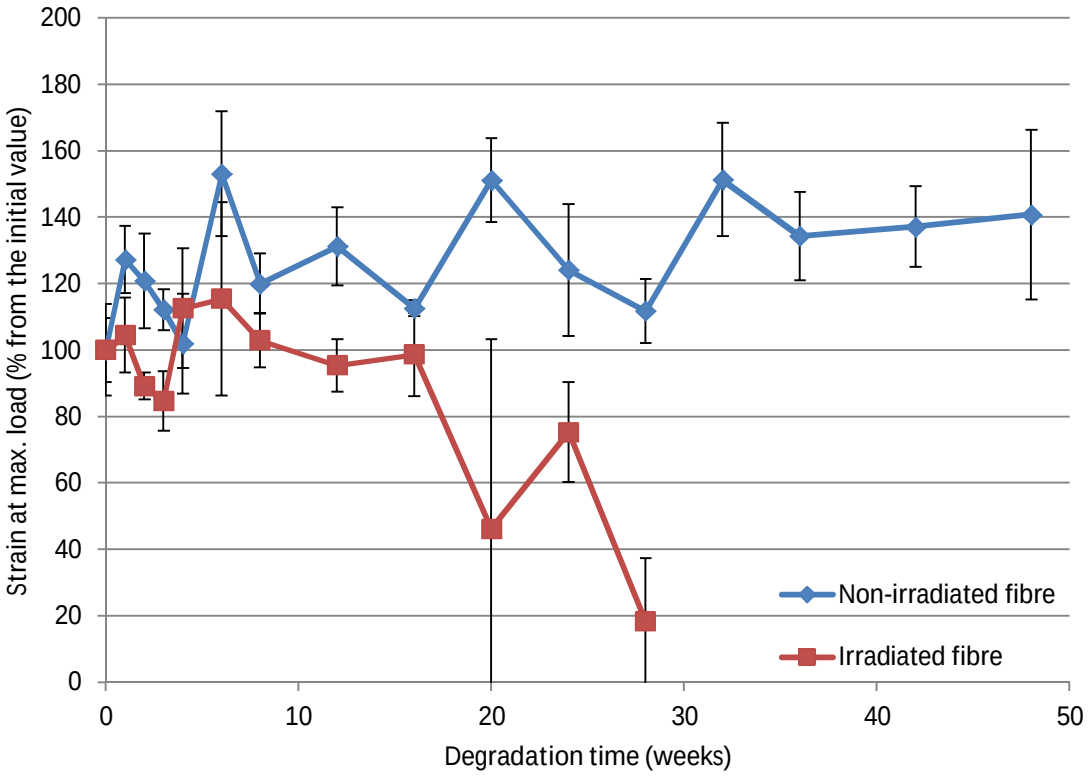

Figure 9.11. *Changes in strain at maximum load in irradiated and non-irradiated fibres during hydrolytic degradation studies (n=3-5).*

The possible error sources of the measurements can be divided to user-related errors, errors deriving from the testing equipment and analysis errors. User-related errors can relate to the similarity of the testing situation; the samples might not have the same tension or they are not completely straight every time they are put between the clamps of the tensile testing machine. These errors have been tried to minimize with paying attention to putting the samples between the clamps, zeroing the device between measurements and taking the hose of the compressed air up so that the upper grip does not drag it when moving. In addition the software can make mistakes in interpreting the curves and calculate the results wrong. The number of parallel samples was 5 but some of the measurements have been ignored due to strange shapes of the curves. This reduced the number of parallel samples in some cases.

10 CONCLUSIONS

There were two objectives in this study: (i) upscaling the production of 4-filament PLA fibre and (ii) providing reference data of the hydrolytic degradation behaviour of the fibre for further studies. The fibre used for the reference hydrolysis studies was manufactured using the conventional set-up.

There were two sets of trials conducted with the upgraded set-up with the slit die. The initial trials were run with a packaging grade material and GMP grade polylactide was used for the second set of trials. The objective was to find relationships characteristic for this set-up between the processing parameters and the properties of the fibre and finally identify optimal parameters for the updated set-up in order to provide fibre with properties corresponding to the fibres manufactured using the conventional processing line.

The results of the trials showed that adding the slit die did not require changes in the extrusion temperatures, but it probably had an effect on the flow of the melt causing single thick or thin filaments to emerge from the spinneret. There was also a problem of high fluctuation in the filament diameters during the initial trials. The main reason was unsteady feeding of the material as the fluctuation was notably smaller in the GMP grade trials where a new gravimetric feeder was used. The choice of the filter pack seemed not to have a large impact on the fluctuation of the filament diameter at least between the filter pack with a single large hole and multiple large holes. The use of the filter pack with small holes resulted in more consistent fibre quality but as the new feeder was introduced in the same trials the effect of the filter pack cannot be specified.

The optimal extrusion temperatures are the lowest inducing no melt fracture and resulting in good melt quality. The thermal degradation of the extrudates was measured and the packaging grade material seemed not to degrade during extrusion but the processing decreased the i.v. of the GMP grade material by one third.

Generally the ideal drawing parameters leading to the best mechanical properties are the highest velocities and highest temperatures on the godets as long as no stress whitening or sticking of the fibres on the godets is occurring. However, in this study it seems that the draw ratio has a higher impact on the mechanical properties of the fibre than the absolute velocities and temperatures. It was concluded that a larger angle between the godet pairs in the DUO units provides better flow of the fibres and minimises fibre overlapping causing unsteady quality of the fibre. No conclusions of the effect of the rounds around the godets on filament diameter or mechanical properties could be drawn.

A fibre with acceptable filament diameter and adequate strength was produced in the initial trials and the filament diameter and the strain values are at an acceptable level in half of the spools produced in the GMP grade trials. There is a need for further optimisation of the mechanical properties of the fibre. However, the ultimate tensile strength of the fibre was not far from the goal.

In conclusion, the updated set-up seems to be capable of producing fibre with properties within the required values although further trials are needed for total optimisation of the processing parameters. Mainly the ultimate tensile strength of the fibre has to be increased without compromising the filament diameter or fibre quality. For this, an increased feed rate and increased draw ratio should be studied together with higher drawing temperatures and closer inspection of where the stress whitening is occurring in the drawing line. The ability to monitor thermal degradation in real time is beneficial in commercial production of fibres from biodegradable polymers as it removes the need of time-consuming and unrepresentative off-line analysis. The implementation of the upgraded production in the manufacturing of the fibre would bring tremendous advantages in production rate and product quality.

A 48-week hydrolysis study was conducted on the fibre produced with the conventional set-up. This was done in order to provide reference data for the *in vitro* studies of the fibre manufactured with the updated set-up. During the hydrolysis study the molecular, rheological, thermal and mechanical properties of the fibre were measured. The M_w, M_n and i.v. of both gamma irradiated and non-irradiated fibre decreased steadily, but the degradation of the irradiated fibre was more prominent.

As expected, the crystallinity of both fibres increased during the hydrolysis period due to increased molecular mobility and the degradation of the amorphous parts. What comes to the profile of the melting peaks it should be noted that the irradiated fibre exhibited a growing clear cold crystallisation and a bimodal melting peak in the second heating which is related to advanced degradation. In the mechanical testing the non-irradiated fibre showed no changes in ultimate tensile during the degradation period. The mechanical performance of the irradiated fibre steadily deteriorated and the fibre could no longer be tested after 28 weeks. In conclusion the results of the hydrolytic degradation studies were mainly in line with earlier studies. The results of this study can be used as a reference for the future hydrolytic degradation studies for the fibre manufactured with the upgraded set-up.

REFERENCES

Abeykoon, C., Li, K., McAfee, M., Martin, P., Niu, Q., Kelly, A. & Deng, J. 2011. A new model based approach for the prediction and optimisation of thermal homogeneity in single screw extrusion. Control Engineering Practice 19, 8, pp. 862–874.

Abeykoon, C., Martin, P., Kelly, A. & Brown, E. 2012. A review and evaluation of melt temperature sensors for polymer extrusion. Sensors and Actuators A 182, pp. 16–27.

Abeykoon, C., McAfee, M., Li, K., Matrin P. & Kelly, A. 2011. The inferential monitoring of screw load torque to predict process fluctuations in polymer extrusion. Journal of Materials Processing Technology 211, 12, pp. 1907–1918.

Abu-Zahra, N.H. 2004a. Measuring melt density in polymer extrusion processes using shear ultrasound waves. International Journal of Advanced Manufacturing Technology 24, pp. 661–666.

Abu-Zahra, N.H. 2004b. Real-time viscosity and density measurements of polymer melts using dielectric and ultrasound sensors fusion. Mechatronics 14, pp. 789–803.

Alig, I., Fischer, D., Lellinger, D. & Steinhoff, B. 2005. Combination of NIR, Raman, Ultrasonic and Dielectric Spectroscopy for In-Line Monitoring of the Extrusion Process. Macromolecular Symposia 230, pp. 51–58.

Alig, I., Steinhoff, B. & Lellinger, D. 2010. Monitoring of polymer melt processing. Measurement Science and Technology 21, pp. 1–19.

Aoyagi, Y., Yamashita, K. & Doi, Y. 2002. Thermal degradation of poly [(R)-3-hydroxybutyrate], poly [ε-caprolactone], and poly [(S)-lactide]. Polymer Degradation and Stability 76, pp. 53–59.

Auras, R., Lim, L-T., Selke, S. & Tsuji, H. 2010. Poly(lactic acid) : synthesis, structures, properties, processing, and applications. Hoboken, New Jersey, John Wiley & Sons, Inc. 499 p.

Bansal, V. & Shambaugh, R.L. 1998. On-line Density and Crystallinity of Polyethylene Terephthalate During Melt Spinning. Polymer Engineering and Science 38, 12, pp. 1959–1968.

Barbas, J.M., Machado, A.V. & Covas, J.A. 2013. In-line Near-Infrared Spectroscopy: A Tool to Monitor the Preparation of Polymer-Clay Nanocomposites in Extruders. Journal of Applied Polymer Science 127, 6, pp. 4899–4909.

Barnes, S.E., Sibley, M.G., Edwards H.G.M. & Coates P.D. 2007. Process monitoring of polymer melts using in-line spectroscopy. Transactions of the Institute of Measurement and Control 29, 5, pp. 453–465.

Battegazzore, D., Bocchini, S. & Frache, A. 2011. Crystallization kinetics of poly(lactic acid)-talc composites. Express Polymer Letters 5, 10, pp. 849–858.

Bendada, A. & Lamontagne, M. 2004. A new infrared pyrometer for polymer temperature measurement during extrusion moulding. Infrared Physics & Technology 46, pp. 11–15.

Blackburn, R.S. 2005. Biodegradable and sustainable fibres. Cambridge, Woodhead Publishing Limited. 456 p.

Bresee, R.R. & Ko, W-C. 2003. Fiber Formation During Melt Blowing. International Nonwovens Journal, pp. 21–28.

Brown, E.C., Kelly, A.L. & Coates, P.D. 2004. Melt temperature field measurement in single screw extrusion using thermocouple meshes. Review of Scientific Instruments 75, 11, pp. 4742-4748.

Brucato, V., Piccarolo, S. & La Carrubba, V. 2002. An experimental methodology to study polymer crystallization under processing conditions . The influence of high cooling rates. Chemical Engineering Science 57, pp. 4129–4143.

Bur, A.J. & Roth, S.C., 2004a. Fluorescence Temperature Measurements: Methodology for Applications to Process Monitoring. Polymer Engineering and Science 44, 5, pp. 898–908.

Bur, A.J. & Roth, S.C. 2004b. Temperature Gradients in the Channels of a Single-Screw Extruder. Polymer Engineering and Science 44, 11, pp. 2148–2157.

Bur, A.J., Roth, S.C. & McBrearty, M. 2002. In-line dielectric monitoring during extrusion of filled polymers. Review of Scientific Instruments 73, 5, p. 2097-2102.

Bur, A.J., Vangel, M.G. & Roth, S.C., 2001. Fluorescence Based Temperature Measurements and Applications to Real-Time Polymer Processing. Polymer Engineering and Science 41, 8, pp. 1380-1389.

Callis, J.B., Illman, D.L. & Kowalski, B.R. 1987. Process Analytical Chemistry. Analytical Chemistry 59, 9, pp. 624–637.

Cam, D. & Marucci, M. 1997. Influence of residual monomers and metals on poly(L-lactide) thermal stability. Polymer 38, 8, pp. 1879–1884.

Canevarolo, S.V., Bertolino, M.K., Pinheiro, L.A., Palermo, V. & Piccarolo S. 2009. The use of in-line quantitative analysis to follow polymer processing. Macromolecular Symposia 279, pp. 191–200.

Carneiro, O.S., Covas, J.A, Ferreira J.A. & Cerqueira, M.F. 2004. On-line monitoring of the residence time distribution along a kneading block of a twin-screw extruder. Polymer Testing 23, pp. 925–937.

Carrasco, F., Pagès, P., Gámez-Pérez, J., Santana, O.O & Maspoch M.L. 2010. Processing of poly(lactic acid): Characterization of chemical structure, thermal stability and mechanical properties. Polymer Degradation and Stability 95, pp. 116–125.

Cartier, L., Okihara, T., Ikada, Y., Tsuji, H., Puiggali, J. & Lotz, B. 2000. Epitaxial crystallization and crystalline polymorphism of polylactides. Polymer 41, 25, pp. 8909–8919.

Chen, X., Zhuo, J. & Jiao, C. 2012. Thermal degradation characteristics of flame retardant polylactide using TG-IR. Polymer Degradation and Stability 97, 11, pp. 2143–2147.

Chen, Z.-L., Chao, P.-Y. & Chiu, S.-H. 2003. Proposal of an empirical viscosity model for quality control in the polymer extrusion process. Polymer Testing 22, 5, pp. 601–607.

Chiu, S.-H. & Lin, C.-C. 1998. Applying the Constrained Minimum Variance Control Theory on In-line Viscosity Control in the Extrusion Molding Process. Journal of Polymer Research 5, 3, pp. 171–175.

Chiu, S.-H., Yiu, H.-C. & Pong, S.-H. 1997. Development of an in-line viscometer in an extrusion molding process. Journal of Applied Polymer Science 63, pp. 919–924.

Chiu, S., & Pong, S. 1999. In-line viscosity control in an extrusion process with a fuzzy gain scheduled PID controller. Journal of Applied Polymer Science 74, pp. 541-555.

Chiu, S., & Pong, S. 2001. In-line viscosity fuzzy control. Journal of Applied Polymer Science 79, pp.1249-1255.

Cicero, J.A., Dorgan, J.R., Garrett, J. Runt, J. & Lin, J.S. 2002a. Effects of molecular architecture on two-step, melt-spun poly(lactic acid) fibers. Journal of Applied Polymer Science 86, 11, pp. 2839–2846.

Cicero, J.A., Dorgan, J.R., Janzen, J., Garrett, J, Runt, J & Lin, J.S. 2002b. Supramolecular morphology of two-step, melt-spun poly(lactic acid) fibers. Journal of Applied Polymer Science 86, 11, pp. 2828–2838.

Cicero, J.A. & Dorgan, J.R. 2001. Physical Properties and Fiber Morphology of Poly(lactic acid) Obtained from Continuous Two-Step Melt Spinning. Journal of Polymers and the Environment 9, 1, pp. 1-10.

Coates, P.D., Barnes, S.E., Sibley, M.G., Brown, E.C., Edwards, H.G.M. & Scowen I.J. 2003. In-process vibrational spectroscopy and ultrasound measurements in polymer melt extrusion. Polymer 44, 19, pp. 5937–5949.

Covas, J.A., Carneiro, O.S., Costa, P., Machado A.V. & Maia, J.M. 2004. Online monitoring techniques for studying evolution of physical, rheological and chemical effects along the extruder. Plastics, Rubbers and Composites 33, 1, pp. 55–61.

Covas, J.A., Maia, J.M., Machado, A.V. & Costa P. 2008. On-line rotational rheometry for extrusion and compounding operations. Journal of Non-Newtonian Fluid Mechanics 148, 1-3, pp. 88–96.

Crowley, M.M. & Zhang F. 2007. Pharmaceutical applications of hot-melt extrusion: part I. Drug development and industrial pharmacy 33, 9, pp. 909–926.

Cui, K. Liu, Y., Meng, L., Li, X., Wang, Z., Chen, X. & Li, L. 2014. A novel apparatus combining polymer extrusion processing and x-ray scattering. Polymer Testing 33, pp. 40–47.

Dauner, M., Muller, E., Wagner, B & Planck, H. 1992. in Degradation Phenomena on Polymeric Biomaterials. Berlin, Springer. p.107.

Deng, J., Li, K., Harkin-Jones, E., Price, M., Fei, M., Kelly, A., Vera-Sorroche, J., Coates, P. & Brown, E. 2013. Low-cost process monitoring for polymer extrusion. Transactions of the Institute of Measurement and Control 0, 0, pp. 382–390.

Dexheimer, S. 2008. Terahertz spectroscopy - Principles and Applications. Boca Raton, CRC Press. 360 p.

Dresselhaus, M.S., Dresselhaus, G., Saito, R. & Jorio A. 2005. Raman spectroscopy of carbon nanotubes. Physics Reports 409, 2, pp. 47–99.

Eling, B., Gogolewski, S. & Pennings, A.J., 1982. Biodegradable materials of poly(l-lactic acid): 1. Melt-spun and solution-spun fibres. Polymer 23, 11, pp. 1587–1593.

Ellä, V., Gomes, M.E., Reis, R.L., Törmälä, P. & Kellomäki, M. 2007. Studies of P(L/D)LA 96/4 non-woven scaffolds and fibres; properties, wettability and cell spreading before and after intrusive treatment methods. Journal of Materials Science: Materials in Medicine 18, 6, pp. 1253–1261.

Ellä, V., Nikkola, L. & Kellomäki, M. 2011a. Process-Induced Monomer on a Medical-Grade Polymer and Its Effect on Short-Term Hydrolytic Degradation. Journal of Applied Polymer Science 119, pp. 2996–3003.

Ellä, V., Annala, T., Länsman, S., Nurminen, M. & Kellomäki, M. 2011b. Knitted polylactide 96/4 L/D structures and scaffolds for tissue engineering: shelf life, *in vitro* and *in vivo* studies. Biomatter 1, 1, pp. 102–113.

Ellä, V. 2012. Effects of Processing Parametres on P(L/D)LA 96/4 Fibers and Fibrous Products for Medical Applications. Dissertation. Tampere. Tampere University of Technology. Publication - Tampere Univerisyt of Technology. Publication 1039. 96 p.

Fambri, L., Pegoretti, A., Fenner, R., Incardona, S.D. & Migliaresi C. 1997. Biodegradable fibres of poly(l-lactic acid) produced by melt spinning. Polymer 38, 1, pp. 79–85.

Fan, Y., Nishida, H., Shirai, Y. & Endo, T. 2004. Thermal stability of poly (l-lactide): influence of end protection by acetyl group. Polymer Degradation and Stability 84, 1, pp. 143–149.

Fang, H., Mighri, F., Ajji, A., Cassagnau, P. & Elkoun S. 2011. Flow Behavior in a Co-rotating Twin-Screw Extruder of Pure Polymers and Blends: Characterization by Fluorescence Monitoring Technique. Journal of Applied Polymer Science 120, pp. 2304-2312.

Fischer, D., Bayer, T., Eichhorn K.-J. & Otto, M. 1997. In-line process monitoring on polymer melts by NIR-spectroscopy. Fresenius' Journal of Analytical Chemistry 359, pp. 74–77.

Fourné, F. 1999. Synthetic Fibers: Machines and Equipment, Manufacture, Properties. Handbook for Plant Engineering, Machine Design, and Operation. Ohio, Hanser Publications. 885 p.

Gao, R.X., Tang, X., Gordon, G. & Kazmer, D.O. 2014. Online product quality monitoring through in-process measurement. CIRP Annals - Manufacturing Technology 63, 1, pp. 493–496.

Garlotta, D. 2002. A Literature Review of Poly (Lactic Acid). Journal of Polymers and the Environment 9, 2, pp. 63-84.

Golzar, M., Beyreuther, R., Brünig, H., Tändler, B. & Vogel, R. 2004. Online temperature measurement and simultaneous diameter estimation of fibers by thermography of the spinline in the melt spinning process. Advances in Polymer Technology 23, 3, pp. 176–185.

Gottwald, A. & Scheler, U. 2005. Extrusion Monitoring of Polymer Melts Using a High-Temperature Surface-NMR Probe. Macromolecular Materials and Engineering 290, 5, pp. 438–442.

Grijpma, D.W., Altpeter, H., Bevis, M.J. & Feijen, J. 2002. Improvement of the mechanical properties of poly(D,L-lactide) by orientation. Polymer International 51, 10, pp. 845–851.

Gupta, A.P. & Kumar, V. 2007. New emerging trends in synthetic biodegradable polymers – Polylactide: A critique. European Polymer Journal 43, 10, pp. 4053–4074.

Gupta, B., Revagade, N. & Hilborn, J. 2007. Poly(lactic acid) fiber: An overview. Progress in Polymer Science 32, 4, pp. 455–482.

Gupta, V.B. & Kothari, V.K. 1997. Manufactured Fibre Technology. London, Chapman & Hall. 661 p.

Gururajan, G. & Ogale, A.A. 2009. Molecular orientation evolution during low-density polyethylene blown film extrusion using real-time Raman spectroscopy. Journal of Raman Spectroscopy 40, 2, pp. 212–217.

Hansen, M.G. & Vedula, S. 1998. In-line fiber-optic near-infrared spectroscopy: Monitoring of rheological properties in an extrusion process. Part I. Journal of Applied Polymer Science 68, pp. 859–872.

Hirsch, J. 2010. Online monitoring of continuous hot melt extrusion. Pharmaceutical Technology Europe, pp. 19–20.

Hoogsteen, W., Postema, A.R., Pennings, A.J. & ten Brinke, G. 1990. Crystal structure, conformation and morphology of solution-spun poly(L-lactide) fibers. Macromolecules 23, 2, pp. 634–642.

Huang, C. & Tang, T. 2007. Development of a New Infrared Device for Monitoring the Coefficient of Variation in Yarns. Journal of Applied Polymer Science 106, pp. 2342-2349.

Hyon, S.H., Jamshidi, K., & Ikada.Y. 1984. in Polymers as Biomaterials. New York, Plenum Press. p. 51.

Ibrahim, S., Militky, J., Kremenakova, D. & Mishra R. 2012. Characterization of yarn diameter measured on different. International Conference: Textiles & Fashion, Bangkok, Thailand, July 3-4, 2012.

Innovative Sensors - Processing of Plastics [WWW]. 2008. Fos Messtechnik GmbH. [accessed on 18.5.2015]. Available at: http://www.fos-messtechnik.de/Innovative_Sensors_2008.pdf.

Jamshidi, K., Hyon, S.-H. & Ikada, Y. 1988. Thermal characterization of polylactides. Polymer, 29, pp. 2229–2234.

Jen, C.-K., Zun, Z. & Kobayashi, M. 2005. Real-time monitoring of barrel thickness and barrel/screw separation using ultrasound. Measurement Science and Technology 16, pp. 842–850.

Jia, J. 2010. Melt spinning of continuous filaments by cold air attenuation. Dissertation. Georgia Institute of Technology, School of Materials Science anf Engineering. 168 p.

Kellomäki, M., Paasimaa, S. & Törmälä, P. 2000. Pliable polylactide plates for guided bone regeneration: Manufacturing and *in vitro*. Proceedings of the Institution of Mechanical Engineers, Part H: Journal of Engineering in Medicine 214, pp. 615–629.

Kelly, A.L., Brown, E.C. & Coates, P.D. 2006. The Effect of Screw Geometry on Melt Temperature Profile in Single Screw Extrusion. Polymer Engineering and Science, pp. 1706-1714.

Kikutani, T., Nakao, K., Takarada, W. & Ito, H. 1999. On-Line Measurement of Orientation Development in the High-speed Melt Spinning Process. Polymer Engineering and Science 39, 12, pp. 2349–2357.

Kindermann, C., Matthée, K., Strohmeyer, J., Sievert, F. & Breitkreutz, J. 2011. Tailor-made release triggering from hot-melt extruded complexes of basic polyelectrolyte and poorly water-soluble drugs. European Journal of Pharmaceutics and Biopharmaceutics 79, 2, pp. 372–381.

Kopinke, F-D., Remmler, M., Mackenzie K., Möder, M. & Wachsen, O. 1996. Thermal decomposition of biodegradable polyesters -11 . Poly(lactic acid). Polymer Degradation and Stability 53, pp. 329–342.

Kracalik, M. & Laske, S. 2011. Elongational and shear flow in polymer-clay nanocomposites measured by on-line extensional and off-line shear rheometry. Rheologica Acta 50, pp. 937–944.
Kricheldorf, H.R. 2001. Syntheses and application of polylactides. Chemosphere 43, 1, pp. 49–54.

Krumbholz, N., Hochrein, T., Vieweg, N., Hasek, T., Kretschmer K., Bastian, M., Mikulics, M. & Koch M. 2009. Monitoring polymeric compounding processes inline with THz time-domain spectroscopy. Polymer Testing 28, 1, pp. 30–35.

Laser measurement devices and systems [WWW]. 2014. Zumbach Electronic AG (H.Q.). [accessed 20.5.2015]. Available at: http://www.zumbach.com/products/product-finder/odac/odac-overview.html.

Lewis, I.R. & Edwards, H.G.M. 2001. Handbook of Raman Spectroscopy: From the Research Laboratory to the Process Line. Boca Raton, CRC Press. 1072 p.

Lim, L.-T., Auras, R. & Rubino, M. 2008. Processing technologies for poly(lactic acid). Progress in Polymer Science 33, 8, pp. 820–852.

Lin, C., Ogale, A.A. & Edie, D.D., 2001. On-line measurements during melt spinning of AR mesophase pitch.

Liu, X., Li, K., McAfee, M. & Deng, J. 2010. 'Soft-sensor' for Real-time Monitoring of Melt Viscosity in Polymer Extrusion Process. 49th IEEE Conference on Decision and Control. Atlanta, Georgia, USA, December 15-16, 2010. pp. 3469–3474.

Liu, X., Li, K., McAfee, M., Nguyen, B.K. & McNally, G.M. 2012. Dynamic Gray-Box Modeling for On-Line Monitoring of Polymer Extrusion Viscosity. Polymer Engineering and Science 52, 6, pp. 1332-1341.

Liu, X., Zou, Y., Li, W., Cao, G. & Chen W. 2006. Kinetics of thermo-oxidative and thermal degradation of poly(D,L-lactide) (PDLLA) at processing temperature. Polymer Degradation and Stability 91, 12, pp. 3259–3265.

Lunt, J. 1998. Large scale production, properties and commercial application of polylactic acid polymers. Polymer Degradation and Stability 59, pp. 145–152.

Marla, V.T., Shambaugh, R.L. & Papavassiliou, D. V. 2009. Online Measurement of Fiber Diameter and Temperature in the Melt-Spinning and Melt-Blowing Processes. Industrial & Engineering Chemistry Research 48, 18, pp. 8736–8744.

McAfee, M. 2007. Enhancing process insight in polymer extrusion by grey box modelling. Transactions of the Institute of Measurement and Control 29, 5, pp. 467–488.

McAfee, M. & McNally, G. 2006. Real-time measurement of melt viscosity in single-screw extrusion. Transactions of the Institute of Measurement and Control 28, 5, pp. 481–497.

McAfee, M. & Thompson, S. 2007. A novel approach to dynamic modelling of polymer extrusion for improved process control. Proceedings of the Institution of Mechanical Engineers, Part I: Journal of Systems and Control Engineering 221, 4, pp. 617–628.

McCreery, R.L. 2000. Raman spectroscopy for Chemical Analysis. Volume 225 / Chemical Analysis: A Series of Monographs on Analtyica Chemistry and Its Applications. USA, Wiley & Sons, Inc. 448 p.

McNeill, I.C. & Leiper, H.A. 1985. Degradation studies of some polyesters and polycarbonates – 2. Polylactide: Degradation under isothermal conditions, thermal degradation mechanism and photolysis of the polymer. Polymer Degradation and Stability 11, 4, pp. 309-326.

Meng, Q., Heuzey, M.-C. & Carreau, P.J. 2012. Control of thermal degradation of polylactide/clay nanocomposites during melt processing by chain extension reaction. Polymer Degradation and Stability 97, 10, pp. 2010–2020.

Mezghani, K. & Spruiell, J.E. 1998. High Speed Melt Spinning of Poly(L-lactic acid) Filaments. Journal of Polymer Science Part B: Polymer Physics 36, pp. 1005–1012.

Middleton, J.C. & Tipton, A.J. 2000. Synthetic biodegradable polymers as orthopedic devices. Biomaterials 21, 23, pp. 2335–2346.

Migler, K.B. & Bur, A.J. 1998. Fluorescence Based Measurement of Temperature Profiles During Polymer Processing. Polymer Engineering and Science 38, 1, pp. 213–221.

Mould, S., Barbas, J., Machado, A.V., Nóbrega, J.M. & Covas, J.A. 2011. Measuring the rheological properties of polymer melts with on-line rotational rheometry. Polymer Testing 30, 6, pp. 602–610.

Nagata, T., Ohshima, M. & Tanigaki, M. 2000. In-line monitoring of polyethylene density using near infrared (NIR) spectroscopy. Polymer Engineering Science 40, 5, pp. 1107–1113.

Nair, L.S. & Laurencin, C.T. 2007. Biodegradable polymers as biomaterials. Progress in Polymer Science 32, 8-9, pp. 762–798.

Nguyen, B.K., McNally, G. & Clarke, A. 2014. Real time measurement and control of viscosity for extrusion processes using recycled materials. Polymer Degradation and Stability 102, pp. 212–221.

Nicolae, C.-A., Grigorescu, M.A. & Gabor, R.A. 2008. An Investigation of Thermal Degradation of Poly(Lactic Acid). Engineering Letter 16, 4.
Von Oepen, R. & Michaeli, W. 1992. Injection Moulding of Biodegradable Implants. Clinical Materials 10, pp. 21–28.

Paakinaho, K., Heino, H., Väisänen, J., Törmälä, P. & Kellomäki, M. 2011. Effects of lactide monomer on the hydrolytic degradation of poly(lactide-co-glycolide) 85L/15G. Journal of the mechanical behavior of biomedical materials 4, 7, pp. 1283–1290.

Paakinaho, K., Ellä, V., Syrjälä, S. & Kellomäki, M. 2009. Melt spinning of poly(L/D)lactide 96/4: Effects of molecular weight and melt processing on hydrolytic degradation. Polymer Degradation and Stability 94, 3, pp. 438–442.

Penning, J., Dijkstra, H. & Pennings, A.J. 1993. Preparation and properties of absorbable fibres from L-lactide copolymers. Polymer 34, 5, pp. 942–951.

Perepelkin, K.E. 2002. Chemistry and Technology of Chemical Fibres - Polylactide Fibres: Fabrication, Properties, Use, Prospects. A Review. Fibre Chemistry 34, 2, pp. 85–100.

Perusich, S. 2000. Dielectric Spectroscopy for Polymer Melt Composition Measurements. Polymer Engineering and Science 40, 1, pp. 214–226.

Pinheiro, L.A., Hu, G-H., Pessan, L.A. & Canevarolo, S.V. 2008. In-Line Measurements of the Morphological Parameters of PP/PA6 Blends During Extrusion in the Transient Mode. Polymer Engineering and Science, pp. 2–10.

PLA Meltblown Process Guide. 2005. NatureWorks. 7 p.

Rajan, V.V, Wäber, R. & Wieser, J. 2010. Online Monitoring of the Thermal Degradation of POM During Melt Extrusion. Journal of Applied Polymer Science 115, pp. 2394–2401.

Rasselet, D., Ruellan, A., Guinault., Miquelard-Garnier, G., Sollogoub, C. & Fayolle, B. 2014. Oxidative degradation of polylactide (PLA) and its effects on physical and mechanical properties. European Polymer Journal 50, pp. 109–116.

Ren, J. 2010. Biodegradable Poly (Lactic Acid) - Synthesis, Modification, Processing and Applications. Beijing, Tsinghua University Press. 314 p.

De Rovére, A. & Shambaugh, R.L. 2001. Melt-Spun Hollow Fibers: Modeling and Experiments. Polymer Engineering and Science 41, 7, pp. 1206–1219.

Saerens, L., Vervaet, C., Remon, J.P. & De Beer, T. 2014. Process monitoring and visualization solutions for hot-melt extrusion: a review. Journal of Pharmacy and Pharmacology 66, 2, pp. 180–203.

Saerens, L., Dierickx, L., Lenain, B., Vervaet, C, Remon, J.P. & De Beer, T. 2011. Raman spectroscopy for the in-line polymer-drug quantification and solid state characterization during a pharmaceutical hot-melt extrusion process. European Journal of Pharmaceutics and Biopharmaceutics 77, 1, pp. 158–163.

Sawai, D. et al., 2002. Preparation of Oriented β-Form Poly (L-lactic acid) by Solid-State Extrusion. Journal of Polymer Science Part B: Polymer Physics 40, pp. 95–104.

Schmack, G., Tändler, B., Vogel, R., Beyreuther, R., Jacobsen, S. & Fritz, H.-G. 1999. Biodegradable Fibers of Poly(L-lactide) Produced by High-Speed Melt Spinning and Spin Drawing. Journal of Applied Polymer Science 73, pp. 2785–2797.

Schmack, G., Jenichen, D., Vogel, R., Tändler, B., Beyreuther, R., Jacobsen, S & Fritz, H.-G. 2001. Biodegradable fibres spun from poly(lactide) generated by reactive extrusion. Journal of Biotechnology 86, pp. 151–160.

Schmack, G. Tändler, B., Optiz, G., Vogel, R., Komber, H., Häußler, L., Voigt, D., Weinmann, S., Heinemann, M & Fritz, H.-G. 2003. High-Speed Melt Spinning of Various Grades of Polylactides. Journal of Applied Polymer Science 91, pp. 800-806.

US3636956 A. Polylactide sutures. Ethicon Inc. (Schneider, A.K). 13.5.1970 (25.1.1972).

Shalaby, S.W. & Johnson, R.A. 1994. Synthetic Absorbable Polyesters. Biodegradable implants in fracture fixation, pp. 1–34.

Signori, F., Coltelli, M.-B. & Bronco, S. 2009. Thermal degradation of poly(lactic acid) (PLA) and poly(butylene adipate-co-terephthalate) (PBAT) and their blends upon melt processing. Polymer Degradation and Stability 94, 1, pp. 74–82.

Silva, J., Santos, A.C. & Canevarolo, S. V. 2015. In-line monitoring flow in an extruder die by rheo-optics. Polymer Testing 41, pp. 63–72.

Slomkowski, S., Penczek, S. & Duda, A. 2014. Polylactides - an overview. Polymers for Advanced Technologies 25, 5, pp. 436–447.

Solarski, S., Ferreira, M. & Devaux, E. 2005. Characterization of the thermal properties of PLA fibers by modulated differential scanning calorimetry. Polymer 46, 25, pp. 11187–11192.

Solarski, S., Ferreira, M. & Devaux, E. 2007. Thermal and mechanical characteristics of polylactide filaments drawn at different temperatures. Journal of the Textile Institute 98, 3, pp. 227–236.

Sparavigna, A., Broglia, E. & Lugli, S. 2004. Beyond capacitive systems with optical measurements for yarn evenness evaluation. Mechatronics 14, 10, pp. 1183–1196.

Södergård, A. & Näsman, J.H. 1996. Melt Stability Study of Various Types of Poly(L - lactide). Industrial & Engineering Chemistry Research 35, pp. 732–735.

Södergård, A. & Näsman, J.H. 1994. Stabilization of poly(l-lactide) in the melt. Polymer Degradation and Stability 1, pp. 25–30.

Södergård, A. & Stolt, M. 2002. Properties of lactic acid based polymers and their correlation with composition. Progress in Polymer Science 27, 6, pp. 1123–1163.

Tadmor, Z. & Gogos, C. 2013. Principles of Polymer Processing. Hoboken, New Jersey, John Wiley & Sons, Inc. 984 p.

Takahashi, K., Sawai, D., Yokoyama, T., Kanamoto, T. & Hyon, S-H. 2004. Crystal transformation from the α- to the β-form upon tensile drawing of poly(l-lactic acid). Polymer 45, 14, pp. 4969–4976.

Takasaki, M., Ito, H. & Kikutani, T. 2003. Development of Stereocomplex Crystal of Polylactide in High-Speed Melt Spinning and Subsequent Drawing and Annealing Processes. Journal of Macromolecular Science Part B - Physics, 3 & 4, pp. 403–420.

Tateishi, T., Chen, G. & Ushida, T. 2002. Biodegradable porous scaffolds for tissue engineering. Journal of Artificial Organs 5, 2, pp. 77–83.

Taubner, V. & Shishoo, R. 2001. Influence of Processing Parameters on the Degradation of Poly(L-lactide) During Extrusion. Journal of Applied Polymer Science 79, pp. 2128–2135.

Teixeira, P.F., Hilliou, L., Covas, J.A. & Maia, J.M. 2013. Assessing the practical utility of the hole-pressure method for the in-line rheological characterization of polymer melts. Rheologica Acta 52, 7, pp. 661–672.

Tsai, I.-S. & Chu, W.-C. 1996. A new photoelectric device for the measurement of yarn diameter and yarn evenness. II. The measurement of yarn diameter and the effect of shape-error factor (SEF) on the measurement of yarn evenness. Journal of the Textile Institute 87, 3, pp. 496–508.

Tsuji, H., Saeki, T., Tsukegi, T., Daimon, H. & Fujie, K. 2008. Comparative study on hydrolytic degradation and monomer recovery of poly(l-lactic acid) in the solid and in the melt. Polymer Degradation and Stability 93, 10, pp. 1956–1963.

Tsuji, H., Shimizu, K. & Sato, Y. 2012. Hydrolytic Degradation of Poly (L-lactic acid): Combined Effects of UV Treatment and Crystallization. Journal of Applied Polymer Science 125, pp. 2394–2406.

Twarowska-Schmidt, K. 2012. Influence of Drawing Parameters on the Properties of Melt Spun Poly(Lactic Acid) Fibres. Fibres and Textiles in Eastern Europe 20, 96, pp. 58–63.

Wachsen, O., Reichert, K.H., Krüger, R.P., Much, H. & Schulz G. 1997. Thermal decomposition of biodegradable polyesters- III. Studies on the mechanisms of thermal degradation of oligo-L-lactide using SEC, LACCC and MALDI-TOF-MS. Polymer Degradation and Stability 55, pp. 225–231.

Wang, D. & Min, K., 2005. In-line monitoring and analysis of polymer melting behavior in an intermeshing counter-rotating twin-screw extruder by ultrasonic waves. Polymer Engineering and Science, pp. 998–1010.

Wang, Y., Steinhoff, Bernd, Brinkmann, C. & Alig, I. 2008. In-line monitoring of the thermal degradation of poly (L-lactic acid) during melt extrusion by UV-vis spectroscopy. Polymer 49, pp. 1257–1265.

Vedula, S. & Hansen, M.G. 1998. In-line fiber-optic near-infrared spectroscopy: Monitoring of rheological properties in an extrusion process. Part II. Journal of Applied Polymer Science 68, pp. 859–872.

Vera-Sorroche, J., Kelly, A., Brown, E., Coates, P., Karnachi, N., Harkin-Jones, E., Li, K. & Deng J. 2013. Thermal optimisation of polymer extrusion using in-process monitoring techniques. Applied Thermal Engineering 53, 2, pp. 405–413.

Wilson, I.D. & Poole, C. 2009. Handbook of methods and instrumentation in separation science. Volume 1. London, Elsevier. 866 p.

Witschnigg, A., Laske, S., Kracalik, M., Feuchter, M., Pinter, G., Maier, G., Märzinger, W., Haberkorn, M., Langecker, G.R. & Holzer C. 2010. In-line characteristization of polypropylene nanocomposites using FT-NIR. Journal of Applied Polymer Science 117, pp. 3047–3053.

Vondra, R. 2003. Optical methods of measuring in textile industries. TU Liberek, Mechatronics and Interdisciplinary Engineering Studies. 7 p.

Yuan, X., Mak, A.F.T., Kwok, K.W., Yung, B.K.O., Yao, K. 2001. Characterization of Poly(L-lactic acid) Fibers Produced by Melt Spinning. Journal of Applied Polymer Science 81, pp. 9–15.

Zhou, C. & Kumar, S. 2010. Thermal instabilities in melt spinning of viscoelastic fibers. Journal of Non-Newtonian Fluid Mechanics 165, 15-16, pp. 879–891.

APPENDIX 1: PROPERTIES AND CONDITIONS FOR MELT-SPUN PLA FIBRES

Reference	Material	Initial Mw (kDa)	Filament count	Drawn filament diameter (μm)	Take-up speed (m/min)	Draw ratio	Molecular weight reduction (%)	As-spun/drawn fibre crystallinity (%)	Tensile strength (GPa)	Young's modulus (GPa)
(Schneider 1972, cited in Fambri et al. 1997)	PLA	19	?	25-500	?	?	?	?	0.48	7
		182	?	25-500	?	?	37	?	0.69	7
(Eling et al. 1982)	PLA	< 300	?	?	0.25-0.35	?	13 - 40	?	0.5	7
(Hyon et al. 1984, cited in Fambri et al. 1997)	PLLA	360	?	150	?	?	69	5 / ?	0.7	8.5
(Dauner et al. 1992, cited in Fambri et al. 1997)	PLLA	98	?	76	?	?	61	?	0.4	?
(Penning et al. 1993)	PLLA	280	1	83	1	0-9	64	42 / 57	0.53	9.3

	PLDLA 85/15	600	1	83	1	0-8	83	0	0.19	5
(Fambri et al. 1997)	PLLA	330	1	80	5-20	6.6-20.5	67	20-40 / ?	0.87	9
(Cicero & Dorgan 2001)	Staple-fibre grade PLDLA 98/2	99	1	?	?	1-8	28	? / 51	0.07-0.38	1.4-3.1
		109	1	?	?	5-7	43	49	0.07-0.38	1.4-3.1
(Yuan et al. 2001)	PLLA	263	1	119-149	3.2	5.1-5.9	46-61	17-18 / 50-61	0.37-0.42	4.1-4.5
		305	1	134-145	3.2	4.7-5.5	57-59	19-20 / 60-64	0.3-0.48	3.9.2005
		495	1	146-151	3.2	4.7	60-77	17-23 / 62-64	0.4-0.5	4.6-5.2
(Cicero et al. 2002a)	Commercial-grade PLDLA 96/4	111	1	?	?	1-8	39	0 / 0 - 35	0.007-0.4	1.5-3
(Cicero et al. 2002b)	Staple-fibre grade PLDLA 98/2	99	1	?	?	1-8	?	0 / 0-51	?	3-10
(Solarski et al. 2005)	PLA	?	40	45-56	?	1-4	?	? / 8.7-40.63	0.258-0.414	4.2-5.7

(Ellä et al. 2007)	GMP grade PLDLA 96/4	?	4	80	?	4,6	30	?	0.336	0.336 / 7.1
(Solarski et al. 2007)	PLDLA 96/4	?	40	43-56	400-700	2-3.5	?	? / 10-38	0.364-0.442	6.5
(Paakinaho et al. 2009)	GMP grade PLDLA 96/4	100	8/12 fil	?	?	?	0	?	?	?
		270	8/12 fil	?	?	?	50	?	?	?
		350	8/12 fil	?	?	?	63	?	?	?

APPENDIX 2: PROCESS ANALYTICAL TOOLS APPLIED IN POLYMER EXTRUSION

Process analytical tool	Interface	In-line or on-line application	Purpose	Reported challenges/disadvantages/shortcomings	References
NIR spectroscopy: reflection	Die	In-line	Drawing force and Young's modulus	Not possible to monitor a transparent formulation (low signal/noise ratio), temperature sensitivity, different aggregate states will affect the chemometric models negatively	(Witschnigg et al. 2010)
NIR spectroscopy: transmission	Die	In-line	Monomer concentration, complex viscosity, density by monitoring polymer chain branches	-	(Hansen & Vedula 1998; Vedula & Hansen 1998; Nagata et al. 2000)
UV-VIS spectroscopy: transmission	Die	In-line	Polymer degradation	The low count rate of the diode leads to a large error, since this area is the wavelength range where the absorption of the optical fibres connecting the probe with the spectrometer becomes dominant	(Wang et al. 2008)
Fluorescence spectroscopy	Die, Mixing zone	In-line	Melt temperature, temperature gradient measurements	Can only be used in development phase with inert fluorescent dyes, accurate temperature measurements require simultaneous acquisition of pressure, dyes need to stable at high temperatures, spectra should show significant changes with varying temperature, dyes should be soluble in polymer resin and chemically inert, sensor needs to be located beyond the end of screw (low shear rate flow region) to minimise the effect of shear heating, these peaks have to be filtered out to calculate average temperatures	(Migler & Bur 1998; Bur et al. 2001; Carneiro et al. 2004; Barnes et al. 2007; Fang et al. 2011; Kindermann et al. 2011)

Terahertz spectroscopy	Die	In-line	Refractive index measurements related to additive component content	Complexity of the system, high costs, high sensitivity to vibration - a new, partially fibre-coupled terahertz spectrometer was developed. Die adaptations were required: silica plates that can withstand pressures only up to 26 bar and temperatures only up to 260 °C. The recording time needs to be reduced: only the amplitude value at a fixed time position is used as an indicator. The pressure and temperature of the melt need to be observed in order to correct the experimental data	(Krumbholz et al. 2009)
Dielectric spectroscopy	Die	In-line	Comonomer concentration, side chain composition, filler concentrations, melt viscosity	At higher temperatures, the analysis becomes more difficult since ions, permanent dipoles and induced dipoles may all have a significant influence at an elevated temperature. Measuring cells are not sensitive for the melt in the centre of the ring, cells should therefore be as narrow as possible. The sensor utilizes a fringe field to monitor the polymer melt, so the field of the measurement is limited to the depth of penetration of the fringe field. Therefore, the dielectric parameters are measured at the surface of the melt stream	(Perusich et al. 2000; Bur et al. 2002; Abu-Zahra 2004b)
Optical probes	Die, mixing zone	In-line	Particle size and concentration of dispersed phase, melting behaviour		(Pinheiro et al. 2008; Canevarolo et al. 2009)
NMR spectroscopy	Die	On-line	Temperature, composition, homogeneity	Increasing temperature decreases the magnetic field strength, ferromagnetic materials in the extruder might deform the static field, low sensitivity which can be overcome by increasing the experiment time for signal accumulation	(Gottwald & Scheler 2005)

Ultrasonic techniques: longitudinal waves	Melting, mixing, pumping zones, die, barrel	In-line	Barrel integrity at melting, mixing and pumping zones, screw and barrel wear, melting phenomena dependent on screw configurations	The channel should be completely filled at measurement position: adaptation in screw configuration/probe location are required	(Jen et al. 2005; Wang & Min 2005)
Ultrasonic techniques: shear waves	Die	In-line	Melt density	Assumption: a change in melt density will be directly seen as a change in extrudate density (accurate for most polymer extrusion applications), the accuracy of the measurements is highly dependent on the condition of the ultrasound transducer and stability of the process: constant cooling of the transducer was necessary. It is essential to keep the melt temperature and pressure within a narrow range during extrusion : a change in either will affect the acoustic properties of the melt and will interfere with the accuracy of the intended measurements: normalization procedures should be applied	(Abu-Zahra 2004a)
Ultrasonic techniques: undefined wave type	Die	In-line	Melt density	-	(Abu-Zahra 2004b)

Rheological techniques:					
Stress and shear rate sensor	Die	In-line	Melt viscosity as a function of shear rate	-	(Chiu et al. 1997)
Capillary rheometer	Barrel	On-line	Torque, shear stress, shear rate, melt flow index, linear viscoelastic behaviour	Large deformations and relatively high shear rates associated with the flow in a capillary rheometer may affect the morphology of the material and consequently its rheological response	(Covas et al. 2004)
Oscillatory rheometer	Barrel	On-line	Linear viscoelastic behaviour	-	(Covas et al. 2004)
Rotational rheometer	Barrel	On-line	Morphology development, reaction kinetics, linear viscoelastic behaviour, storage and loss modulus of polymer melts	-	(Covas et al. 2008; Mould et al. 2011)
Extensional rheometer	Die	On-line	Melt strength	-	(Kracalik & Laske 2011)
Slit die	Die	In-line	Thermal degradation of polymer	-	(Rajan et al. 2010)
Monitoring of motor current	Motor	In-line	Friction, torque, identification of conveying issues	Since the screw load torque signal is dominated by the solids conveying torque, it is not sensitive enough to identify unstable melting issues	(Abeykoon et al. 2011)

Temperature measurements:					
Thermocouple	Die	In-line	Melt temperature	Slow response time, measurements are highly dominated by barrel/die wall metal temperature	(Abeykoon et al. 2012)
IR sensor	Die	In-line	Melt temperature	Temperature information is limited to a small volume of the melt flow, IR measurements may be affected by polymer type and sensor calibration accuracy	(Abeykoon et al. 2012)
Thermocouple mesh	Die	In-line	Melt temperature	Melt flow may be slightly disturbed, measurements are slightly influenced by shear heating depending on the size of the mesh wires and junctions, mesh wires may be damaged under poor melting conditions (e.g. Highly viscous or unmelted materials)	(Abeykoon et al. 2012)

APPENDIX 3: GPC RESULTS

Hydrolysis week	Sterility	Mw (Da)	S. D.	Mn (Da)	S.D.	PDI	S.D.
0	no	184804	4912	81282	1872	2.27	0.11
1	no	166051	1250	78077	679	2.13	0.03
8	no	152898	815	73221	201	2.09	0.02
16	no	134867	3177	63691	2542	2.12	0.03
24	no	117695	1012	57902	1687	2.03	0.08
28	no	107448	25	52804	696	2.04	0.03
36	no	89312	2768	44543	2762	2.01	0.06
0	yes	41751	735	20774	886	2.01	0.05
1	yes	38901	243	19229	496	2.02	0.04
8	yes	31633	260	15169	624	2.09	0.10
16	yes	25957	769	12108	278	2.14	0.01
24	yes	20579	98	9870	503	2.09	0.10
28	yes	17480	402	8007	660	2.19	0.13
36	yes	9393	541	3642	701	2.61	0.35

APPENDIX 4: DSC RESULTS

Hydrolysis week	Sterility	Tm (°C)	S. D.	Tg (°C)	S.D.	Xc (%)	S.D.
0	no	159.1	0.66	62.7	0.22	29.8	0.57
1	no	157.4	0.28	61.8	0.16	31.1	0.42
8	no	159.3	0.91	62.6	0.06	31.1	0.28
16	no	157.5	1.24	62.0	0.42	32.1	0.11
24	no	156.8	0.37	62.0	0.21	34.0	1.68
28	no	156.9	0.59	62.1	0.24	32.1	0.27
36	no	156.2	0.49	61.8	0.11	35.3	0.04
0	yes	153.7	0.16	60.1	0.11	41.0	0.60
1	yes	155.6	0.16	60.5	0.05	41.8	0.71
8	yes	156.5	0.47	60.2	0.21	42.7	0.86
16	yes	157.1	0.06	59.3	0.06	43.3	0.01
24	yes	157.0	0.19	58.4	0.72	43.5	2.24
28	yes	156.3	0.06	57.1	0.48	44.3	0.01
36	yes	153.2	0.09	55.5	0.31	42.9	1.60

APPENDIX 5: TENSILE TESTING RESULTS

Hydrolysis week	Irradiated	Dry/wet	n	Stress at max. Load (MPa)	S. D.	Load at max. Load (N)	S.D.	Strain at max. Load (%)	S.D.
0	no	dry	5	417.4	32.7	12.5	0.9	51.7	3.1
0	no	wet	5	378.1	52.0	10.1	1.3	39.8	5.5
1	no	wet	5	363.7	69.1	10.5	0.8	50.7	4.0
2	no	wet	5	331.5	52.1	10.8	1.3	48.1	5.7
3	no	wet	4	377.9	53.1	9.4	1.3	44.7	2.4
4	no	wet	4	377.8	25.0	9.3	1.2	40.6	6.0
6	no	wet	4	327.8	29.4	11.9	1.5	60.9	7.5
8	no	wet	4	333.6	33.4	9.7	1.0	47.8	3.6
12	no	wet	4	355.3	24.0	10.3	0.7	52.3	4.7
16	no	wet	4	344.7	28.0	10.0	0.8	44.8	1.0
20	no	wet	5	393.0	28.7	11.4	0.8	60.2	5.0
24	no	wet	5	332.2	76.8	9.6	2.2	49.4	7.9
28	no	wet	5	360.0	42.1	10.4	1.2	44.5	3.8
32	no	wet	5	387.8	63.1	11.2	1.8	60.3	6.8
36	no	wet	5	364.9	30.8	10.6	0.9	53.5	5.3
42	no	wet	5	354.1	26.6	10.3	0.8	54.6	4.9
48	no	wet	5	306.4	69.9	8.9	2.0	56.1	10.2
0	yes	dry	4	308.8	21.6	8.5	0.9	50.3	5.2
0	yes	wet	4	243.9	15.6	9.1	0.8	54.7	5.3
1	yes	wet	3	241.8	15.6	8.2	0.8	57.1	6.2
2	yes	wet	5	240.0	17.6	6.9	0.8	48.7	2.2
3	yes	wet	4	222.5	15.4	5.4	0.3	46.2	4.9
4	yes	wet	5	214.1	14.5	6.4	0.6	61.5	9.9
6	yes	wet	5	215.8	40.2	6.0	1.1	63.1	15.9
8	yes	wet	5	209.4	32.2	5.8	0.9	56.3	4.5
12	yes	wet	5	206.4	13.6	5.7	0.4	52.1	4.3
16	yes	wet	5	211.8	21.1	5.8	0.6	53.9	6.8
20	yes	wet	5	158.0	41.9	4.4	1.2	25.2	31.3
24	yes	wet	5	158.8	10.4	4.4	0.3	41.1	8.2
28	yes	wet	3	114.1	41.4	3.2	1.1	10.0	12.6